TECHNISCHE UNIVERSITÄT DARMSTADT

# Tailor-made antibodies by multidimensional functional screening

**Vom Fachbereich Chemie**
**der Technischen Universität Darmstadt**

zur Erlangung des Grades
Doctor rerum naturalium
(Dr. rer. nat.)

Dissertation

Von

Steffen Christiano Hinz, M. Sc.

Erstgutacher: Prof. Dr. Harald Kolmar

Zweitgutachter: Prof. Dr. Siegfried Neumann

Darmstadt 2021

Hinz, Steffen Christiano: Tailor-made antibodies by multidimensional functional screening

Darmstadt, Technische Universität Darmstadt

Jahr der Veröffentlichung der Dissertation auf TUprints: 2021

URN: urn:nbn:de:tuda-tuprints-145982

URL: https://tuprints.ulb.tu-darmstadt.de/id/eprint/14598

Tag der Einreichung: 24.11.2020

Tag der mündlichen Prüfung: 01.02.2021

Die vorliegende Arbeit wurde unter der Leitung von Herrn Prof. Dr. Harald Kolmar am Clemens-Schöpf-Institut für Organische Chemie und Biochemie der Technischen Universität Darmstadt im Zeitraum von November 2016 bis April 2020 angefertigt.

## Publications derived from this work

J. Grzeschik*, **S. C. Hinz***, D. Könning*, T. Pirzer, S. Becker, S. Zielonka, H. Kolmar. A simplified procedure for antibody engineering by yeast surface display: Coupling display levels and target binding by ribosomal skipping. *Biotechnology Journal*, 2017, 12(2), 1600454. DOI: 10.1002/biot.201600454

J. Grzeschik, D. Könning, **S. C. Hinz**, S. Krah, C. Schröter, M. Empting, H. Kolmar, S. Zielonka. Generation of Semi-Synthetic Shark IgNAR Single-Domain Antibody Libraries. *Methods in Molecular Biology*, 2018, 1701:147-167. DOI: 10.1007/978-1-4939-7447-4_8

D. Könning, **S. Hinz**, J. Grzeschik, C. Schröter, S. Krah, S. Zielonka, H. Kolmar. Construction of Histidine-Enriched Shark IgNAR Variable Domain Antibody Libraries for the Isolation of pH-Sensitive vNAR Fragments. *Methods in Molecular Biology*, 2018, 1827:109-127. DOI: 10.1007/978-1-4939-8648-4_6

J. P. Bogen*, **S. C. Hinz***, J. Grzeschik, A. Ebenig, S. Krah, S. Zielonka, H. Kolmar. Dual Function pH Responsive Bispecific Antibodies for Tumor Targeting and Antigen Depletion in Plasma. *Frontiers in Immunology*, 2019, 10:1892. DOI: 10.3389/fimmu.2019.01892

J. Grzeschik*, D. Yanakieva*, L. Roth, S. Krah, **S. C. Hinz**, A. Elter, T. Zollmann, G. Schwall, S. Zielonka,, H. Kolmar. Yeast surface display in combination with fluorescence-activated cell sorting enables the rapid isolation of antibody fragments derived from immunized chickens. *Biotechnology Journal*, 2019, 14(4):e1800466. DOI: 10.1002/biot.201800466

L. Roth*, J. Grzeschik*, **S. C. Hinz**, S. Becker, L. Toleikis, M. Busch, H. Kolmar, S. Krah, S. Zielonka. Facile generation of antibody heavy and light chain diversities for yeast surface display by Golden Gate Cloning. *Biological Chemistry*, 2019, 400(3):383-393. DOI: 10.1515/hsz-2018-0347

**S. C. Hinz***, A. Elter*, J. Grzeschik, J. Habermann, B. Becker, H. Kolmar. Simplifying the Detection of Surface Presentation Levels in Yeast Surface Display by Intracellular tGFP Expression. *Methods in Molecular Biology*, 2020, 2070:211-222. DOI: 10.1007/978-1-4939-9853-1_12

**S. C. Hinz***, A. Elter*, O. Rammo, A. Schwämmle, A. Ali, S. Zielonka, T. Herget, H. Kolmar. A generic procedure for the isolation of pH- and magnesium-responsive chicken scFvs for downstream purification of human antibodies. *Frontiers in Bioengineering and Biotechnology*, 2020, 8:688. DOI: 10.3389/fbioe.2020.00688

L. Pekar, M. Busch, B. Valldorf, **S. C. Hinz**, L. Toleikis, S. Krah, S. Zielonka. Biophysical and biochemical characterization of a VHH-based IgG-like bi- and trispecific antibody platform. MAbs, 2020, 12(1): p. 1812210. DOI: 10.1080/19420862.2020.1812210

A. Elter*, J. P. Bogen*, **S. C. Hinz**, D. Fiebig, A. Macarrón Palacios, J. Grzeschik, B. Hock, H. Kolmar. Humanization of Chicken-derived scFv Using Yeast Surface Display and NGS Data Mining, *Biotechnology Journal*, 2020, Online ahead of print. DOI: 10.1002/biot.202000231

* shared first author

## Contributions to Conferences

**S. C. Hinz**, D. Könning, J. Grzeschik, S. Zielonka, L. Deweid, H. Kolmar. *Shark-antibody derived biomolecules for downstream processing of antibodies*. GDCh-Wissenschaftsforum Chemie 2017 – Jubiläumskongress „GDCh – 150 Jahre“, Berlin, Deutschland (10.-14.09.2017)

**S. C. Hinz**, D. Könning, J. Grzeschik, S. Zielonka, L. Deweid, H. Kolmar. *Shark-antibody derived biomolecules for downstream processing of antibodies*. 6th Halle Conference on Recombinant Proteins, Halle, Deutschland (08.-09.03.2018)

**S. C. Hinz**, A. Elter, J. Grzeschik, D. Könning S. Zielonka, G. Schwall, H. Kolmar. *Shark-antibody derived biomolecules for downstream processing*. PEGS Europe – Protein & Antibody Engineering Summit, Lissabon, Portugal (12.-16.11.2018)

**S. C. Hinz**, A. Elter, E. Baum, H. Kolmar. *Chicken scFv molecules for downstream processing of sophisticated antigens*. PEGS Europe – Protein & Antibody Engineering Summit, Lissabon, Portugal (18.-22.11.2019)

**S. C. Hinz** & J. Bogen. *Dual function pH responsive bispecific antibodies for tumor targeting and antigen depletion in plasma*. Virtual Summit on Cancer and Immunology Research 2020, Online conference carried out by Science Select (11.-13.05.2020)

## Table of Content

## Zusammenfassung und wissenschaftlicher Erkenntnisgewinn

Die Vielseitigkeit von Antikörpern in den modernen Biowissenschaften oder auch der Medizin beruht nicht nur auf ihrer Fähigkeit, Antigene mit sehr hoher Affinität zu binden, sondern auch auf der intrinsischen Stabilität, die es ermöglicht, Antikörper mit maßgeschneiderten Eigenschaften zu erzeugen.

Das erste Projekt, das in dieser Arbeit vorgestellt wird, konzentrierte sich auf pH-schaltbare bispezifische Antikörper (bsAbs) mit *sweeping*-Funktion. bsAbs haben - im Gegensatz zu herkömmlichen Antikörpern - zwei Antigenspezifitäten, die zur Erzeugung immunologischer Synapsen und nachfolgender Zielstrukturzerstörung genutzt werden können. Werden jedoch solide tumor-assoziierte Antigene anvisiert, kann *antibody buffering* die Wirksamkeit des bsAb minimieren, wenn das Antigen auch in löslicher Form im Blutstrom vorhanden ist. Ein Phänomen was insbesondere im Kontext von monoklonalen Antikörpern beschrieben wurde. In aktuellen Publikationen wird die Erzeugung von *recycling*- und *sweeping*-Antikörpern beschrieben, die eine pH- oder Kalzium-responsive Antigenbindung aufweisen, um *antibody buffering* zu umgehen. Zu diesem Zusammenhang wird der Antigen-Antikörper-Komplex von Endothelzellen internalisiert und bei Änderung der Kalziumkonzentration oder des pH-Wertes dissoziiert das Antigen. Während der Antikörper sezerniert wird und wieder in der Lage ist, Antigen zu binden, wird das Antigen im Lysosom abgebaut. Unser Ansatz beschreibt die erste Implementierung einer Recyclingfunktion in einen bsAb, welcher *common light chains* (cLC) besitzt. Zu diesem Zweck wurde eine Histidin-angereicherte cLC-Bibliothek generiert und auf Antigen-Bindung bei pH 7,4 und Antigen-Freisetzung bei pH 5,0 durchmustert. Der parentale Antikörper wurde aus einer Immunisierung von OmniFlic Tieren mit den Kolorektalkarzinom-assoziierten Proteinen CEACAM5 und CEACAM6 generiert und in diesem Zusammenhang wurde auch die hier genutzt cLC entdeckt. Zusätzlich wurde beabsichtigt, die pH-Responsivität nur für eines der Antigene – CEACAM5 – zu implementieren. Die isolierten Kandidaten wurden hinsichtlich Schmelztemperatur und Antigenaffinität charakterisiert und zeigten nur geringe Unterschiede im Vergleich zur parentalen cLC. Wichtiger noch, es wurde untersucht und bestätigt, dass die erzeugte cLC ihre Eigenschaften als cLC behält und für einen CEACAM5/CEACAM6-spezifisches bsAb verwendet werden kann. Diese Arbeit vermittelt tiefere Einblicke in cLCs und zeigt, dass cLCs detailliert auf Einzelanwendungs-spezifische Anforderungen zugeschnitten werden können. In der dargestellten Arbeit war dies die Etablierung von pH-Responsivität für nur eine der beiden Antigen-Bindestellen.

Die zweite Untersuchung konzentrierte sich auf die Erzeugung von Hühnerantikörperfragmenten im Format der *single chain Fragment variable* (scFv) basierend auf Hühnerimmunisierungen, um die Verwendung von Hühnerantikörpern als Affinitätsliganden in Proteinreinigungsverfahren zu untersuchen. Die Affinitätschromatographie ist ein leistungsfähiges Werkzeug zur Reinigung von Proteinen aus komplexen Lösungen. Insbesondere im Zusammenhang mit Antikörpern ermöglichen natürlich vorkommende Liganden wie Protein A nicht nur eine Vereinfachung, sondern auch eine Beschleunigung des Reinigungsprozesses. Jedoch ist die hohe Affinität von Protein A zu Immunoglobulinen zeitgleich ein entscheidender Nachteil während des

Reinigungsprozesses, da hierdurch harsche Elutionsbedingungen wie beispielsweise Puffer mit niedrigem pH-Wert oder hoher Ionenstärke benötigt werden, welche Ausbeuteverluste durch Proteindegradation zur Folge haben könnten. Dies ist einer der Gründe, wieso für die Reinigung von Antikörpern oft Affinitätsliganden erzeugt werden, welche intrisische Responsivitätselemente aufweisen, die mildere Elutionsbedingungen ermöglichen. Wir wollten Affinitätsliganden auf der Basis von Hühnerantikörpern erzeugen. Hühner-Antikörper sind für eine einfache Bibliothekserzeugung und intrinsische thermische Stabilität bekannt und können durch einen einfachen Immunisierungsprozess erzeugt werden. Darüber hinaus sind Hühner keine Säugetiere, was die Chance erhöht, bei Immunisierung mit einem Säugetierprotein im Gegensatz zu Nagetierwirten eine Immunreaktion auszulösen. Für unsere Studien wählten wir das scFv-Format, um eine kostengünstige und einfache Herstellung durch bakterielle Expression zu ermöglichen. Unsere generierte Hühner-scFv-Bibliothek konnte verwendet werden, um eine Vielzahl verschiedener scFvs gegen unser Modellprotein - ein humaner IgG Antikörper - zu isolieren, die nicht nur eine hohe Affinität aufwiesen, sondern auch ein pH- und/oder Magnesium-responsives Bindungsverhalten zeigten. Dies sollte als zusätzliches Sortierkriterium milde Elutionsbedingungen in einem *Downstream Processing Setup (DSP)* ermöglichen. Nach der Kopplung der scFvs an ein voraktiviertes Festphase wurden Chromatographien durchgeführt, die sowohl die Spezifität als auch das pH-/Magnesium-responsive Bindungsverhalten in einem DSP-Setup bestätigten. Unser experimentelles Design erwies sich als ein sehr zeiteffizientes Verfahren zur Isolierung potenter Affinitätsliganden für die Reinigung menschlicher Proteine unter Anwendung milder Elutionsbedingungen.

Der dritte Teil dieser Arbeit konzentrierte sich auf die Methode des Hefe-Displays selbst und dessen Verbesserung. Das Online-Monitoring bei der Sortierung von Hefe-Display-Bibliotheken wird durch Immunfluoreszenzfärbung ermöglicht. Aufgrund der Färbung muss vor der Sortierung Zeit für die Vorbereitung der Bibliothek aufgewendet werden. Um dieses Verfahren zu umgehen, haben wir ein Expressionssystem entwickelt, bei dem die Oberflächenpräsentation mit intrazellulärer tGFP-Expression gekoppelt ist. Zu diesem Zweck wurde eine ribosomale Skipping-Sequenz (auch als 2A-Peptid bekannt) genetisch mit dem 3'-Ende des präsentierten Proteins und dem 5'-Ende von tGFP verknüpft. Nach der Translation wird die Polypeptidkette bis zum letzten Codon des 2A-Peptidgens verlängert, wo ein Strangbruch stattfindet, ohne dass das Ribosom stoppt, sondern die Translation mit einer zweiten Polypeptidkette (in dieser Arbeit tGFP) fortgesetzt wird, bis ein Stoppcodon erkannt wird. Dieser Aufbau ermöglicht den Nachweis von Oberflächenproteinkonstrukten in voller Länge ohne Verwendung von immunologischer Färbung, was eine zeit- und kostenfreundlichere Alternative zur immunologischen Färbung darstellt.

## Scientific Novelty and Significance

The versatility of antibodies in modern life science or medicine is based not only on their ability to bind antigens with very high affinity but also on intrinsic stability, which allows for multiple protein engineering approaches to generate antibodies with tailor-made characteristics. This work focused on expanding the applicability of antibodies with responsive binding elements for in vitro and *in vivo* experiments while streamlining the screening process by optimizing the library preparation.

The first project presented in this work focuses on pH-responsive sweeping bispecific antibodies (bsAbs). bsAbs comprise – in contrast to conventional antibodies – two antigen specificities that can be utilized to generate immunological synapses and subsequent target degradation. However, if solid tumor-associated antigens are targeted, bsAbs can suffer from antibody buffering if the antigen is also present in soluble form in the bloodstream, just as monospecific antibodies do. Recent publications describe the generation of recycling and sweeping antibodies which comprise pH-responsive or Calcium-responsive antigen binding in order to circumvent antibody buffering. This mechanism is based on the internalization of the antigen-antibody complex by endothelial cells and subsequent calcium concentration and pH change during vesicle maturation causing the antigen to dissociate. While the antibody is secreted and again able to bind antigen, the antigen is degraded in the forming lysosome. Our approach describes the first implementation of a recycling function into a bsAb equipped with common light chains. To this end, a histidine-doped common light chain library was generated based on the common light chain of a CEACAM5/CEACAM6 bsAb. This bsAb was isolated from an Omniflic immunization with the antigens CEACAM5 and CEACAM6, respectively, both relevant markers for colorectal cancer. As an additional goal, we aimed at introducing the pH-responsive binding solely for CEACAM5. The his-doped cLC library was screened for antigen-binding at pH 7.4 and antigen-release at pH 5.0. Isolated candidates were characterized towards melting temperature and antigen affinity, only showing minor differences compared to the parental common light chain. More importantly, it was examined and confirmed that the generated common light chain remains a common light chain which can be used for a CEACAM5/CEACAM6 specific bsAb. This work mediates more profound insights into the engineering of common light chains for tailor-made binding characteristics resulting in a molecule where one antibody arm gains pH-responsive behavior while one arm remains pH-independent.

The second investigation focuses on the generation of *single chain Fragment variable* molecules (scFvs) generated by chicken immunization as affinity ligands for affinity chromatography, expanding the utilization of chicken immunization derived antibody fragments. Affinity chromatography is a powerful tool to purify protein from complex solutions. Especially in the context of antibodies, naturally occurring ligands such as Protein A enable simplifying and accelerating the purification process. But the very high affinity of Protein A also comes with the drawback of requiring harsh elution conditions such as low pH or high ionic strength, resulting in antibody degradation during purification. Therefore, newly generated ligands for antibody purification are often

engineered to include responsive binding elements allowing mild elution conditions during purification. We aimed at creating affinity ligands based on chicken antibodies, which are known for easy library generation, intrinsic thermal stability, and can be generated by a simple immunization process.

Additionally, chickens are not mammals increasing the chance of provoking an immune reaction upon immunization with a mammal protein, unlike rodent hosts. Our chosen format – scFv – should also allow easy and fast production in bacterial hosts to ensure favorable production. The generated chicken scFv library could be utilized to isolate a plethora of different scFvs against our model protein, a human IgG scaffold. The resulting variants showed high affinity and comprised pH- and/or Magnesium-responsive binding behavior, which was an additional sorting criterion to enable mild elution conditions in a DSP setup in the end. After coupling the scFvs to a solid support, chromatographies were performed confirming the specificity as well as the pH-/Magnesium-responsive binding behavior in a DSP setup. Our experimental design proved to be a very time-efficient procedure to isolate potent affinity ligands enabling a mild elution purification of human proteins.

The third part of this work focuses on the method of yeast display itself and the refinement thereof. The online monitoring during the sorting of yeast display libraries is enabled by immunofluorescent staining. Due to the staining, time has to be spent to prepare the library prior sorting. We developed an expression system where the surface presentation is entangled with intracellular tGFP expression to circumvent this procedure. To this end, a ribosomal skipping sequence (also known as 2A peptide) was genetically fused to the 3’ of the presented protein and 5’ of tGFP. Upon translation, the polypeptide chain is elongated until the last codon of the 2A peptide gene. A strand break occurs without causing the ribosome to stop but rather to continue translation with a second polypeptide chain (tGFP in this work) until a stop codon is recognized. This setup allows the detection of full-length surface protein constructs without utilizing immunological staining resulting in a more time- and cost-friendly alternative to immunological staining.

## Individuelle Beiträge von S. Hinz zum kumulativen Teil der Dissertation

1. J. P. Bogen*, **S. C. Hinz***, J. Grzeschik, A. Ebenig, S. Krah, S. Zielonka, H. Kolmar. Dual function pH-responsive bispecific antibodies for tumor targeting and antigen depletion in plasma. *Frontiers in Immunology*, 2019, 10:1892. DOI: 10.3389/fimmu.2019.01892

   Beiträge von S. C. Hinz:

   - Durchführung von 40% der im Artikel beschriebenen Experimente
   - Design und Anfertigung der im Artikel dargestellten Abbildungen zusammen mit J. P. Bogen
   - Schreiben des Artikels zusammen mit H. Kolmar und J. P. Bogen
   - Wissenschaftliche Betreuung der in diesem Zusammenhang durchgeführten Masterarbeit von J. P. Bogen

   **Der Anteil von S. C. Hinz an dieser Publikation beläuft sich auf 40%.** Der Anteil von J. P. Bogen beläuft sich als Co-Erstautor ebenfalls auf 40%. Die verbleibenden 20% verteilen sich auf die übrigen Koautoren für die initialen Expressionen der Proteine in Zellkultur, die Koordination des Projektes wie auch das kritische Korrigieren des Manuskriptes.

2. **S. C. Hinz***, A. Elter*, J. Grzeschik, J. Habermann, B. Becker, H. Kolmar. Simplifying the Detection of Surface Presentation Levels in Yeast Surface Display by Intracellular tGFP Expression. *Methods in Molecular Biology*, 2020, 2070:211-222, 10.1007/978-1-4939-9853-1_12. DOI: 10.1007/978-1-4939-9853-1_12

   Beiträge von S. C. Hinz:

   - Design der in dem Artikel dargestellten Abbildungen
   - Gemeinsames Schreiben des Artikels mit A. Elter

   **Der Anteil von S. C. Hinz an dieser Publikation beläuft sich auf 45%.** Der Anteil von A. Elter beläuft sich als Co-Erstautor ebenfalls auf 45%. Die verbleibenden 10% verteilen sich auf die übrigen Koautoren für das Korrigieren des Manuskriptes.

3. **S. C. Hinz***, A. Elter*, O. Rammo, A. Schwämmle, A. Ali, S. Zielonka, T. Herget, H. Kolmar. A generic procedure for the isolation of pH- and magnesium-responsive chicken scFvs for downstream purification of human antibodies. *Frontiers in Bioengineering and Biotechnology*, 2020, 8:688. DOI: 10.3389/fbioe.2020.00688

Beiträge von S. C. Hinz:

- Initiale Literaturrecherche zusammen mit A. Elter, T. Herget und H. Kolmar
- Durchführung von 60% der im Artikel beschriebenen Experimenten
- Design und Anfertigung der im Artikel dargestellten Abbildungen zusammen mit A. Elter
- Erweiterung des Projektes auf Magnesium-responsive Antikörperfragmente
- Verfassen des Manuskriptes mit A. Elter und H. Kolmar

**Der Anteil von S. C. Hinz an dieser Publikation beläuft sich auf 40%.** Der Anteil von A. Elter beläuft sich als Co-Erstautor ebenfalls auf 40%. Die verbleibenden 20% verteilen sich auf die übrigen Koautoren für die kritische Diskussion der experimentellen Ergebnisse, wie auch das kritische Korrigieren des Manuskriptes.

# 1 Introduction

Throughout millions of years, multicellular organisms developed defense mechanisms against microorganisms to which they are exposed to in nearly every natural habitat. More developed organisms, such as vertebrates and invertebrates, comprise defense mechanisms referred to as the immune system. This system is responsible for the identification of pathogens and subsequent neutralization thereof. To enable a fast response to a pathogen, some mechanisms of the immune system are immediately activated upon pathogen contact. The trade-off, however, is that the initial immune reaction is less pathogen-specific and, therefore, less efficient in pathogen neutralization. Still, it is capable of recognizing a wide range of pathogens by *pathogen-associated molecular patterns* (PAMPs) present on the surface of pathogens. This so-called innate immune system relies on *i.a*. macrophages, dendritic cells, and granulocytes [1-3] expressing *pathogen recognition receptors* (PRRs), which are evolutionary highly conserved [2, 4-7]. If a PAMP is identified and bound by a cell of the innate immune system, the reaction can lead to the pathogen's opsonization or the expression of antimicrobial peptides and inflammatory cytokines [8-10]. Different mechanisms of the innate immune system rely on natural killer cells (NK cells), which are activated upon pathogen binding [11, 12]. Not only molecular interactions are summarized as the innate immune system but also the physical barriers formed by mucosal surfaces and epithelial cells preventing pathogens from entering the host organism [13].

In contrast to the innate immune system, the second line of defense – the adaptive immune system – is only activated upon encountering pathogenic threats. Key components are lymphocytes called B-cells and T-cells. In contrast to the PRRs, antigen-recognition receptors present on B-cells and T-cells are not germline coded and comprise a very high diversity through recombination-activating gene-protein (RAG-protein) initiated somatic recombination events [14-16]. This allows the expression of tailor-made B-cell receptors (BCRs) or T-cell receptors (TCRs), respectively, specifically binding to imminent threats [17, 18]. This high diversity comes at a cost. During maturation of B-cells and T-cells and generation of BCRs and TCRs, the host has to circumvent the appearance of receptor variants targeting host-self antigens to prevent autoimmune reactions. This process, referred to as central tolerance, occurs during maturation of both cell types [19-21].

TCRs do not recognize solely soluble antigen but rather a pathogenic peptide (derived from a degraded pathogenic protein), which is presented by *antigen-presenting cells* (APCs) in complex with the *major histocompatibility complex* (MHC) receptor [22, 23]. Depending on the co-receptor on the T-cell – either CD4 or CD8 – the T-cell activation by TCR-signaling will lead to the secretion of cytokines and accumulation of immune system cells like phagocytes, natural killer cells and cytotoxic T-cells for cell killing or direct cell-killing by cytotoxic T-cells, respectively [16, 24-26].

Additionally, BCRs are responsible for inducing the humoral response of the adaptive immune system.

B-cell activation is initiated by antigen binding to the BCR either in as soluble antigen or in complex with MHC [27]. With the addition of a co-stimulatory signal of maturated and pre-activated T-cells, the B-cell can further differentiate into a plasma call and develop the ability to secrete soluble forms of the BCR called immunoglobulins or antibodies to “label” pathogens [16]. An alternative differentiation pathway will lead to the formation of memory cells, which serve as B-cells on hold, which can be reactivated very fast upon exposure to a known pathogen.

## 1.1 Antibodies

### 1.1.1 Structure and Diversity

Antibodies are glycoproteins secreted by plasma cells. They are comprised of two heavy chains and two light chains, which are interconnected by disulfide bonds. Whereas the heavy chains of most antibodies contain one variable domain called $V_H$ and up to three constant domains termed $C_{H1}$, $C_{H2}$, and $C_{H3}$, the light chain only comprises two domains: one variable domain named $V_L$ and one constant domain $C_L$, respectively (Figure 1). Two different light chain variants are genetically encoded in humans, the κ and the λ light chain [28]. Early experiments with the protease papain showed that IgG-isotype antibodies could be cleaved between $C_{H1}$ and $C_{H2}$, resulting in a $C_{H2}$-$C_{H3}$ homodimer termed *Fragment crystalline* (Fc) and two heterodimers of the light chain domains $V_L$-$C_L$ and the heavy chain domains $V_H$-$C_{H1}$ called *Fragment antigen-binding* (Fab). Additionally, the cleavage region is located in a spacer sequence termed *Hinge* since it facilitates the flexibility of the Fab arms [29].

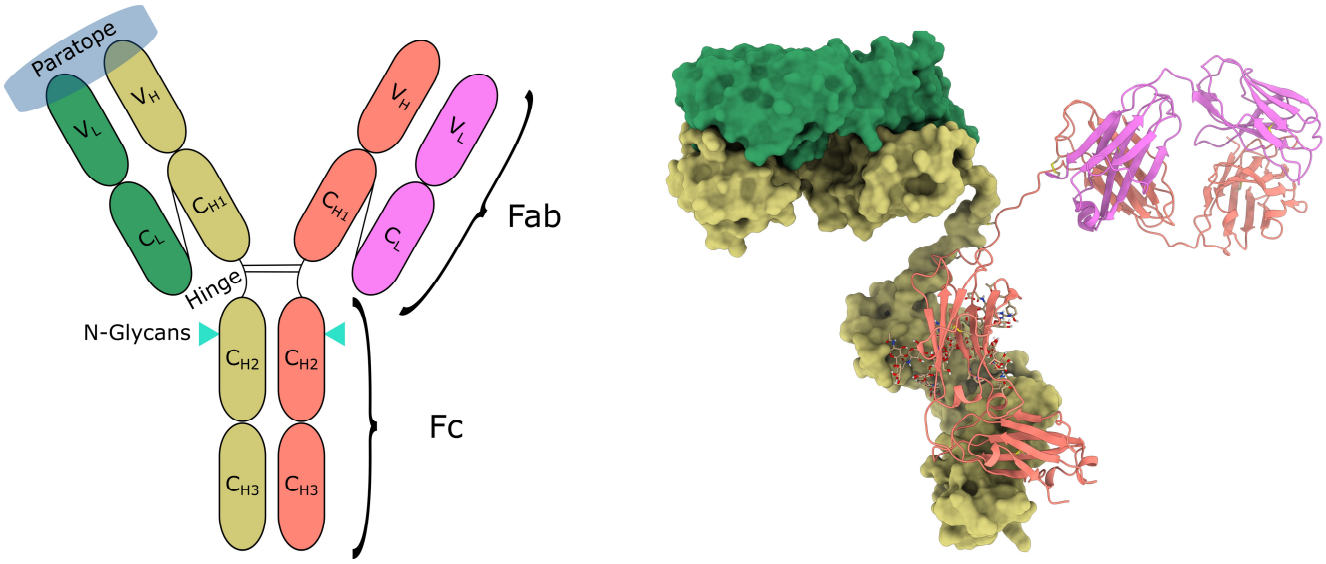


**Figure 1. Schematic depiction of an IgG antibody and its three-dimensional model in ribbon and surface presentation.** Light chains are depicted in green and pink, respectively. Heavy chains are shown in olive green and coral, respectively. N-glycans are depicted as ball and sticks or indicated with cyan triangles on the schematic drawing. Additionally, the paratope, the hinge region, the Fab, and the Fc are indicated on the schematic IgG. Disulfide bridges are shown in yellow on the three-dimensional model, which is based on PDB entry 1igt.

The first steps of generating antibody diversity are the rearrangement of gene fragments coding for the either the variable domain of the heavy and the light chain. The gene fragments are categorized as *variable* (V), *diversifying* (D) or *joining* (J) segments, of which only V and J are utilized for $V_L$ generation [30]. These recombination events are initiated by the activation of RAG-1 and RAG-2, which are almost exclusively expressed in non-matured lymphocytes [31]. RAG proteins introduce double-strand breaks at designated recombination signal sequences (RSS) located between individual V, D and J segments, respectively [32]. These double-strand breaks are repaired by nonhomologous end-joining, which creates imprecise joins at the coding ends, serving as a template for the terminal deoxynucleotidyl transferase (TdT). The TdT is only expressed in human lymphocytes and it may add non-germline encoded nucleotides to the coding end of the recombination fragment [29], introducing an additional element of diversity. The locus for the κ light chain variable domain contains 40 V segments and 5 J segments located on chromosome 2p11.2 [28, 33]. The joining of V and J segments is located in the *complementarity determining region 3* (CDR3) one of three CDR loops located in each variable domain responsible for antigen binding. The antigen recognition site – the paratope - is determined by the three CDRs of the variable domain of the light chain and three CDRs of the variable domain of the heavy chain. The λ locus exhibits a slightly different organization. It contains 32 V segments and, additionally, four fixed J-C segments, which also encode for the constant domain of the λ light chain [29].

The genetic organization of the heavy chain variable domain locus is considerably more complex. Located on chromosome 14q32.33, the locus is divided into 39 V segments, 27 D segments and 6 J segments [30, 34]. During recombination one D and one J segments are joint first, whereas the V segment is added last [35]. Due to the three-segment joining process, TdT-assisted nucleotide addition can occur between V-D and D-J, which increases the diversification significantly [29]. Each of the VDJ variable domains of the heavy chain can be juxtaposed to any of nine different constant domain genes [36], a process referred to as *class switch recombination* (CSR). These constant domain genes encode for specific constant domains and hinge regions, also giving the option of expressing a membrane-bound antibody or a secreted antibody upon alternative splicing. These different heavy chains are responsible for specific effector functions, which are discussed in the next paragraph. The switching of individual heavy chain genes (*class switch recombination* (CSR)) is mediated by the *activation-induced cytidine deaminase* (AID). This enzyme is also responsible for an additional element of antibody diversification, namely *somatic hypermutation* (SHM) [31, 37]. AID deaminates ssDNA cytidines during transcription in RGYW (purine/G/pyrimidine/A) motifs [38], which can be processed by several repair pathways. Base excision repair, mismatch repair as well as *non-homologous end-joining* (NHEJ) appear to be necessary for either CSR or SHM [39, 40]. The absence of AID activity leads to severe immunodeficiencies called Hyper-IgM syndrome, highlighting the importance of the immune system's aforementioned recombination processes [31]. All in all, the pool of possible antibody sequences is estimated to exceed $1 \times 10^{12}$ [30].

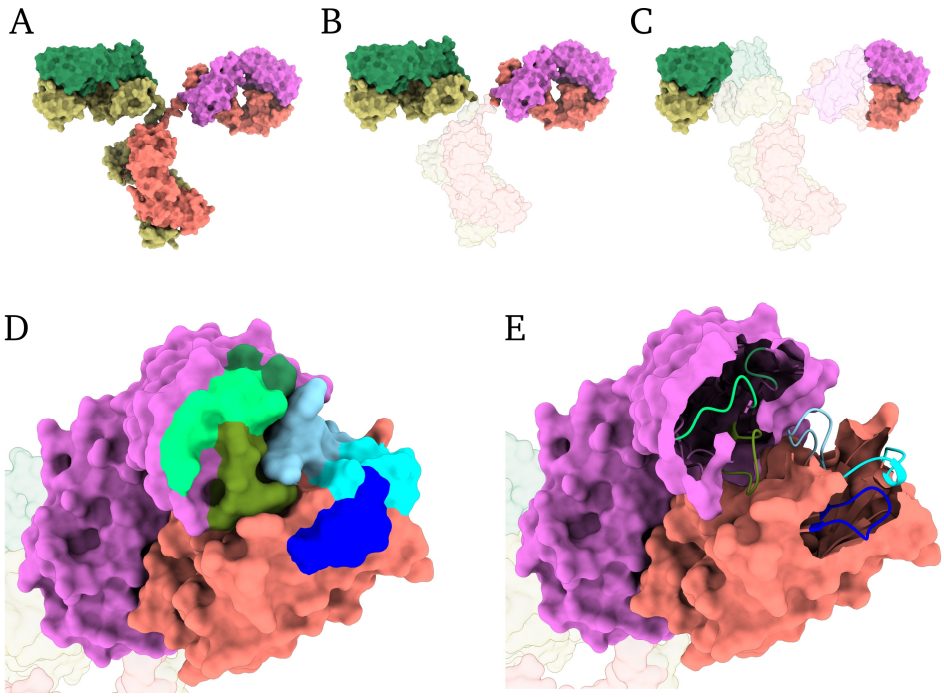


**Figure 2.** **Depiction of a full-length IgG antibody (A), Fab fragments (B) and scFv molecules (C).** Light chains are depicted in green and pink, respectively. Heavy chains are shown in olive green and coral, respectively. CDRs of the light chains are shown in green tones, CDRs of the heavy chain in blue tones (D + E). The model is based on PDB entry 1igt with CDR annotation according to IMGT [41]. Scfv molecules are displayed without interconnecting linker sequences.

### 1.1.2 Function

The human heavy chain is encoded by one of nine heavy chain genes, each differing in hinge flexibility, tissue accessibility, glycosylation pattern and effector function of the antibody. Effector functions summarize the ability of antibodies to mediate pathogen neutralization pathways upon antigen binding. It can be distinguished between cellular-dependent and cellular-independent effector functions [42]. The *antibody-dependent cellular cytotoxicity* (ADCC) describes the neutralization of antigens after antibody binding and subsequent effector cell recruitment, such as NK cells and monocytes mediated by various Fc receptors [29, 43]. The effect of antibody-induced phagocytosis is named *antibody-dependent cell-mediated phagocytosis* (ADCP), which is also cell dependent [44]. Cellular-independent effector functions rely on *complement-dependent cytotoxicity* (CDC) mediated by C1q binding to the Fc and subsequent target cell lysis.

The default isotype being expressed first after antigen recognition and before SHM and CSR occur is IgM (encoded by Cμ) exhibiting only low affinity towards the antigen, which is compensated by its pentameric form resulting in ten antigen binding sites and therefore high avidity. Its size limits IgM mainly to the bloodstream and, to a lesser degree, to the lymph [30]. Due to the pentameric form, IgM shows very high complement system activation. IgD (encoded by Cδ) is also expressed early in the development of B-cells on B-cell surfaces simultaneously to IgM and seems to activate basophils [45] and can substitute to some extend low IgM expression levels [46]. The least abundant isotype is IgE (encoded by Cε), which mediates hypersensitivity and is often linked to allergic reactions. Infections with helminths and metazoan parasites also induce elevated IgE

production [47]. Due to its high affinity to the FcεRI and FcεRII, which are mostly found on mast cells and basophils, it can initiate the production of proinflammatory molecules like histamine and cytokines [48]. IgA can be subdivided into IgA1 and IgA2 (encoded by Cα1 or Cα2, respectively) and mainly exist in a dimeric form. This isotype activates effector functions to a low degree and is found primarily in secretory fluids such as breast milk and saliva and on mucosal surfaces [49]. The most abundant isotype in humans is the IgG isotype, which is subdivided into IgG1, IgG2, IgG3 and IgG4 (encoded by Cγ1, Cγ2, Cγ3 and Cγ4, respectively) [50]. It reaches concentrations up to 10 mg/ml in the blood plasma, representing 10-20% of total plasma protein [51]. IgG1 and IgG3 show higher complement activation [52] than IgG2 and IgG4, mainly caused by less efficient binding of C1q of the latter isotypes [53]. Accordingly, ADCC activation also differs between IgG isotypes. Whereas IgG1 and IgG3 show very strong ADCC activation, IgG4 and IgG2 fall significantly behind [54, 55]. Due to the binding to the neonatal Fc-receptor (FcRn), all IgG isotypes exhibit a significantly increased half-life of up to 21 days [56-59]. An additional effect of FcRn-binding is the transfer of IgG antibodies across the placenta, the blood-brain-barrier and epithelial barriers in general [60-63], emphasizing the importance of the IgG isotype for the immune system.

The glycosylation of the antibody influences not only the effector function capabilities but also enhances the stability of the Fc-heterodimer [64, 65]. Individual antibody isotypes defined by the heavy chain gene and class differ significantly by their glycosylation pattern. The relative weight of the glycans can be as high as 12% w/w for IgE with six N-glycosylation sites in contrast to IgG with only one conserved N-glycosylation site [65, 66]. Additionally, it is reported that the glycosylation pattern can influence the secretion efficiency as well as the hinge flexibility [67, 68].

### 1.2 Antibodies in a therapeutic context

The success story of antibodies is tightly connected to the history of cancer therapeutics. Almost eighty years ago, experiments were performed by Charles Huggins in order to treat prostate cancer with hormones [69], indicating that treatment might be possible for cancer indications. Further developments included studies performed during the second world war, which stated that alkylating agents such as mustard gas initiate non-Hodgkin lymphoma regression [70]. However, side effects were severe and improvements during the following decades not only focused on the efficacy of fighting cancer but also on minimizing side effects caused by the treatment [71]. A promising way of reducing side effects is the utilization of targeted therapeutics, therapeutics that do not rely on diffusion into tissue and eventually face a cancer cell at some point but rather therapeutics that comprise cancer cell recognition sites that do not impact healthy tissue. Antibodies are naturally occurring molecules with such recognition sites and seemed to be promising tools for therapeutics in general, not limited to cancer indications. The first utilization of antibody-based therapeutics dates back to the late 19$^{th}$ century when Bering and Kitasato discovered that the sera from rabbits which faced a *Clostridium tetani* infection can be used to protect mice against infections with the very same pathogen [72, 73]. This discovery quickly led to

the development of a diphtheria therapeutics made from horse sera used to treat diphtheria suffering children with great success [74]. However, side effects were severe and some children may have died due to anaphylactic reaction against the horse serum instead of diphtheria [75]. However, it took some more decades until protein engineering developed technics for the production of defined antibody therapeutics, which will be discussed in the following paragraph.

Due to their highly versatile characteristics, antibodies are accepted and essential biomolecules in modern medicine. More than 80 antibody-based therapeutics were approved by the *food and drug administration* (FDA) in the USA, with many more to come in the following years for indications in the fields of oncology, immunology and hematology [76-78]. In total, more than 550 antibodies were evaluated in clinical studies with 62 being in late-stage studies in 2019 [79]. Additionally, antibodies are also used for analytical purposes such as labeling agents in enzyme-linked immunosorbent assay, lateral-flow devices, affinity ligands in affinity chromatography and Western Blots [80-83].

### 1.2.1 Monoclonal antibodies

One of the most important techniques which allowed the utilization of antibodies in a therapeutic context was the development of the hybridoma technology by Köhler and Milstein in 1975. This technology relies on the fusion of an immortalized myeloma cell with an antibody-producing B-cell, resulting in an immortalized hybridoma cell that produces an antibody with defined specificity [84].

In 1986 the first antibody – muromonab - was approved by the FDA to enter the US market [85] to treat kidney transplant patients immune to steroid treatment. Thirty-two years later, the bestselling antibody adalimumab (Humira) reached a market capitalization of 19.34 bn $ [86]. First antibodies were generated by immunization of mice resulting in murine antibody therapeutics with potential immunogenicity risks [87, 88] and significantly reduced Fc-mediated effector functions due to the non-human Fc [89]. Even though the generation strategy did not change in the beginning, important changes were performed on antibody candidates for therapy to make the antibody “more human,” and therefore reducing the probability of encountering immunogenicity [90]. In 1994 abciximab was approved for the treatment of platelet aggregation, and in contrast to muromonab, it was engineered to comprise only murine variable domains grafted onto human constant domains [91, 92]. The same was performed for rituximab, the first monoclonal antibody (mAb) approved for an oncologic indication [93]. One step further towards complete human antibodies was the grafting of murine CDRs onto fully human frameworks [94]. The first mAb utilizing this method was daclizumab, approved in 1997 by the FDA [90]. But still, immunogenicity was a problem due to the rise of anti-idiotypic antibodies that could recognize non-human CDR sequences [95, 96]. Besides the appearance of *in vitro* screening technologies, which will be discussed in section 1.4, the engineering of transgenic animals allowed the generation of fully human antibodies [97-99] and subsequent approval of the FDA [100, 101]. To this end, the human immunoglobulin genes are inserted into the

genome of the animal, replacing endogenous immunoglobulin genes resulting in the expression of human antibodies upon immune system activation [102, 103]. A significant drawback of immunization-derived antibodies is the restriction to non-toxic target molecules and low immunogenicity against proteins with high homology in mammals [104, 105].

### 1.2.2 Novel antibody formats and novel modes of action

Besides utilizing antibodies resembling the natural-occurring IgG format, many different antibody-based formats have been developed throughout the years. To facilitate better tissue penetration and reduce steric hindrance, Fab and *single chain variable fragment* (scFv) molecules have been engineered, which comprise a drastic reduction in molecule size [106-108] (Figure 2). An scFv consists of only VH and VL domains connected by a flexible linker sequence devoid of any constant domains of a conventional antibody molecule. Engineering of the Fc to obtain decreased or increased effector function activation is also described in literature [109-111]. Additionally, these small antibody-based molecules are easier to produce in prokaryotic expression systems due to their less complex structure [112]. However, the small size comes with a drawback, namely renal clearing. With approx. 28 kDa in size, scFv molecules show half-lives in the blood of 10 min, the utilization of Fabs only increases the half-live to 28 minutes [113]. To circumvent renal clearance, the multimerization of small antibody-based molecules can increase the overall molecular size as well as the attachment of polymers like e.g., *polyethylene glycol* (PEG) to elongate circulation duration [112, 114-116].

Other strategies utilize the antibody as a carrier protein. In antibody-drug conjugates (ADCs), the antibody mediates the highly specific binding to tumor-associated antigens while the antibody-conjugated payload is responsible for tumor cell neutralization. This payload can be toxins [117, 118], radionucleotides [119] or cytokines [120, 121] for regiospecific effector cell accumulation.

Alternative approaches focus on implementing novel modes of action like sweeping and recycling antibodies to counter the accumulation of antigen-antibody complexes in the bloodstream. This phenomenon is restricted to soluble antigens and is also known as antibody buffering [122-124]. In order to prevent antibody buffering, sweeping and recycling antibodies can be utilized to degrade antigen by binding it and “directing” it into the cell for lysosomal degradation (Figure 3). Sweeping antibodies require the engineering of the Fc as well as the paratope. Sweeping antibodies comprise an alternative Fc-scaffold with an increased affinity to either FcRn or FcγRIIb [125, 126].

Additionally, the binding of the antigen to the antibody needs to be pH-dependent in order to release the antigen at pH <6.5. Upon binding of the antigen-antibody complex to the Fc receptor and subsequent uptake into an endothelial cell, the antigen is released due to the incremental acidification of the forming sorting endosome. The soluble antigen is subsequently degraded by the lysosome. In contrast, the Fc receptor-antibody complex is

brought back to the cell surface where the antibody can bind again a new antigen. This cycle can be performed multiple times [127]. In contrast to sweeping antibodies, a recycling antibody does not comprise an alternated Fc molecule but only a pH-responsive paratope [128]. This allows utilizing the antibody for soluble antigen depletion while retaining its ability to move through the bloodstream to reach the tumor site. Additionally, it is reported that this strategy can be used to deplete soluble antigen, which would block and therefore prevent the antibody from reaching its site of action [129]. Alternative approaches have been undertaken with calcium-responsive antibodies instead of pH-responsive antibodies because endosome formation also results in increasing calcium levels [130].

Besides Fc-mediated effects, antibodies can also act as an antagonist by either binding to the ligand or the respective receptor denying the interaction thereof and as agonist by binding and clustering of receptors, which can lead to apoptosis [131].

Besides developing next-generation monospecific antibodies, engineering approaches enabled the production of antibodies that comprise two specificities, *i.e*., target a different epitope with each Fab arm. These bispecific antibodies have gained a lot of attention in recent decades and will be discussed in the following paragraph.

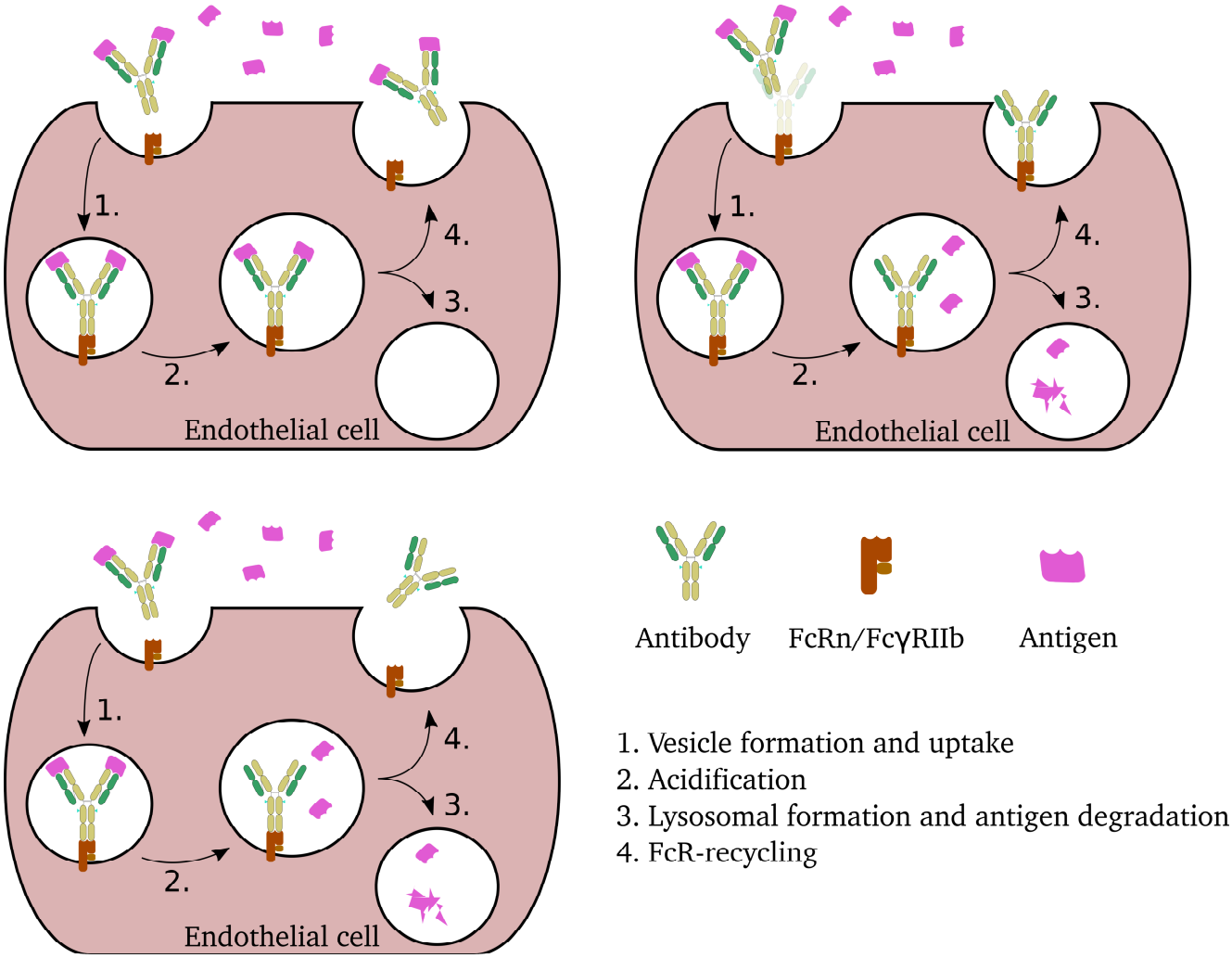


**Figure 3.** **Mechanism of sweeping and recycling antibodies.** The endothelial cell is depicted in dark red. Upon binding the antigen (pink), the antibody (green tones) is internalized. Acidification leads to the dissociation of the antigen from engineered IgGs and the association of the IgG to Fc receptors. The antigen is degraded in the formed lysosome while the antibody is recycled to the cell surface capable of binding new antigen either as soluble antibody (C) or bound to the Fc receptor (B).

### 1.3 Bispecific antibodies

A plethora of different strategies has been developed in order to generate bispecific molecules. In 2019, 57 bsAbs constructs were in clinical trials underlining the importance of this format [132]. Most simple strategies involve the linkage of monospecific antibodies or antibody fragments which was done for the bispecific T-cell engager (BiTE) molecules where two scFvs are linked by a peptide chain [133]. Its mechanism relies on recognizing a tumor cell-associated antigen such as EpCAM or CD19 and the simultaneous binding of an effector cell-associated antigen like CD3 located on T-cells. This close proximity leads to the formation of an immunological synapse and, subsequently, tumor cell neutralization [134]. The success of the BiTE technology quickly led to the development of additional T-cell engaging bispecific antibodies against hematological, solid tumor and other indications [135-137]. One of the major characteristics of BiTE is the lack of an Fc, which is a shared feature for “non-IgG”-bispecifics including DART, TandAb, F(ab`)2 molecules and others [138]. However, the lack of the Fc prevents the molecule from mediating effector functions and the recycling mechanism of the

FcRn receptor, drastically decreasing its half-life in serum [139, 140]. The first approved full-length IgG-like bsAb was catumaxomab in 2009 for the treatment of malignant ascites [141]. The first production strategies of IgGs relied on the fusion of an antibody-secreting B-cell with an immortalized myeloma cell resulting in a hybridoma cell producing soluble antibody [84]. Applying this expression strategy to bsAbs involves the subsequent fusion of two hybridoma cell lines forming hybrid-hybridoma cells. However, hybrid-hybridoma cells will produce not only the desired bsAb but also a mixture of LC/HC variants which do not comprise desired properties (Figure 4A) [142]. With only 12.5% of all possible variants, the desired product would have to face an inefficient and uneconomical manufacturing process. The first experiments to improve the production of correctly assembled bsAbs were undertaken in 1995 with the quadroma technology [143]. This method relies on the fusion of a mouse hybridoma and a rat hybridoma cell line since LC/HC pairing was found to be species-specific. In order to avoid the chain-mispairing issue on fully human IgGs, engineering approaches have resulted in technologies for guided heavy chain heterodimerization. In 1996, Ridgway and coworkers developed the *Knobs-into-holes* (KiH) technology which is based on mutation of single amino acids in the $C_{H3}$ domain [144]. These mutations create a "knob" in one $C_{H3}$ by replacing threonine with tyrosine (T366Y) and a "hole" by replacing a tyrosine residue with threonine (Y407T) on the opposite $C_{H3}$. However, the heterodimerization is not perfect and homodimers of hole-HC is commonly observed which is not true for the knob-HC [145]. For increasing the chance of purifying only correctly assembled variants, Protein A variants – a naturally occurring Ig-binding protein that will be discussed in chapter 1.6.2 - have been engineered to discriminate between heavy chain homo and heterodimers. This is achieved by introducing two amino acid exchanges in the $C_{H3}$ domain changing HY to RF, significantly reducing Protein A affinity and allowing clean separation by applying a pH-gradient during elution [146]. Alternative approaches have focused on more complex exchanges in order to achieve dimerization. The *strand-exchanged engineered domains* (SEED) technology utilizes the inability of IgA and IgG antibodies to form dimers. By exchanging β-strands from IgG $C_{H3}$ and IgA $C_{H3}$ asymmetrically, heavy chains are formed that preferably dimerize with their asymmetric counterpart [147]. This results in a heterodimerization platform with unaltered Fc-receptor interaction characteristics [148]. Alternative approaches have been made to generate new heavy chain scaffolds with preferable heterodimerization capabilities [149, 150]. However, correct arrangement of heavy chains in bsAbs increases the yield of correctly assembled antibodies only to 25%, which is still not sufficient for large scale production of therapeutics. Consequently, technologies for the correct assembly of light chains have been developed. The CrossMab platform developed by Roche is based on the exchange of $C_L$ and $C_{H1}$ domains resulting in a $V_L$-$C_{H1}$ light chain and a $V_H$-$C_L$-$C_{H2}$-$C_{H3}$ exploiting the inability of $C_{H1}$ and $C_L$ domains to form homodimers [151] (Figure 4C). However, it is known that the association of LC and HC can be driven by the VL and VH interaction. In that case, CrossMab cannot be used to solve the LC/HC mispairing problem. Lewis and coworkers published a strategy to circumvent the mispairing by introducing amino acid exchanges in the dimerization interface of $V_H$-$C_{H1}$ and $V_L$-$C_L$ [152]. Based on SEED-Abs, Dietrich *et al.* recently showed that the replacement of $C_L$ and $C_{H1}$ with $C_{H3}$ domains can also result in

correct LC-HC association [153]. Alternatively, light chains can be used that show promiscuous binding behavior and can act as common light chains (cLCs) shared between heavy chains. CLCs can be generated by utilizing screening technologies with restricted light chain repertoires [154, 155] or by testing HC/LC combinations for retained antigen binding [156]. Emicizumab, a cLC bsAb, was approved by the FDA in 2017 [157]. Ideally, the combination of Fc-heterodimerization and guided light chain association can result in yields of up to 100% of correctly assembled bsAbs.

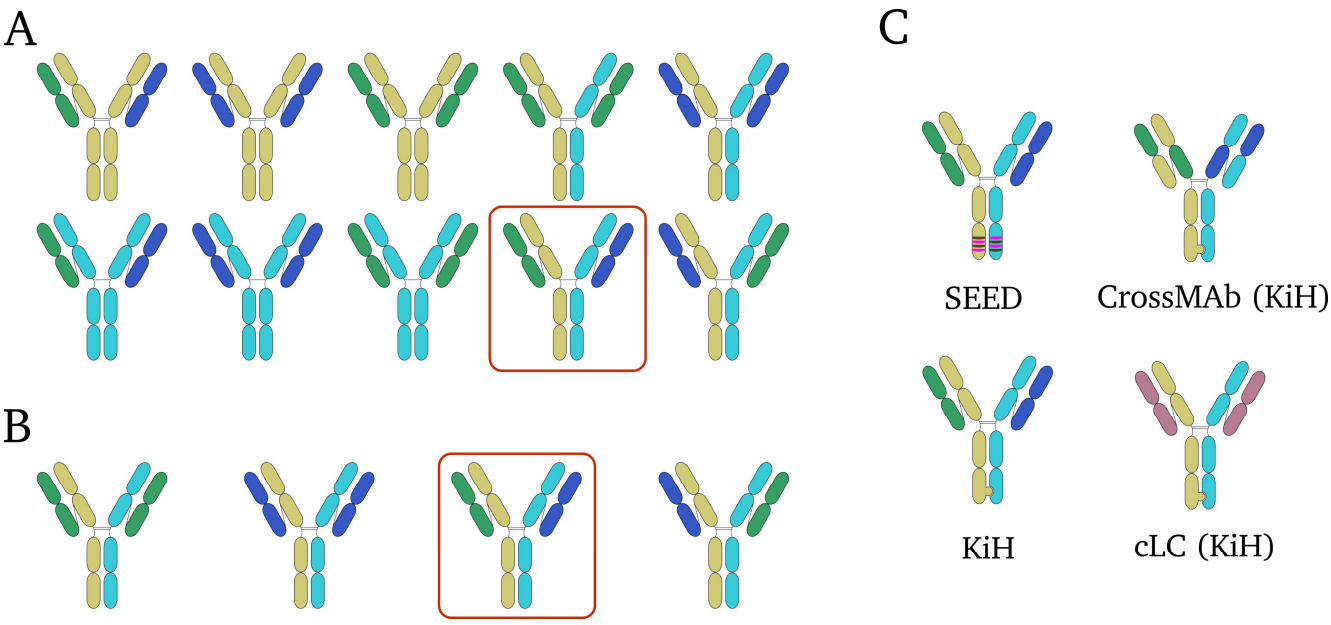


**Figure 4.** **Possible products during production of bispecific antibodies without heterodimerization techniques and schematic depiction thereof. (A)** Representation of all possible products during bsAb manufacturing without guided LC/HC pairing, the correctly assembled antibody is highlighted in red. **(B)** Possible products during bsAb manufacturing with implemented heavy chain heterodimerization methods. The correctly assembled antibody is highlighted in red. **(C)** Depiction of two different heterodimerization strategies for HC assembly (SEED + KiH) as well as two approaches to circumvent LC mispairing (CrossMAb + cLC).

## 1.4 Antibody discovery

Generating monoclonal antibodies started as a labor-intensive and time-consuming process. Upon immunization, the host's immune system generated antigen-specific antibody-secreting B-cells that were isolated from the animal's spleen after sacrifice. The isolated B-cells are subsequently utilized to generate hybridoma cells, with each hybridoma cell producing a single antibody species. Single hybridoma cells are isolated by dilution, and secreted antibodies are subsequently screened for antigen binding. Positive clones can be sequenced and used for antibody production [84, 158]. A negative characteristic is the tedious and cumbersome screening procedure with very low throughput.

Alternatively, screening technologies for monoclonal antibodies have emerged which utilize extracted B-cell mRNA, which is used to amplify $V_L$ and $V_H$ genes and convert them into cDNA [159]. This cDNA can be used in multiple screening setups, which will be discussed in the following paragraph.

The first high throughput screening technology was developed by McCafferty and coworkers in 1990. This *phage display* technology is based on the genetic fusion of $V_L$ and $V_H$ fragments as scFv to a phage coat protein on the surface of filamentous bacteriophages [160]. Phage display libraries are extended by infecting *Escherichia coli* cells and soluble phages are applied to a matrix with immobilized antigen. By washing the matrix, unbound phages are eliminated and binding phages can be eluted separately. Since the DNA of the displayed antibody fragment is wrapped in the very same phage, which displays it, the so-called genotype-phenotype coupling allows obtaining the antibody sequence of the bound antibody. Already in 1991, the repertoire of phage display was extended by Fab molecules by simultaneous expression of coat protein-fused HC and periplasmic expressed LC [161]. Although very powerful, the display of sophisticated proteins like antibodies or antibody fragments remains challenging in a bacterial expression set-up [162]. Alternative approaches have been developed in the past decades, including cell-free display systems such as ribosomal [163], mRNA [164] and DNA display [165], as well as cell-based display systems utilizing different host cells of insect [166], bacteria [167], mammalian [168] and yeast cells [169]. In general, cell-free display systems allow the utilization of larger library sizes compared to cell-based display systems. They therefore enable the screening of antibody diversities up to $1 \times 10^{14}$ [170], but only cell-based systems allow for a convenient ultra-high throughput real-time analysis [171]. Even though phage display remains a key technology up to this date for antibody discovery, yeast display was able to establish itself as a strong competitor allowing the isolation of antibodies with femtomolar affinities [172]. In contrast to prokaryote-based display systems, yeast cells comprise advantageous properties with regards to providing rudimentary glycosylation of displayed proteins [173, 174] as well as comprising post-translational modifications that allow for correct protein folding and disulfide bridge formation [170].

When it comes to targeting difficult-to-address antigens, alternative binding scaffolds have been examined. This includes antibodies derived from bovines, which comprise extremely elongated CDR3 loops in the VH domain of up to 70 amino acids providing unique antigen-binding surfaces [175, 176]. In contrast to conventional antibodies, camelids possess additional antibody isotypes devoid of light chains. The antigen-binding domain of these heavy chain-only antibodies are called VHH domains and comprise excellent production properties in bacterial expression setups and excel with their small size [177, 178]. Heavy chain-only antibodies have also been found in cartilaginous fish. With approx. 12 kDa, the variable domain of this antibody isotype – the so-called *variable new antigen receptor* (vNAR) - is the smallest known binding domain in the animal kingdom. The structural basis for the small size is the deletion of the CDR2 loop. However, a highly diverse and elongated CDR3 can compensate for the missing CDR loop since the non-planar binding surface allows for the binding of cryptic epitopes [179-181].

### 1.4.1 Antibody discovery with yeast display

Yeast display utilizes the surface-exposed protein Aga2p, which is covalently linked by two disulfide bonds to the GPI-anchored Aga1p on the cell wall (Figure 5). The Aga1p-Aga2p heterodimer is a naturally occurring

protein of *Saccharomyces cerevisiae* and it is involved in mating events and also referred to as a-agglutinin [182]. In *yeast display* (also known as *yeast surface display*; YSD), the peptide or protein which should be presented on the cell surface is genetically fused to either the *N*- or *C*-terminus of Aga2p as demonstrated by Boder and Wittrup [169, 170]. In this setup, Aga1p is encoded in the yeast genome, while Aga2p is encoded by the respective gene on a plasmid. This enables the fast and easy fusion of genes 5' and 3' of AGA2P by commonly used cloning methods like homologous recombination or restriction cloning. Both AGA1P and AGA2P are controlled by an inducible GAL1 promoter enabling the expression of both proteins upon galactose supplementation of the cultivation medium. Upon induction of surface presentation, up to $1 \times 10^5$ Aga2p-fusion molecules are displayed on a single yeast cell [169]. To ensure genotype-phenotype coupling, a single copy *origin of replication* (ori) is utilized [183, 184].

Non-different to competing display methods, YSD allows for the *in vitro* selection of naïve, immune and synthetic antibody repertoires [185]. In order to achieve very large libraries, Benatuil and coworkers developed a scalable transformation protocol for the generation of libraries easily surpassing $1 \times 10^9$ transformants [186].

Additional epitope tags flanking the *protein of interest* (POI) are implemented to verify surface presentation by immunofluorescent staining. Especially C-terminal tags help to identify non-frameshifted full-length variants acting as a quality control. The same methods apply for the verification of antigen-binding by the displayed antibody-fragment. Convenient staining strategies detect tags on the antigen used for antigen purification, such as His-tag and Strep-tag [173, 187, 188]. Alternatively, the antigen can be modified *in vitro* by conjugation with agents like NHS-Biotin conjugates, enabling the detection with fluorophore-streptavidin conjugates. Also, the direct conjugation of the antigen with a fluorophore is a valid strategy. After the staining process, the yeast cells exhibit a certain fluorescence signal depending on the bound fluorophores. This can be detected by flow cytometry and utilized for cell sorting by *fluorescence-activated cell sorting* (FACS). During cell sorting, cells with positive fluorescence signals for antigen binding and surface display are collected and submitted for cell expansion before subsequent sorting rounds. After approx. 3-5 sorting rounds, the cell population is utilized for plasmid rescue and the antibody genes can be reformatted for expression [189, 190].

New staining strategies can be utilized not only for the isolation of highly affine antibodies but also to identify variants with increased thermal stability, switchable binding behavior, and the expression profile [191]. Recently, 2A peptides have been introduced into YSD. 2A peptides can be used to entangle the expression of two proteins [192]. To this end, the 2A peptide gene is genetically fused in between the two protein genes. Upon translation of the mRNA, the formation of the 2A peptide leads to the termination of the polypeptide chain without stopping the ribosome from translating the second gene [193, 194]. This mechanism was implemented in order to substitute for surface display immunostaining by entangling Aga2p-POI and eGFP expression [195, 196] and also for enabling simultaneous surface presentation and secretion of soluble protein by utilizing an inefficiently cleaving 2A peptide [197].

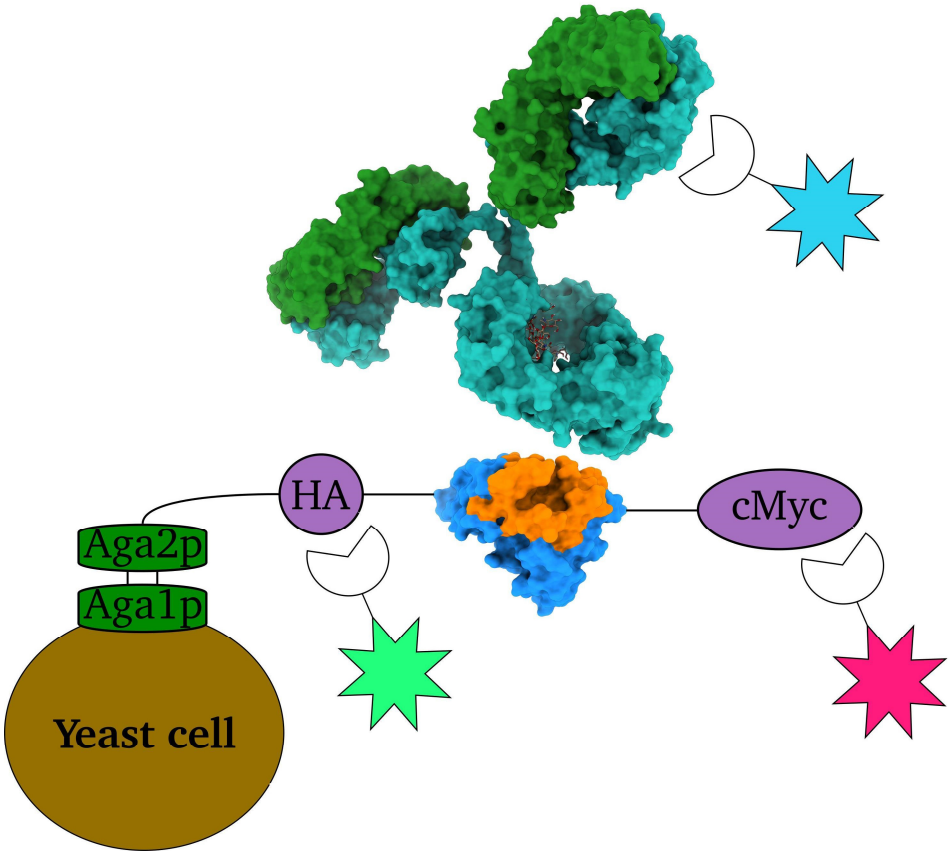


**Figure 5.** **Schematic depiction of yeast surface display.** The displaying yeast cell is depicted as a brown circle with the GPI-anchored Aga1p-Aga2p protein (green) on the cell wall. The scFv molecule (PDB: 4p48) is depicted in blue with the CDRs shown in orange. Bound antibody is shown in blue (HCs) and green (LCs) with glycosylation shown as balls and sticks (PDB: 1igt). Tags for verification of surface presentation are highlighted in violet. Labeling agents are shown as incomplete circles with attached stars that resemble the fluorophores (green, pink, blue).

### 1.4.2 Generation of responsive antibodies

As already mentioned in the context of sweeping/recycling antibodies, antibody engineering focuses not only on the generation of high affinity antibodies but rather on a plethora of different properties, enabling tailor-made antibodies with custom characteristics. YSD has been utilized to develop antibodies that can be switched from antigen-binding to antigen-nonbinding by external factors such as temperature, pH, and supplementation of chemicals [129, 195, 198]. Therapeutic applications can benefit from binding-finetuning since pH values differ across tissues. The tumor microenvironment is a good example, with potential pH values reported being as low as pH 5.9 [199, 200]. This enables to target antigens specifically within certain tissues conveying regiospecificity. As already mentioned in the context of recycling and sweeping antibodies, pH-switches allow new modes of action for antigen depletion to avoid antigen buffering [122]. The implementation of pH-switches can be achieved by multiple strategies, explained in the following paragraphs. A common theme for many of them is the focus on histidine residues, since histidine comprises an averaged pKa value of 6.6 (±1.0), which translates into a charge change upon slight acidification [201-203].

Positions that can be addressed by amino acid exchange to implement histidine residues can be identified by structure-guided approaches, in particular, if protein-protein interaction surfaces are known [204]. However, success is not guaranteed since small changes in proximity to the histidine side chain can influence the protonation state [205]. Combinatorial histidine scanning libraries utilize a more general approach to identify possible positions for implementing histidine residues, which does not rely on in-depth knowledge of the protein-protein interaction surface [128]. Additionally, amino acid substitutions can also be implemented in the protein framework, which is not involved in antigen binding. Upon acidification, the histidine residues will mediate structural changes leading to interruption of protein-antigen binding [128, 201, 206]. Murtaugh *et al.* identified synergistic effects of histidine residues in close proximity emphasizing pH-responsive behavior, which was shown for the engineering of a pH-responsive RNase A binding VHH antibody fragment [202].

Alternative approaches utilize ultra-high throughput display technologies like phage or yeast display to identify pH-responsive antibodies in complex libraries with more than $1 \times 10^8$ different antibody variants [207, 208]. Since this methodology can also be used for semi-synthetic and synthetic antibody/antibody fragment libraries, a plethora of different screening methods can be applied in order to isolate pH-responsive proteins only limited by either the library diversity or the creativity of the experimenter. Usually, these screening approaches start with the enrichment of antigen-specific antibodies. This pool is subsequently subjected to negative sorting rounds, which differ from “regular” screening round by an additional wash step after incubation with the target protein. This wash step is performed at a pH value where the antibody should not encompass antigen binding. After this wash step, the immunofluorescent staining of epitope tags for surface presentation is continued. If the displayed antibody comprises pH-responsive binding behavior, the displaying-entity should only exhibit surface presentation but no antigen-binding [83, 204, 209]. To accelerate the isolation procedure, histidine-doped libraries have been created for phage display and yeast display, which comprise higher than average rates of histidines in randomized binding loops. This strategy was implemented in the screening process of scFvs and alternative binding scaffolds such as vNARs (*variable new antigen receptor*) [207, 208]. Similar to the generation of pH-responsive binding behavior, antibodies have also been engineered from naïve and immune libraries to comprise calcium- and magnesium-responsive binding modalities by adjusting the screening methods accordingly [83, 130, 210-214]. Besides developing pH-switchable antibodies for therapeutic applications, these strategies can also be used to isolate affinity ligands for chromatographic applications, which will be further discussed in chapter 1.6.2.

## 1.5 Antibodies against human proteins

To prevent the formation of self-host reactive antibodies, developing B-cells undergo clonal selection in which self-host reactive receptors lead to inactivation of the B-cell [215, 216]. Genetic mutations can lead to an interruption of this sorting process, causing severe autoimmune diseases [217]. However, this phenomenon has

also to be considered during immunization campaigns since it will inhibit the generation of antibodies if the antigen comprises high homology to host-self proteins, which has been reported for mouse (*Mus musculus*) immunization [218-220]. Subsequent methods have been tested where the murine homolog protein was specifically knocked out to overcome immune tolerance. Furthermore, the utilization of immune-deficient mice has been reported to enable the generation of antibodies recognizing highly conserved antigens [221-223]. The fusion of highly conserved antigens with immune response enhancers such as peptides based on diphtheria and tetanus toxins did show positive results in mice and allowed subsequent target-specific antibody isolation [224].

An example of orthogonal approaches is the immunization of chickens (*Gallus gallus domesticus*) to generate antibodies against highly conserved epitopes on proteins in mammalians. A major consideration of utilizing chicken for immunization is the phylogenetic distance between mammals and chickens, increasing the probability of raising antigen-specific antibodies against highly conserved mammalian proteins [225, 226]. Also, favorable characteristics like enhanced stability due to elevated cystine levels and elevated body temperature in avians are described in the literature [227, 228]. Additionally, advantageous is the easy isolation of $V_H$ and $V_L$ genes due to the genetic arrangement of the antibody genes enabling the isolation of the respective gene fragment by defined primer pairs [229, 230].

## 1.6 Production of antibodies

The commercial success of antibodies led to a demand for economical large-scale production. This need was not satisfied with initial hybridoma production setups due to the instability of the hybridoma cells [231]. Alternative cell lines for the production of monoclonal antibodies have been developed like HEK293, NS0, PER.C6 and CHO, each capable of producing antibodies in the range of $> 1\ g/L$ [232-236]. In 2014, 84% of all commercially available antibodies were produced in CHO cells [237]. This is caused by the fact that CHO cells enable easy cell line engineering, fast and versatile adaption to a wide range of cultivation conditions, high cell densities in combination with high productivity, and human-like post-translational modifications [238]. Even though non-mammalian cell system can be utilized for the production of antibodies such as plant [239], yeast [240], insect [241], and bacterial cells [242], the vast majority of production processes are still relying on mammalian cells for the production of antibodies due to post-translational modifications such as glycosylation [243, 244]. Besides choosing the correct cell lines for production, main considerations comprise the scale and setup of the cell culture during *upstream processing* (USP) and the purification strategy, usually referred to as *downstream processing* (DSP).

### 1.6.1 Upstream processing

After choosing a cell line for expression, the production process is tailor-made for every produced antibody. Critical parameters in cell culture are pH, temperature, seeding density, oxygen transfer rate, and glucose concentration, among others [245, 246]. Additionally, amino acid concentrations and supplemental chemicals

(e.g., dextran sulfate, copper, cysteine, ascorbic acid) are known for influencing the yields of active antibody species [245, 247-249]. All these variables can be tested in small scale format prior to upscaling in multititer plate formats with cell culture volumes of less than 1 mL [250, 251]. In the next stages, bioreactors with volumes of several liters to hundreds of liters are used to confirm and polish production conditions before inoculating production bioreactors, which can comprise several thousand liters of cell culture with optimized yields of up to 20 g/L [246, 252].

### 1.6.2 Downstream processing

After harvest, the antibody has to be extracted and purified from the cell culture supernatant, referred to as downstream processing (DSP). This is done by several chromatographic steps starting with affinity chromatography to reduce impurities and also sample volume [253, 254]. Multistep purification of antibodies is the major cost-driving factor during the whole production with up to 90% of total costs [255, 256] with Protein A affinity chromatography contributing 25% of total DSP costs [257]. Additional chromatographic steps such as ion-exchange chromatography are commonly applied to reduce host proteins (HCP), DNA and other impurities [258]. Early affinity chromatography resins for antibody purification utilized immobilized Protein A. Protein A is a protein produced by *Staphylococcus aureus* to evade degradation by the immune system by binding to a broad range of antibody isotypes and render them non-functional[259, 260].

Interestingly, Protein A does not only comprise affinity to its main binding site located in the junction of CH2 and CH3 but also to family 3 VH domains [261, 262]. In general, Protein A chromatography is performed by loading the antibody-containing solution onto a chromatography column. Impurities are removed by wash steps and the bound antibody is subsequently eluted by applying elution buffer. A shared characteristic for Protein A chromatography is the required pH shift during elution. Commonly used buffers such as glycine buffer or citrate buffer comprise pH values in the range of 2.8-3.5 for elution. However, strongly acidic elution conditions may lead to irreversible damage to the purified protein and, eventually, protein loss, which is further enhanced by low pH virus inactivation steps [263-267]. Besides protein aggregation, deamidation events, as well as succinimide formation with subsequent amino acid isomerization or even backbone cleavage can occur but depend strongly on the individual antibody amino acid sequence [268-270]. Virus inactivation can be achieved by alternative methods such as UV radiation, heat treatment or even membrane filters, omitting the need for harsh potential protein-damaging virus inactivation steps [271].

For more than three decades, engineering approaches enabled the improvement of Protein A to become more acid/base stable, show less leakage and allow for shorter contact times during purification [272-274]. This includes depletion of all domains of Protein A but antibody-binding domain B (also known as Z-domain), which shows superior stability against NaOH while simultaneously allowing higher ligand density and, therefore, higher binding column capacity [275]. The stability against NaOH is a very important factor in the context of resin

lifetime since NaOH is utilized to sanitize and clean the column material between runs [276-278]. But also, the suboptimal elution conditions have been addressed. Gülich *et al.* elongated loop regions of the Z-domain, which resulted in reversible pH-dependent unfolding and subsequent affinity loss against IgG, allowing purification at pH 4.5 with a recovery of 97% [279]. Structure-guided approaches, either in combination with histidine scanning phage libraries or without library-assisted screening methods, did result in the isolation of Protein A variants with superior elution conditions at pH 5.0 [280, 281]. Watanabe et al. were able to isolate Z-domain mutants enabling an efficient elution at pH 5.0 while retaining NaOH-resistance [282]. Alternatively, elution based on temperature-dependent Protein A derivatives has been described [198]. Upon the incorporation of a calcium-binding loop between two of the three Z-domain helices, a calcium-dependent Z-domain was generated that binds antibodies only while calcium ions are present [283, 284]. Subsequent elution can be achieved by utilizing an EDTA-containing solution at pH 5.5.

In addition to engineering scaffolds based on Protein A, scientists developed orthogonal purification platforms relying on either proteins with naturally occurring antibody affinity (Protein G/Protein L) or engineered semi-synthetic proteins (i.g. affimers). In comparison with Protein A, Protein G is also derived from *Staphylococcus aureus* and shows a slightly higher affinity against human IgG antibodies. However, the unique selling proposition of Protein G is the high affinity towards murine antibodies, which can be purified with ease, whereas Protein A exhibits only a low affinity to murine antibodies [285]. The higher affinity comes with the drawback of requiring even lower pH for elution, but protein engineering allowed the generation of pH-switchable Protein G variants that enable elution at pH 4.5 [286, 287].

Additionally, antibody-derived molecules such as VHHs have been engineered to comprise IgG-specificity and switchable binding characteristics. Upon camelid immunization, a plethora of variants has been isolated, enabling the purification of multiple antibody isotypes and formats [214, 288, 289]. Of these VHH variants, the variants specific for IgA-CH1 and IgG-CH3 (named *FcXL*) can be used for mild elution upon addition of either high concentrations of magnesium chloride of 2 M (IgA-CH1) or supplementation of the elution buffer with magnesium chloride (1 M) and propylene glycol (40%). Publications suggest the suitability of vNAR proteins to comprise pH-responsive binding behavior as well as the capability of recognizing antibodies isotypes and even idiotypes [188, 207, 290]. Shark-derived single domain antibodies (vNARs) are not yet commercially available for purification of antibodies.

Similar approaches have been made with non-immunoglobulin scaffolds. *Affitins* are based on Sso7D, a naturally occurring protein in hyperthermophilic crenarchaea, which binds DNA but can be engineered for altered specificity. Variants have been identified by YSD, which could be used for small-scale DSP experiments at an elution pH of 4.5 [201, 291]. In this work, chicken-derived antibody fragments and their suitability for DSP applications were examined.

## 2 Objective

The objective of this doctoral thesis was the development of responsive antibody scaffolds either for therapeutic application or for downstream processing applications utilizing yeast display. Additionally, improvements of the screening procedure should also be considered and implemented.

The first project presented in this work will focus on pH-responsive sweeping bispecific antibodies (bsAbs). To increase the manufacturability of correctly assembled bsAbs, heterodimerization strategies for the heavy chains, as well as the light chains can be implemented. The chosen parental molecule – a CEACAM5/CEACAM6 specific bsAb – utilizes the *knob-in-hole* (KiH) strategy for heavy chain- and the *common light chain* (cLC) technique for light chain heterodimerization. Assuming the targeted antigen is located on a solid tumor but also occures in the blood stream, antibody therapeutics can be intercepted by the soluble antigen and will not be able to make an impact at the tumor site – a phenomenon called *antibody buffering*. However, implementing a pH- or calcium-responsive binding element at the antibody will support antigen degradation, as shown by recent publications, usually referred to as antibody sweeping. This concept is based on the dissociation of the antibody-antigen-complex during lysosome formation. This is caused by changes in pH and calcium concentration after the complex was internalized into endothelial cells. The objective of this part of the thesis will be the implementation of a sweeping function into the mentioned parental common light chains, but it should only compromise pH-responsive binding for one of both antigens proven the engineerability of cLCs in general while retaining high affinity and stability.

The second investigation will focus on the generation of affinity ligands for affinity purification of human proteins. One of the best protein purification methods is affinity chromatography due to the very high specificity between protein-of-interest and the ligand, often omitting the need for several chromatography steps. Especially in antibody purification, naturally occurring ligands such as Protein A and Protein G enable fast purification. But neither Protein A nor Protein G are free from drawbacks. Necessary harsh elution conditions can result in lower antibody yield due to protein degradation. Therefore, the generation of new affinity ligands with tailor-made elution conditions is an attractive alternative approach. However, the generation of an affinity ligand can be cumbersome and time-intensive. Therefore, we decided to generate affinity ligands based on chicken antibodies since immunization of chicken and subsequent library generation is cost-effective and easy to perform. Additionally, during affinity chromatography, mild elution conditions would be beneficial for proteins prone to aggregation, wherefore we also wanted to include pH-responsive behavior with non-binding at pH 5.0. The screening should be performed accordingly and the isolated variants should be expressed in a bacterial host, immobilized on a solid support, and then tested towards chromatographic characteristics.

An additional effort was put into setting up an improved version of yeast display. One of the advantages of yeast display is the online-monitoring of the sorting process possible due to immunofluorescent staining of epitope

tags. The staining has to be performed prior to the sorting and can include multiple steps according to the number of stained epitope tags. Since the library preparation requires time and consumes – sometimes expensive – staining agents, we aimed at simplifying the detection of surface presentation by entangling intracellular tGFP expression with surface presentation. To this end, we aimed at utilizing a ribosomal skipping sequence (also known as 2A peptide) genetically fused in between the genes of the protein of interest, which should be displayed and tGFP. Due to the properties of the 2A-peptide, two separate polypeptide chains are translated during translation. This is caused by the helix-like structure of the translated amino acid sequence favoring polypeptide chain formation termination without stopping the ribosome's translation process, which continues with translation until facing a stop codon. Upon generating the 2A-peptide construct for yeast display, a proof of concept sorting campaign should be performed against EpCAM and isolated variants should be compared to isolated variants derived from a classical library. This comparison would include thermal stability and binding kinetics.

In summary, the presented work aims at generating pH-responsive antibodies that can either be used in a therapeutic context, enhancing the efficacy of a bispecific antibody *in vivo* or for purification of antibodies with favorable elution conditions resulting in less protein loss due to degradation. Also, the screening procedure's efficacy should be improved by implementing a 2A-tGFP system omitting the need for immunofluorescent for surface presentation in yeast display.

## 3 References


1. Akira, S., S. Uematsu, and O. Takeuchi, *Pathogen Recognition and Innate Immunity.* Cell, 2006. **124**(4): p. 783-801.
2. Kumagai, Y. and S. Akira, *Identification and functions of pattern-recognition receptors.* J Allergy Clin Immunol, 2010. **125**(5): p. 985-92.
3. Aristizábal B. and G. Á., *Innate immune system*, in *Autoimmunity: From Bench to Bedside*, S.Y. Anaya JM., Rojas-Villarraga A., Levy RA., Cervera R., Editor. 2013, El Rosario University Press: Bogota (Colombia).
4. Hoffmann, J.A., *The immune response of Drosophila.* Nature, 2003. **426**(6962): p. 33-8.
5. Akira, S. and K. Takeda, *Toll-like receptor signalling.* Nat Rev Immunol, 2004. **4**(7): p. 499-511.
6. Beutler, B., *Inferences, questions and possibilities in Toll-like receptor signalling.* Nature, 2004. **430**(6996): p. 257-63.
7. Takeuchi, O. and S. Akira, *Pattern Recognition Receptors and Inflammation.* Cell, 2010. **140**(6): p. 805-820.
8. Stahl, P.D. and R.A.B. Ezekowitz, *The mannose receptor is a pattern recognition receptor involved in host defense.* Current Opinion in Immunology, 1998. **10**(1): p. 50-55.
9. Fraser, I.P., H. Koziel, and R.A. Ezekowitz, *The serum mannose-binding protein and the macrophage mannose receptor are pattern recognition molecules that link innate and adaptive immunity.* Semin Immunol, 1998. **10**(5): p. 363-72.
10. Medzhitov, R. and C. Janeway, Jr., *Innate immune recognition: mechanisms and pathways.* Immunol Rev, 2000. **173**: p. 89-97.
11. Iwasaki, A. and R. Medzhitov, *Control of adaptive immunity by the innate immune system.* Nat Immunol, 2015. **16**(4): p. 343-53.
12. Lanier, L.L., *NK cell recognition.* Annu Rev Immunol, 2005. **23**: p. 225-74.
13. Hato, T. and P.C. Dagher, *How the Innate Immune System Senses Trouble and Causes Trouble.* Clinical journal of the American Society of Nephrology : CJASN, 2015. **10**(8): p. 1459-1469.
14. Kennedy, M.A., *A Brief Review of the Basics of Immunology: The Innate and Adaptive Response.* Veterinary Clinics of North America: Small Animal Practice, 2010. **40**(3): p. 369-379.
15. Schatz, D.G., M.A. Oettinger, and M.S. Schlissel, *V(D)J recombination: molecular biology and regulation.* Annu Rev Immunol, 1992. **10**: p. 359-83.
16. Bonilla, F.A. and H.C. Oettgen, *Adaptive immunity.* Journal of Allergy and Clinical Immunology, 2010. **125**(2): p. S33-S40.
17. Tonegawa, S., *Somatic generation of antibody diversity.* Nature, 1983. **302**(5909): p. 575-581.
18. Schatz, D.G. and P.C. Swanson, *V(D)J Recombination: Mechanisms of Initiation.* Annual Review of Genetics, 2011. **45**(1): p. 167-202.
19. Schubert, D.A., et al., *Self-reactive human CD4 T cell clones form unusual immunological synapses.* J Exp Med, 2012. **209**(2): p. 335-52.
20. Ramsay, A.G., et al., *Chronic lymphocytic leukemia T cells show impaired immunological synapse formation that can be reversed with an immunomodulating drug.* J Clin Invest, 2008. **118**(7): p. 2427-37.
21. Hardy, R.R., et al., *B-cell commitment, development and selection.* Immunological Reviews, 2000. **175**(1): p. 23-32.
22. Hennecke, J. and D.C. Wiley, *T Cell Receptor-MHC Interactions up Close.* Cell, 2001. **104**(1): p. 1-4.
23. Scholer, A., et al., *Intercellular Adhesion Molecule-1-Dependent Stable Interactions between T Cells and Dendritic Cells Determine CD8+ T Cell Memory.* Immunity, 2008. **28**(2): p. 258-270.
24. Dustin, M.L., *The immunological synapse.* Cancer immunology research, 2014. **2**(11): p. 1023-1033.
25. Grakoui, A., et al., *The Immunological Synapse: A Molecular Machine Controlling T Cell Activation.* Science, 1999. **285**(5425): p. 221.
26. Dustin, M.L., *The cellular context of T cell signaling.* Immunity, 2009. **30**(4): p. 482-492.

27. Depoil, D., et al., *CD19 is essential for B cell activation by promoting B cell receptor–antigen microcluster formation in response to membrane-bound ligand.* Nature Immunology, 2008. **9**(1): p. 63-72.
28. Janeway, C.A., Jr., et al., *Immunobiology: The Immune System in Health and Disease.* 2001, New York: Garland Science.
29. Schroeder, H.W., Jr. and L. Cavacini, *Structure and function of immunoglobulins.* The Journal of allergy and clinical immunology, 2010. **125**(2 Suppl 2): p. S41-S52.
30. Alberts, B., et al., *Molecular Biology of the Cell*. 4th Edition ed. 2002, New York: Garland Science. 1616.
31. Dudley, D.D., et al., *Mechanism and Control of V(D)J Recombination versus Class Switch Recombination: Similarities and Differences*, in *Advances in Immunology*, F.W. Alt, Editor. 2005, Academic Press. p. 43-112.
32. Jung, D. and F.W. Alt, *Unraveling V(D)J recombination; insights into gene regulation.* Cell, 2004. **116**(2): p. 299-311.
33. Zachau, H., *Immunoglobulin genes.* Immunology today, 1989. **10**(8): p. S9-10.
34. Corbett, S.J., et al., *Sequence of the human immunoglobulin diversity (D) segment locus: a systematic analysis provides no evidence for the use of DIR segments, inverted D segments, "minor" D segments or D-D recombination.* J Mol Biol, 1997. **270**(4): p. 587-97.
35. Sleckman, B.P., et al., *Mechanisms that direct ordered assembly of T cell receptor beta locus V, D, and J gene segments.* Proc Natl Acad Sci U S A, 2000. **97**(14): p. 7975-80.
36. Honjo, T., *Immunoglobulin genes.* Annu Rev Immunol, 1983. **1**: p. 499-528.
37. Neuberger, M.S., *Antibody diversification by somatic mutation: from Burnet onwards.* Immunol Cell Biol, 2008. **86**(2): p. 124-32.
38. Dörner, T., et al., *Somatic hypermutation of human immunoglobulin heavy chain genes: targeting of RGYW motifs on both DNA strands.* Eur J Immunol, 1998. **28**(10): p. 3384-96.
39. Petersen-Mahrt, S.K., R.S. Harris, and M.S. Neuberger, *AID mutates E. coli suggesting a DNA deamination mechanism for antibody diversification.* Nature, 2002. **418**(6893): p. 99-103.
40. Chaudhuri, J. and F.W. Alt, *Class-switch recombination: interplay of transcription, DNA deamination and DNA repair.* Nat Rev Immunol, 2004. **4**(7): p. 541-52.
41. Lefranc, M.P., et al., *IMGT unique numbering for immunoglobulin and T cell receptor variable domains and Ig superfamily V-like domains.* Dev Comp Immunol, 2003. **27**(1): p. 55-77.
42. Hansel, T.T., et al., *The safety and side effects of monoclonal antibodies.* Nature Reviews Drug Discovery, 2010. **9**(4): p. 325-338.
43. Abbas, A., A. Lichtman, and S. Pillai, *Cellular and Molecular Immunology*. 5th Edition ed. 2014, Philadelphia: Saunders.
44. Mazor, Y., et al., *Enhancement of Immune Effector Functions by Modulating IgG's Intrinsic Affinity for Target Antigen.* PLOS ONE, 2016. **11**(6): p. e0157788.
45. Chen, K., et al., *Immunoglobulin D enhances immune surveillance by activating antimicrobial, proinflammatory and B cell-stimulating programs in basophils.* Nature immunology, 2009. **10**(8): p. 889-898.
46. Lutz, C., et al., *IgD can largely substitute for loss of IgM function in B cells.* Nature, 1998. **393**(6687): p. 797-801.
47. Fitzsimmons, C.M., F.H. Falcone, and D.W. Dunne, *Helminth Allergens, Parasite-Specific IgE, and Its Protective Role in Human Immunity.* Frontiers in immunology, 2014. **5**: p. 61-61.
48. Senger, K., et al., *Antibody Isotype Switching in Vertebrates.* Results Probl Cell Differ, 2015. **57**: p. 295-324.
49. Woof, J.M. and J. Mestecky, *Mucosal immunoglobulins.* Immunol Rev, 2005. **206**: p. 64-82.
50. Schur, P.H., *IgG subclasses. A historical perspective.* Monogr Allergy, 1988. **23**: p. 1-11.
51. Vidarsson, G., G. Dekkers, and T. Rispens, *IgG subclasses and allotypes: from structure to effector functions.* Frontiers in immunology, 2014. **5**: p. 520-520.
52. Bindon, C.I., et al., *Human monoclonal IgG isotypes differ in complement activating function at the level of C4 as well as C1q.* The Journal of experimental medicine, 1988. **168**(1): p. 127-142.

53. Tao, M.H., R.I. Smith, and S.L. Morrison, *Structural features of human immunoglobulin G that determine isotype-specific differences in complement activation.* J Exp Med, 1993. **178**(2): p. 661-7.
54. van Erp, E.A., et al., *Fc-Mediated Antibody Effector Functions During Respiratory Syncytial Virus Infection and Disease.* Frontiers in Immunology, 2019. **10**(548).
55. Srivastava, V., et al., *Identification of dominant antibody-dependent cell-mediated cytotoxicity epitopes on the hemagglutinin antigen of pandemic H1N1 influenza virus.* Journal of virology, 2013. **87**(10): p. 5831-5840.
56. Anderson, C.L., et al., *Perspective-- FcRn transports albumin: relevance to immunology and medicine.* Trends Immunol, 2006. **27**(7): p. 343-8.
57. Borvak, J., et al., *Functional expression of the MHC class I-related receptor, FcRn, in endothelial cells of mice.* Int Immunol, 1998. **10**(9): p. 1289-98.
58. Akilesh, S., et al., *Neonatal FcR expression in bone marrow-derived cells functions to protect serum IgG from catabolism.* J Immunol, 2007. **179**(7): p. 4580-8.
59. Booth, B.J., et al., *Extending human IgG half-life using structure-guided design.* mAbs, 2018. **10**(7): p. 1098-1110.
60. Junghans, R.P. and C.L. Anderson, *The protection receptor for IgG catabolism is the beta2-microglobulin-containing neonatal intestinal transport receptor.* Proc Natl Acad Sci U S A, 1996. **93**(11): p. 5512-6.
61. Yoshida, M., et al., *Human neonatal Fc receptor mediates transport of IgG into luminal secretions for delivery of antigens to mucosal dendritic cells.* Immunity, 2004. **20**(6): p. 769-83.
62. Claypool, S.M., et al., *Bidirectional transepithelial IgG transport by a strongly polarized basolateral membrane Fcgamma-receptor.* Mol Biol Cell, 2004. **15**(4): p. 1746-59.
63. Spiekermann, G.M., et al., *Receptor-mediated immunoglobulin G transport across mucosal barriers in adult life: functional expression of FcRn in the mammalian lung.* J Exp Med, 2002. **196**(3): p. 303-10.
64. Liu, H., G.G. Bulseco, and J. Sun, *Effect of posttranslational modifications on the thermal stability of a recombinant monoclonal antibody.* Immunol Lett, 2006. **106**(2): p. 144-53.
65. Arnold, J.N., et al., *The Impact of Glycosylation on the Biological Function and Structure of Human Immunoglobulins.* Annual Review of Immunology, 2007. **25**(1): p. 21-50.
66. Dorrington, K.J. and H.H. Bennich, *Structure-function relationships in human immunoglobulin E.* Immunological reviews, 1978. **41**(1): p. 3-25.
67. Sun, Z., et al., *Semi-extended solution structure of human myeloma immunoglobulin D determined by constrained X-ray scattering.* J Mol Biol, 2005. **353**(1): p. 155-73.
68. Gala, F.A. and S.L. Morrison, *The role of constant region carbohydrate in the assembly and secretion of human IgD and IgA1.* J Biol Chem, 2002. **277**(32): p. 29005-11.
69. Huggins, C. and C.V. Hodges, *Studies on prostatic cancer. I. The effect of castration, of estrogen and of androgen injection on serum phosphatases in metastatic carcinoma of the prostate. 1941.* J Urol, 2002. **167**(2 Pt 2): p. 948-51; discussion 952.
70. Goodman, L.S., M.M. Wintrobe, and et al., *Nitrogen mustard therapy; use of methyl-bis (beta-chloroethyl) amine hydrochloride and tris (beta-chloroethyl) amine hydrochloride for Hodgkin's disease, lymphosarcoma, leukemia and certain allied and miscellaneous disorders.* J Am Med Assoc, 1946. **132**: p. 126-32.
71. DeVita, V.T., Jr. and E. Chu, *A history of cancer chemotherapy.* Cancer Res, 2008. **68**(21): p. 8643-53.
72. Behring, E.v., *Ueber das zustandekommen der diphtherie-immunität und der tetanus-immunität bei thieren.* 1890.
73. Behring, E.v., *Untersuchungen ueber das Zustandekommen der Diphtherie-Immunität bei thieren.* 1890.
74. Kaufmann, S.H.E., *Remembering Emil von Behring: from Tetanus Treatment to Antibody Cooperation with Phagocytes.* mBio, 2017. **8**(1): p. e00117-17.
75. Zeiss, H. and R. Bieling, *Behring: Gestalt und Werk*. 1940: B. Schultz.
76. Scolnik, P.A., *mAbs: a business perspective.* mAbs, 2009. **1**(2): p. 179-184.
77. Reichert, J.M. *Antibody therapeutics approved or in regulatory review in the EU or US*. 2020 [cited 2020 09.06.2020]; Available from: https://www.antibodysociety.org/resources/approved-antibodies/.

78. Grilo, A.L. and A. Mantalaris, *The Increasingly Human and Profitable Monoclonal Antibody Market.* Trends Biotechnol, 2019. **37**(1): p. 9-16.
79. Kaplon, H. and J.M. Reichert, *Antibodies to watch in 2019.* mAbs, 2019. **11**(2): p. 219-238.
80. Burnette, W.N., *"Western blotting": electrophoretic transfer of proteins from sodium dodecyl sulfate--polyacrylamide gels to unmodified nitrocellulose and radiographic detection with antibody and radioiodinated protein A.* Anal Biochem, 1981. **112**(2): p. 195-203.
81. Engvall, E. and P. Perlmann, *Enzyme-linked immunosorbent assay (ELISA). Quantitative assay of immunoglobulin G.* Immunochemistry, 1971. **8**(9): p. 871-4.
82. Posthuma-Trumpie, G.A., J. Korf, and A. van Amerongen, *Lateral flow (immuno)assay: its strengths, weaknesses, opportunities and threats. A literature survey.* Anal Bioanal Chem, 2009. **393**(2): p. 569-82.
83. Hinz, S.C., et al., *A Generic Procedure for the Isolation of pH- and Magnesium-Responsive Chicken scFvs for Downstream Purification of Human Antibodies.* Frontiers in Bioengineering and Biotechnology, 2020. **8**(688).
84. Köhler, G. and C. Milstein, *Continuous cultures of fused cells secreting antibody of predefined specificity.* nature, 1975. **256**(5517): p. 495-497.
85. Emmons, C. and L.G. Hunsicker, *Muromonab-CD3 (Orthoclone OKT3): the first monoclonal antibody approved for therapeutic use.* Iowa Med, 1987. **77**(2): p. 78-82.
86. AbbVie. *AbbVie Reports Full-Year and Fourth-Quarter 2018 Financial Results*. 2019 08.06.2020]; Available from: https://news.abbvie.com/news/abbvie-reports-full-year-and-fourth-quarter-2018-financial-results.htm.
87. Sgro, C., *Side-effects of a monoclonal antibody, muromonab CD3/orthoclone OKT3: bibliographic review.* Toxicology, 1995. **105**(1): p. 23-9.
88. Harding, F.A., et al., *The immunogenicity of humanized and fully human antibodies: residual immunogenicity resides in the CDR regions.* mAbs, 2010. **2**(3): p. 256-265.
89. Lu, R.-M., et al., *Development of therapeutic antibodies for the treatment of diseases.* Journal of Biomedical Science, 2020. **27**(1): p. 1.
90. Tsurushita, N., P.R. Hinton, and S. Kumar, *Design of humanized antibodies: from anti-Tac to Zenapax.* Methods, 2005. **36**(1): p. 69-83.
91. Ibbotson, T., J.K. McGavin, and K.L. Goa, *Abciximab: an updated review of its therapeutic use in patients with ischaemic heart disease undergoing percutaneous coronary revascularisation.* Drugs, 2003. **63**(11): p. 1121-63.
92. Morrison, S.L., et al., *Chimeric human antibody molecules: mouse antigen-binding domains with human constant region domains.* Proc Natl Acad Sci U S A, 1984. **81**(21): p. 6851-5.
93. Maloney, D.G., et al., *IDEC-C2B8 (Rituximab) anti-CD20 monoclonal antibody therapy in patients with relapsed low-grade non-Hodgkin's lymphoma.* Blood, 1997. **90**(6): p. 2188-95.
94. Jones, P.T., et al., *Replacing the complementarity-determining regions in a human antibody with those from a mouse.* Nature, 1986. **321**(6069): p. 522-5.
95. Hakimi, J., et al., *Reduced immunogenicity and improved pharmacokinetics of humanized anti-Tac in cynomolgus monkeys.* The Journal of Immunology, 1991. **147**(4): p. 1352.
96. Schneider, W.P., et al., *The anti-idiotypic response by cynomolgus monkeys to humanized anti-Tac is primarily directed to complementarity-determining regions H1, H2, and L3.* The Journal of Immunology, 1993. **150**(7): p. 3086.
97. Lonberg, N., et al., *Antigen-specific human antibodies from mice comprising four distinct genetic modifications.* Nature, 1994. **368**(6474): p. 856-9.
98. Mendez, M.J., et al., *Functional transplant of megabase human immunoglobulin loci recapitulates human antibody response in mice.* Nat Genet, 1997. **15**(2): p. 146-56.
99. Murphy, A.J., et al., *Mice with megabase humanization of their immunoglobulin genes generate antibodies as efficiently as normal mice.* Proc Natl Acad Sci U S A, 2014. **111**(14): p. 5153-8.
100. Bartlett, B.L. and S.K. Tyring, *Ustekinumab for chronic plaque psoriasis.* Lancet, 2008. **371**(9625): p. 1639-40.

101. Church, L.D. and M.F. McDermott, *Canakinumab, a fully-human mAb against IL-1beta for the potential treatment of inflammatory disorders.* Curr Opin Mol Ther, 2009. **11**(1): p. 81-9.
102. Green, L.L., et al., *Antigen-specific human monoclonal antibodies from mice engineered with human Ig heavy and light chain YACs.* Nat Genet, 1994. **7**(1): p. 13-21.
103. Almagro, J.C., et al., *Progress and Challenges in the Design and Clinical Development of Antibodies for Cancer Therapy.* Frontiers in Immunology, 2018. **8**(1751).
104. Ulivieri, C., et al., *Generation of a monoclonal antibody to a defined portion of the Helicobacter pylori vacuolating cytotoxin by DNA immunization.* J Biotechnol, 1996. **51**(2): p. 191-4.
105. Zhang, C., et al., *Potent monoclonal antibodies against Clostridium difficile toxin A elicited by DNA immunization.* Hum Vaccin Immunother, 2013. **9**(10): p. 2157-64.
106. Ward, E.S., et al., *Binding activities of a repertoire of single immunoglobulin variable domains secreted from Escherichia coli.* Nature, 1989. **341**(6242): p. 544-546.
107. Jain, R.K., *Physiological barriers to delivery of monoclonal antibodies and other macromolecules in tumors.* Cancer Res, 1990. **50**(3 Suppl): p. 814s-819s.
108. Yokota, T., et al., *Rapid tumor penetration of a single-chain Fv and comparison with other immunoglobulin forms.* Cancer Res, 1992. **52**(12): p. 3402-8.
109. Umaña, P., et al., *Engineered glycoforms of an antineuroblastoma IgG1 with optimized antibody-dependent cellular cytotoxic activity.* Nature Biotechnology, 1999. **17**(2): p. 176-180.
110. Idusogie, E.E., et al., *Engineered antibodies with increased activity to recruit complement.* J Immunol, 2001. **166**(4): p. 2571-5.
111. Shields, R.L., et al., *High resolution mapping of the binding site on human IgG1 for Fc gamma RI, Fc gamma RII, Fc gamma RIII, and FcRn and design of IgG1 variants with improved binding to the Fc gamma R.* J Biol Chem, 2001. **276**(9): p. 6591-604.
112. Sanz, L., et al., *Antibody engineering: facing new challenges in cancer therapy.* Acta Pharmacol Sin, 2005. **26**(6): p. 641-8.
113. Xenaki, K.T., S. Oliveira, and P.M.P. van Bergen En Henegouwen, *Antibody or Antibody Fragments: Implications for Molecular Imaging and Targeted Therapy of Solid Tumors.* Frontiers in immunology, 2017. **8**: p. 1287-1287.
114. Schlapschy, M., et al., *PASylation: a biological alternative to PEGylation for extending the plasma half-life of pharmaceutically active proteins.* Protein Eng Des Sel, 2013. **26**(8): p. 489-501.
115. Schellenberger, V., et al., *A recombinant polypeptide extends the in vivo half-life of peptides and proteins in a tunable manner.* Nat Biotechnol, 2009. **27**(12): p. 1186-90.
116. Yurkovetskiy, A.V., et al., *A Polymer-Based Antibody-Vinca Drug Conjugate Platform: Characterization and Preclinical Efficacy.* Cancer Res, 2015. **75**(16): p. 3365-72.
117. Kommineni, N., et al., *Antibody drug conjugates: Development, characterization, and regulatory considerations.* Polymers for Advanced Technologies, 2020. **31**(6): p. 1177-1193.
118. Appelbaum, F.R. and I.D. Bernstein, *Gemtuzumab ozogamicin for acute myeloid leukemia.* Blood, 2017. **130**(22): p. 2373-2376.
119. Iagaru, A., et al., *131I-Tositumomab (Bexxar) vs. 90Y-Ibritumomab (Zevalin) therapy of low-grade refractory/relapsed non-Hodgkin lymphoma.* Mol Imaging Biol, 2010. **12**(2): p. 198-203.
120. Bachanova, V., et al., *Remission induction in a phase I/II study of an anti-CD20-interleukin-2 immunocytokine DI-Leu16-IL2 in patients with relapsed B-cell lymphoma*. 2015, American Society of Hematology Washington, DC.
121. Neri, D. and P.M. Sondel, *Immunocytokines for cancer treatment: past, present and future.* Current opinion in immunology, 2016. **40**: p. 96-102.
122. Byrd, J.C., et al., *Phase 1 study of lumiliximab with detailed pharmacokinetic and pharmacodynamic measurements in patients with relapsed or refractory chronic lymphocytic leukemia.* Clin Cancer Res, 2007. **13**(15 Pt 1): p. 4448-55.
123. Xiao, J.J., et al., *Pharmacokinetics of anti-hepcidin monoclonal antibody Ab 12B9m and hepcidin in cynomolgus monkeys.* Aaps j, 2010. **12**(4): p. 646-57.

124. Haringman, J.J., et al., *A randomized controlled trial with an anti-CCL2 (anti-monocyte chemotactic protein 1) monoclonal antibody in patients with rheumatoid arthritis.* Arthritis Rheum, 2006. **54**(8): p. 2387-92.
125. Igawa, T., et al., *Engineered monoclonal antibody with novel antigen-sweeping activity in vivo.* PLoS One, 2013. **8**(5): p. e63236.
126. Iwayanagi, Y., et al., *Inhibitory FcγRIIb-Mediated Soluble Antigen Clearance from Plasma by a pH-Dependent Antigen-Binding Antibody and Its Enhancement by Fc Engineering.* J Immunol, 2015. **195**(7): p. 3198-205.
127. Igawa, T., K. Haraya, and K. Hattori, *Sweeping antibody as a novel therapeutic antibody modality capable of eliminating soluble antigens from circulation.* Immunol Rev, 2016. **270**(1): p. 132-51.
128. Igawa, T., et al., *Antibody recycling by engineered pH-dependent antigen binding improves the duration of antigen neutralization.* Nature Biotechnology, 2010. **28**(11): p. 1203-1207.
129. Bogen, J.P., et al., *Dual Function pH Responsive Bispecific Antibodies for Tumor Targeting and Antigen Depletion in Plasma.* Front Immunol, 2019. **10**: p. 1892.
130. Hironiwa, N., et al., *Calcium-dependent antigen binding as a novel modality for antibody recycling by endosomal antigen dissociation.* mAbs, 2016. **8**(1): p. 65-73.
131. Ludwig, D.L., et al., *Monoclonal antibody therapeutics and apoptosis.* Oncogene, 2003. **22**(56): p. 9097-9106.
132. Suurs, F.V., et al., *A review of bispecific antibodies and antibody constructs in oncology and clinical challenges.* Pharmacol Ther, 2019. **201**: p. 103-119.
133. Baeuerle, P.A. and C. Reinhardt, *Bispecific T-cell engaging antibodies for cancer therapy.* Cancer Res, 2009. **69**(12): p. 4941-4.
134. Löffler, A., et al., *A recombinant bispecific single-chain antibody, CD19× CD3, induces rapid and high lymphoma-directed cytotoxicity by unstimulated T lymphocytes.* Blood, The Journal of the American Society of Hematology, 2000. **95**(6): p. 2098-2103.
135. Velasquez, M.P., C.L. Bonifant, and S. Gottschalk, *Redirecting T cells to hematological malignancies with bispecific antibodies.* Blood, The Journal of the American Society of Hematology, 2018. **131**(1): p. 30-38.
136. Yu, S., et al., *Recent advances of bispecific antibodies in solid tumors.* Journal of hematology & oncology, 2017. **10**(1): p. 155.
137. Bargou, R., et al., *Tumor regression in cancer patients by very low doses of a T cell–engaging antibody.* Science, 2008. **321**(5891): p. 974-977.
138. Fan, G., et al., *Bispecific antibodies and their applications.* J Hematol Oncol, 2015. **8**: p. 130.
139. Kontermann, R.E. and U. Brinkmann, *Bispecific antibodies.* Drug Discov Today, 2015. **20**(7): p. 838-47.
140. Lorenczewski, G., et al., *Generation of a half-life extended anti-CD19 BiTE® antibody construct compatible with once-weekly dosing for treatment of CD19-positive malignancies.* Blood, 2017. **130**(Supplement 1): p. 2815-2815.
141. Seimetz, D., H. Lindhofer, and C. Bokemeyer, *Development and approval of the trifunctional antibody catumaxomab (anti-EpCAM×anti-CD3) as a targeted cancer immunotherapy.* Cancer Treatment Reviews, 2010. **36**(6): p. 458-467.
142. Jain, M., N. Kamal, and S.K. Batra, *Engineering antibodies for clinical applications.* Trends in Biotechnology, 2007. **25**(7): p. 307-316.
143. Lindhofer, H., et al., *Preferential species-restricted heavy/light chain pairing in rat/mouse quadromas. Implications for a single-step purification of bispecific antibodies.* The Journal of Immunology, 1995. **155**(1): p. 219.
144. Ridgway, J.B., L.G. Presta, and P. Carter, *'Knobs-into-holes' engineering of antibody CH3 domains for heavy chain heterodimerization.* Protein Eng, 1996. **9**(7): p. 617-21.
145. Chen, T., et al., *Monitoring removal of hole-hole homodimer by analytical hydrophobic interaction chromatography in purifying a bispecific antibody.* Protein Expression and Purification, 2019. **164**: p. 105457.
146. Tustian, A.D., et al., *Development of purification processes for fully human bispecific antibodies based upon modification of protein A binding avidity.* mAbs, 2016. **8**(4): p. 828-838.

147. Davis, J.H., et al., *SEEDbodies: fusion proteins based on strand-exchange engineered domain (SEED) CH3 heterodimers in an Fc analogue platform for asymmetric binders or immunofusions and bispecific antibodies†.* Protein Engineering, Design and Selection, 2010. **23**(4): p. 195-202.
148. Muda, M., et al., *Therapeutic assessment of SEED: a new engineered antibody platform designed to generate mono- and bispecific antibodies.* Protein Eng Des Sel, 2011. **24**(5): p. 447-54.
149. Von Kreudenstein, T.S., et al. *Improving biophysical properties of a bispecific antibody scaffold to aid developability: quality by molecular design*. in *MAbs*. 2013. Taylor & Francis.
150. Gunasekaran, K., et al., *Enhancing antibody Fc heterodimer formation through electrostatic steering effects applications to bispecific molecules and monovalent IgG.* Journal of Biological Chemistry, 2010. **285**(25): p. 19637-19646.
151. Schaefer, W., et al., *Immunoglobulin domain crossover as a generic approach for the production of bispecific IgG antibodies.* Proceedings of the National Academy of Sciences, 2011. **108**(27): p. 11187.
152. Lewis, S.M., et al., *Generation of bispecific IgG antibodies by structure-based design of an orthogonal Fab interface.* Nature Biotechnology, 2014. **32**(2): p. 191-198.
153. Dietrich, S., et al., *Constant domain-exchanged Fab enables specific light chain pairing in heterodimeric bispecific SEED-antibodies.* Biochimica et Biophysica Acta (BBA) - Proteins and Proteomics, 2020. **1868**(1): p. 140250.
154. Merchant, A.M., et al., *An efficient route to human bispecific IgG.* Nat Biotechnol, 1998. **16**(7): p. 677-81.
155. Jackman, J., et al., *Development of a two-part strategy to identify a therapeutic human bispecific antibody that inhibits IgE receptor signaling.* J Biol Chem, 2010. **285**(27): p. 20850-9.
156. Smith, E.J., et al., *A novel, native-format bispecific antibody triggering T-cell killing of B-cells is robustly active in mouse tumor models and cynomolgus monkeys.* Sci Rep, 2015. **5**: p. 17943.
157. Blair, H.A., *Emicizumab: A Review in Haemophilia A.* Drugs, 2019. **79**(15): p. 1697-1707.
158. Li, F., A. Shen, and A. Amanullah, *Cell culture processes in monoclonal antibody production.* Pharmaceutical Sciences Encyclopedia: Drug Discovery, Development, and Manufacturing, 2010: p. 1-38.
159. Orlandi, R., et al., *Cloning immunoglobulin variable domains for expression by the polymerase chain reaction.* Proc Natl Acad Sci U S A, 1989. **86**(10): p. 3833-7.
160. McCafferty, J., et al., *Phage antibodies: filamentous phage displaying antibody variable domains.* Nature, 1990. **348**(6301): p. 552-4.
161. Hoogenboom, H.R., et al., *Multi-subunit proteins on the surface of filamentous phage: methodologies for displaying antibody (Fab) heavy and light chains.* Nucleic Acids Res, 1991. **19**(15): p. 4133-7.
162. Frenzel, A., T. Schirrmann, and M. Hust, *Phage display-derived human antibodies in clinical development and therapy.* mAbs, 2016. **8**(7): p. 1177-1194.
163. Hanes, J. and A. Plückthun, *In vitro selection and evolution of functional proteins by using ribosome display.* Proceedings of the National Academy of Sciences, 1997. **94**(10): p. 4937.
164. Nemoto, N., et al., *In vitro virus: bonding of mRNA bearing puromycin at the 3'-terminal end to the C-terminal end of its encoded protein on the ribosome in vitro.* FEBS Lett, 1997. **414**(2): p. 405-8.
165. Odegrip, R., et al., *CIS display: In vitro selection of peptides from libraries of protein-DNA complexes.* Proc Natl Acad Sci U S A, 2004. **101**(9): p. 2806-10.
166. Ernst, W., et al., *Baculovirus surface display: Construction and screening of a eukaryotic epitope library.* Nucleic Acids Research, 1998. **26**(7): p. 1718-1723.
167. Freudl, R., et al., *Cell surface exposure of the outer membrane protein OmpA of Escherichia coli K-12.* Journal of Molecular Biology, 1986. **188**(3): p. 491-494.
168. Beerli, R.R., et al., *Isolation of human monoclonal antibodies by mammalian cell display.* Proc Natl Acad Sci U S A, 2008. **105**(38): p. 14336-41.
169. Boder, E.T. and K.D. Wittrup, *Yeast surface display for screening combinatorial polypeptide libraries.* Nat Biotechnol, 1997. **15**(6): p. 553-7.
170. Cherf, G.M. and J.R. Cochran, *Applications of Yeast Surface Display for Protein Engineering.* Methods Mol Biol, 2015. **1319**: p. 155-75.

171. Doerner, A., et al., *Therapeutic antibody engineering by high efficiency cell screening.* FEBS Lett, 2014. **588**(2): p. 278-87.
172. Boder, E.T., K.S. Midelfort, and K.D. Wittrup, *Directed evolution of antibody fragments with monovalent femtomolar antigen-binding affinity.* Proc Natl Acad Sci U S A, 2000. **97**(20): p. 10701-5.
173. Mei, M., et al., *Prompting Fab Yeast Surface Display Efficiency by ER Retention and Molecular Chaperon Co-expression.* Frontiers in Bioengineering and Biotechnology, 2019. **7**(362).
174. Gerngross, T.U., *Advances in the production of human therapeutic proteins in yeasts and filamentous fungi.* Nat Biotechnol, 2004. **22**(11): p. 1409-14.
175. Haakenson, J.K., R. Huang, and V.V. Smider, *Diversity in the Cow Ultralong CDR H3 Antibody Repertoire.* Frontiers in immunology, 2018. **9**: p. 1262-1262.
176. Stanfield, R.L., et al., *The Unusual Genetics and Biochemistry of Bovine Immunoglobulins.* Advances in immunology, 2018. **137**: p. 135-164.
177. Muyldermans, S., *Single domain camel antibodies: current status.* J Biotechnol, 2001. **74**(4): p. 277-302.
178. Veggiani, G. and A. de Marco, *Improved quantitative and qualitative production of single-domain intrabodies mediated by the co-expression of Erv1p sulfhydryl oxidase.* Protein Expr Purif, 2011. **79**(1): p. 111-4.
179. Stanfield, R.L., et al., *Crystal structure of a shark single-domain antibody V region in complex with lysozyme.* Science, 2004. **305**(5691): p. 1770-3.
180. Nuttall, S.D., et al., *A naturally occurring NAR variable domain binds the Kgp protease from Porphyromonas gingivalis.* FEBS Lett, 2002. **516**(1-3): p. 80-6.
181. Nuttall, S.D., et al., *Isolation of the new antigen receptor from wobbegong sharks, and use as a scaffold for the display of protein loop libraries.* Mol Immunol, 2001. **38**(4): p. 313-26.
182. Wojciechowicz, D., et al., *Cell surface anchorage and ligand-binding domains of the Saccharomyces cerevisiae cell adhesion protein alpha-agglutinin, a member of the immunoglobulin superfamily.* Mol Cell Biol, 1993. **13**(4): p. 2554-63.
183. Ghosh, S.K., S. Hajra, and M. Jayaram, *Faithful segregation of the multicopy yeast plasmid through cohesin-mediated recognition of sisters.* Proc Natl Acad Sci U S A, 2007. **104**(32): p. 13034-9.
184. Liu, Y.T., C.H. Ma, and M. Jayaram, *Co-segregation of yeast plasmid sisters under monopolin-directed mitosis suggests association of plasmid sisters with sister chromatids.* Nucleic Acids Res, 2013. **41**(7): p. 4144-58.
185. Hoogenboom, H.R., *Selecting and screening recombinant antibody libraries.* Nature Biotechnology, 2005. **23**(9): p. 1105-1116.
186. Benatuil, L., et al., *An improved yeast transformation method for the generation of very large human antibody libraries.* Protein Eng Des Sel, 2010. **23**(4): p. 155-9.
187. Rosowski, S., et al., *A novel one-step approach for the construction of yeast surface display Fab antibody libraries.* Microbial Cell Factories, 2018. **17**(1): p. 3.
188. Könning, D., et al., *Semi-synthetic vNAR libraries screened against therapeutic antibodies primarily deliver anti-idiotypic binders.* Scientific Reports, 2017. **7**(1): p. 9676.
189. Boder, E.T., M. Raeeszadeh-Sarmazdeh, and J.V. Price, *Engineering antibodies by yeast display.* Arch Biochem Biophys, 2012. **526**(2): p. 99-106.
190. Chao, G., et al., *Isolating and engineering human antibodies using yeast surface display.* Nature Protocols, 2006. **1**(2): p. 755-768.
191. Shusta, E.V., et al., *Yeast polypeptide fusion surface display levels predict thermal stability and soluble secretion efficiency.* J Mol Biol, 1999. **292**(5): p. 949-56.
192. Chng, J., et al., *Cleavage efficient 2A peptides for high level monoclonal antibody expression in CHO cells.* mAbs, 2015. **7**(2): p. 403-412.
193. de Felipe, P., et al., *Inhibition of 2A-mediated 'cleavage' of certain artificial polyproteins bearing N-terminal signal sequences.* Biotechnol J, 2010. **5**(2): p. 213-23.
194. Donnelly, M.L.L., et al., *Analysis of the aphthovirus 2A/2B polyprotein 'cleavage' mechanism indicates not a proteolytic reaction, but a novel translational effect: a putative ribosomal 'skip'.* J Gen Virol, 2001. **82**(Pt 5): p. 1013-1025.

195. Hinz, S.C., et al., *Simplifying the Detection of Surface Presentation Levels in Yeast Surface Display by Intracellular tGFP Expression.* Methods Mol Biol, 2020. **2070**: p. 211-222.
196. Grzeschik, J., et al., *A simplified procedure for antibody engineering by yeast surface display: Coupling display levels and target binding by ribosomal skipping.* Biotechnol J, 2017. **12**(2).
197. Cruz-Teran, C.A., et al., *Inefficient Ribosomal Skipping Enables Simultaneous Secretion and Display of Proteins in Saccharomyces cerevisiae.* ACS Synth Biol, 2017. **6**(11): p. 2096-2107.
198. Koguma, I., et al., *Novel purification method of human immunoglobulin by using a thermo-responsive protein A.* J Chromatogr A, 2013. **1305**: p. 149-53.
199. Wike-Hooley, J.L., J. Haveman, and H.S. Reinhold, *The relevance of tumour pH to the treatment of malignant disease.* Radiother Oncol, 1984. **2**(4): p. 343-66.
200. Sulea, T., et al., *Structure-based engineering of pH-dependent antibody binding for selective targeting of solid-tumor microenvironment.* mAbs, 2020. **12**(1): p. 1682866-1682866.
201. Gera, N., et al., *Design of pH sensitive binding proteins from the hyperthermophilic Sso7d scaffold.* PLoS One, 2012. **7**(11): p. e48928.
202. Murtaugh, M.L., et al., *A combinatorial histidine scanning library approach to engineer highly pH-dependent protein switches.* Protein Sci, 2011. **20**(9): p. 1619-31.
203. Pace, C.N., G.R. Grimsley, and J.M. Scholtz, *Protein ionizable groups: pK values and their contribution to protein stability and solubility.* J Biol Chem, 2009. **284**(20): p. 13285-9.
204. Schröter, C., et al., *A generic approach to engineer antibody pH-switches using combinatorial histidine scanning libraries and yeast display.* mAbs, 2015. **7**(1): p. 138-151.
205. Sampogna, R.V. and B. Honig, *Environmental effects on the protonation states of active site residues in bacteriorhodopsin.* Biophys J, 1994. **66**(5): p. 1341-52.
206. Boyken, S.E., et al., *De novo design of tunable, pH-driven conformational changes.* Science, 2019. **364**(6441): p. 658.
207. Könning, D., et al., *Isolation of a pH-sensitive IgNAR variable domain from a yeast-displayed, histidine-doped master library.* Mar Biotechnol (NY), 2016. **18**(2): p. 161-7.
208. Bonvin, P., et al., *De novo isolation of antibodies with pH-dependent binding properties.* mAbs, 2015. **7**(2): p. 294-302.
209. Traxlmayr, M.W., et al., *Construction of pH-sensitive Her2-binding IgG1-Fc by directed evolution.* Biotechnol J, 2014. **9**(8): p. 1013-22.
210. Slootstra, J.W., et al., *Structural aspects of antibody-antigen interaction revealed through small random peptide libraries.* Molecular diversity, 1996. **1**(2): p. 87-96.
211. Ohlin, A.K. and J. Stenflo, *Calcium-dependent interaction between the epidermal growth factor precursor-like region of human protein C and a monoclonal antibody.* J Biol Chem, 1987. **262**(28): p. 13798-804.
212. Dixit, V.M., et al., *Monoclonal antibodies that recognize calcium-dependent structures of human thrombospondin. Characterization and mapping of their epitopes.* J Biol Chem, 1986. **261**(4): p. 1962-8.
213. Eifler, N., et al., *Development of a novel affinity chromatography resin for platform purification of lambda fabs.* Biotechnol Prog, 2014. **30**(6): p. 1311-8.
214. Hermans, P., H. Adams, and F. Detmers, *Purification of antibodies and antibody fragments using CaptureSelect affinity resins.* Methods Mol Biol, 2014. **1131**: p. 297-314.
215. Gonzalez, S., et al., *Conceptual aspects of self and nonself discrimination.* Self/nonself, 2011. **2**(1): p. 19-25.
216. Reth, M., J. Wienands, and W.W. Schamel, *An unsolved problem of the clonal selection theory and the model of an oligomeric B-cell antigen receptor.* Immunol Rev, 2000. **176**: p. 10-8.
217. Hofmann, K., A.-K. Clauder, and R.A. Manz, *Targeting B Cells and Plasma Cells in Autoimmune Diseases.* Frontiers in immunology, 2018. **9**: p. 835-835.
218. Sinclair, N.R., *B cell/antibody tolerance to our own antigens.* Front Biosci, 2004. **9**: p. 3019-28.
219. Hrabovska, A., V. Bernard, and E. Krejci, *A novel system for the efficient generation of antibodies following immunization of unique knockout mouse strains.* PLoS One, 2010. **5**(9): p. e12892.
220. Andrievskaia, O., et al., *Generation of antibodies against bovine recombinant prion protein in various strains of mice.* Clin Vaccine Immunol, 2006. **13**(1): p. 98-105.

221. Zhou, H., et al., *Generation of monoclonal antibodies against highly conserved antigens.* PloS one, 2009. **4**(6): p. e6087-e6087.
222. Fisher, C.L., R.A. Eisenberg, and P.L. Cohen, *Quantitation and IgG subclass distribution of antichromatin autoantibodies in SLE mice.* Clin Immunol Immunopathol, 1988. **46**(2): p. 205-13.
223. Bell, D.A., et al., *Anti DNA antibody production by lymphoid cells of NZB-W mice and human systemic lupus erythematosus (SLE).* Clin Immunol Immunopathol, 1973. **1**(3): p. 293-303.
224. Percival-Alwyn, J.L., et al., *Generation of potent mouse monoclonal antibodies to self-proteins using T-cell epitope "tags".* mAbs, 2015. **7**(1): p. 129-137.
225. Davies, E.L., et al., *Selection of specific phage-display antibodies using libraries derived from chicken immunoglobulin genes.* J Immunol Methods, 1995. **186**(1): p. 125-35.
226. Kasahara, M. and Y. Sutoh, *Chapter Two - Two Forms of Adaptive Immunity in Vertebrates: Similarities and Differences*, in *Advances in Immunology*, F.W. Alt, Editor. 2014, Academic Press. p. 59-90.
227. Prinzinger, R., A. Preßmar, and E. Schleucher, *Body temperature in birds.* Comparative Biochemistry and Physiology Part A: Physiology, 1991. **99**(4): p. 499-506.
228. Wu, L., et al., *Fundamental characteristics of the immunoglobulin VH repertoire of chickens in comparison with those of humans, mice, and camelids.* J Immunol, 2012. **188**(1): p. 322-33.
229. McCormack, W.T., L.W. Tjoelker, and C.B. Thompson, *Immunoglobulin gene diversification by gene conversion.* Prog Nucleic Acid Res Mol Biol, 1993. **45**: p. 27-45.
230. Thompson, C.B. and P.E. Neiman, *Somatic diversification of the chicken immunoglobulin light chain gene is limited to the rearranged variable gene segment.* Cell, 1987. **48**(3): p. 369-78.
231. Kunert, R. and D. Reinhart, *Advances in recombinant antibody manufacturing.* Applied microbiology and biotechnology, 2016. **100**(8): p. 3451-3461.
232. Dumont, J., et al., *Human cell lines for biopharmaceutical manufacturing: history, status, and future perspectives.* Critical reviews in biotechnology, 2016. **36**(6): p. 1110-1122.
233. Ho, Y., et al., *Computational approach for understanding and improving GS-NS0 antibody production under hyperosmotic conditions.* J Biosci Bioeng, 2012. **113**(1): p. 88-98.
234. Nallet, S., et al., *Glycan variability on a recombinant IgG antibody transiently produced in HEK-293E cells.* N Biotechnol, 2012. **29**(4): p. 471-6.
235. Kuczewski, M., et al., *A single-use purification process for the production of a monoclonal antibody produced in a PER.C6 human cell line.* Biotechnol J, 2011. **6**(1): p. 56-65.
236. Reinhart, D., et al., *Benchmarking of commercially available CHO cell culture media for antibody production.* Applied microbiology and biotechnology, 2015. **99**(11): p. 4645-4657.
237. Walsh, G., *Biopharmaceutical benchmarks 2018.* Nat Biotechnol, 2018. **36**(12): p. 1136-1145.
238. Jayapal, K.P., et al., *Recombinant protein therapeutics from CHO cells-20 years and counting.* Chemical engineering progress, 2007. **103**(10): p. 40.
239. Diamos, A.G., et al., *High Level Production of Monoclonal Antibodies Using an Optimized Plant Expression System.* Frontiers in Bioengineering and Biotechnology, 2020. **7**(472).
240. Kuroda, K., et al., *Efficient Antibody Production upon Suppression of O Mannosylation in the Yeast Ogataea minuta.* Applied and Environmental Microbiology, 2008. **74**(2): p. 446.
241. Yamaji, H., *Production of Antibody in Insect Cells*, in *Antibody Expression and Production*, M. Al-Rubeai, Editor. 2011, Springer Netherlands: Dordrecht. p. 53-76.
242. Jalalirad, R., *Production of antibody fragment (Fab) throughout Escherichia coli fed-batch fermentation process: Changes in titre, location and form of product.* Electronic Journal of Biotechnology, 2013. **16**(3): p. 9-9.
243. Ghaderi, D., et al., *Production platforms for biotherapeutic glycoproteins. Occurrence, impact, and challenges of non-human sialylation.* Biotechnology and Genetic Engineering Reviews, 2012. **28**(1): p. 147-176.
244. Durocher, Y. and M. Butler, *Expression systems for therapeutic glycoprotein production.* Curr Opin Biotechnol, 2009. **20**(6): p. 700-7.
245. Chung, S., et al., *Industrial bioprocessing perspectives on managing therapeutic protein charge variant profiles.* Biotechnol Bioeng, 2018. **115**(7): p. 1646-1665.

246. Gronemeyer, P., R. Ditz, and J. Strube, *Trends in Upstream and Downstream Process Development for Antibody Manufacturing.* Bioengineering (Basel), 2014. **1**(4): p. 188-212.
247. Hyoung Park, J., et al., *The molecular weight and concentration of dextran sulfate affect cell growth and antibody production in CHO cell cultures.* Biotechnol Prog, 2016. **32**(5): p. 1113-1122.
248. Hazeltine, L.B., et al., *Chemically defined media modifications to lower tryptophan oxidation of biopharmaceuticals.* Biotechnol Prog, 2016. **32**(1): p. 178-88.
249. Trexler-Schmidt, M., et al., *Identification and prevention of antibody disulfide bond reduction during cell culture manufacturing.* Biotechnol Bioeng, 2010. **106**(3): p. 452-61.
250. Fisher, A.C., et al., *The Current Scientific and Regulatory Landscape in Advancing Integrated Continuous Biopharmaceutical Manufacturing.* Trends Biotechnol, 2019. **37**(3): p. 253-267.
251. Long, Q., et al., *The development and application of high throughput cultivation technology in bioprocess development.* J Biotechnol, 2014. **192 Pt B**: p. 323-38.
252. Tripathi, N.K. and A. Shrivastava, *Recent Developments in Bioprocessing of Recombinant Proteins: Expression Hosts and Process Development.* Frontiers in bioengineering and biotechnology, 2019. **7**: p. 420-420.
253. Fahrner, R.L., et al., *Industrial purification of pharmaceutical antibodies: development, operation, and validation of chromatography processes.* Biotechnol Genet Eng Rev, 2001. **18**: p. 301-27.
254. Low, D., R. O'Leary, and N.S. Pujar, *Future of antibody purification.* J Chromatogr B Analyt Technol Biomed Life Sci, 2007. **848**(1): p. 48-63.
255. Straathof, A.J.J., *2.57 - The Proportion of Downstream Costs in Fermentative Production Processes*, in *Comprehensive Biotechnology (Second Edition)*, M. Moo-Young, Editor. 2011, Academic Press: Burlington. p. 811-814.
256. Farid, S.S., *Process economics of industrial monoclonal antibody manufacture.* J Chromatogr B Analyt Technol Biomed Life Sci, 2007. **848**(1): p. 8-18.
257. Costioli, M.D., et al., *Cost of goods modeling and quality by design for developing cost-effective processes.* BioPharm International, 2010. **23**: p. 26-35.
258. Singh, N., et al., *Clarification technologies for monoclonal antibody manufacturing processes: Current state and future perspectives.* Biotechnol Bioeng, 2016. **113**(4): p. 698-716.
259. Goudswaard, J., et al., *Protein A reactivity of various mammalian immunoglobulins.* Scand J Immunol, 1978. **8**(1): p. 21-8.
260. Pauli, N.T., et al., *Staphylococcus aureus infection induces protein A-mediated immune evasion in humans.* The Journal of experimental medicine, 2014. **211**(12): p. 2331-2339.
261. Graille, M., et al., *Crystal structure of a Staphylococcus aureus protein A domain complexed with the Fab fragment of a human IgM antibody: structural basis for recognition of B-cell receptors and superantigen activity.* Proc Natl Acad Sci U S A, 2000. **97**(10): p. 5399-404.
262. Moks, T., et al., *Staphylococcal protein A consists of five IgG-binding domains.* Eur J Biochem, 1986. **156**(3): p. 637-43.
263. Vázquez-Rey, M. and D.A. Lang, *Aggregates in monoclonal antibody manufacturing processes.* Biotechnology and Bioengineering, 2011. **108**(7): p. 1494-1508.
264. Jin, W., et al., *Protein aggregation and mitigation strategy in low pH viral inactivation for monoclonal antibody purification.* mAbs, 2019. **11**(8): p. 1479-1491.
265. Mazzer, A.R., et al., *Protein A chromatography increases monoclonal antibody aggregation rate during subsequent low pH virus inactivation hold.* J Chromatogr A, 2015. **1415**: p. 83-90.
266. Liu, B., et al., *Acid-induced aggregation propensity of nivolumab is dependent on the Fc.* MAbs, 2016. **8**(6): p. 1107-17.
267. Ejima, D., et al., *Effects of acid exposure on the conformation, stability, and aggregation of monoclonal antibodies.* Proteins, 2007. **66**(4): p. 954-62.
268. Lu, X., et al., *Deamidation and isomerization liability analysis of 131 clinical-stage antibodies.* MAbs, 2019. **11**(1): p. 45-57.
269. Linhult, M., S. Gulich, and S. Hober, *Affinity ligands for industrial protein purification.* Protein Pept Lett, 2005. **12**(4): p. 305-10.

270. Pace, A.L., et al., *Asparagine Deamidation Dependence on Buffer Type, pH, and Temperature.* Journal of Pharmaceutical Sciences, 2013. **102**(6): p. 1712-1723.
271. Sommerfeld, S. and J. Strube, *Challenges in biotechnology production—generic processes and process optimization for monoclonal antibodies.* Chemical Engineering and Processing: Process Intensification, 2005. **44**(10): p. 1123-1137.
272. Fishman, J.B. and E.A. Berg, *Protein A and Protein G Purification of Antibodies.* Cold Spring Harb Protoc, 2019. **2019**(1).
273. Ramos-de-la-Peña, A.M., J. González-Valdez, and O. Aguilar, *Protein A chromatography: Challenges and progress in the purification of monoclonal antibodies.* J Sep Sci, 2019. **42**(9): p. 1816-1827.
274. Duhamel, R.C., et al., *pH gradient elution of human IgG1, IgG2 and IgG4 from protein A-Sepharose.* Journal of Immunological Methods, 1979. **31**(3): p. 211-217.
275. Hober, S., K. Nord, and M. Linhult, *Protein A chromatography for antibody purification.* J Chromatogr B Analyt Technol Biomed Life Sci, 2007. **848**(1): p. 40-7.
276. Gulich, S., et al., *Engineering streptococcal protein G for increased alkaline stability.* Protein Eng, 2002. **15**(10): p. 835-42.
277. Hahn, R., et al., *Comparison of protein A affinity sorbents III. Life time study.* Journal of Chromatography A, 2006. **1102**(1): p. 224-231.
278. Zhang, J., et al., *Maximizing the functional lifetime of Protein A resins.* Biotechnology Progress, 2017. **33**(3): p. 708-715.
279. Gulich, S., M. Uhlen, and S. Hober, *Protein engineering of an IgG-binding domain allows milder elution conditions during affinity chromatography.* J Biotechnol, 2000. **76**(2-3): p. 233-44.
280. Tsukamoto, M., et al., *Engineered protein A ligands, derived from a histidine-scanning library, facilitate the affinity purification of IgG under mild acidic conditions.* Journal of Biological Engineering, 2014. **8**(1): p. 15.
281. Pabst, T.M., et al., *Engineering of novel Staphylococcal Protein A ligands to enable milder elution pH and high dynamic binding capacity.* J Chromatogr A, 2014. **1362**: p. 180-5.
282. Watanabe, H., et al., *Structure-based histidine substitution for optimizing pH-sensitive Staphylococcus protein A.* Journal of Chromatography B, 2013. **929**: p. 155-160.
283. Kanje, S., et al., *Protein engineering allows for mild affinity-based elution of therapeutic antibodies.* J Mol Biol, 2018. **430**(18 Pt B): p. 3427-3438.
284. Scheffel, J., et al., *Optimization of a calcium-dependent Protein A-derived domain for mild antibody purification.* MAbs, 2019. **11**(8): p. 1492-1501.
285. Choe, W., T.A. Durgannavar, and S.J. Chung, *Fc-Binding Ligands of Immunoglobulin G: An Overview of High Affinity Proteins and Peptides.* Materials (Basel), 2016. **9**(12).
286. Watanabe, H., et al., *Optimizing pH response of affinity between protein G and IgG Fc: how electrostatic modulations affect protein-protein interactions.* J Biol Chem, 2009. **284**(18): p. 12373-83.
287. Watanabe, H., et al., *Histidine-mediated intramolecular electrostatic repulsion for controlling pH-dependent protein-protein interaction.* ACS Chem Biol, 2019.
288. Klooster, R., et al., *Improved anti-IgG and HSA affinity ligands: clinical application of VHH antibody technology.* J Immunol Methods, 2007. **324**(1-2): p. 1-12.
289. Detmers, F., et al., *Novel affinity ligands provide for highly selective primary capture.* BioProcess Internatl, 2010. **8**: p. 50-54.
290. Buschhaus, M.J., et al., *Isolation of highly selective IgNAR variable single-domains against a human therapeutic Fc scaffold and their application as tailor-made bioprocessing reagents.* Protein Engineering, Design and Selection, 2019. **32**(9): p. 385-399.
291. Behar, G., et al., *Affitins as robust tailored reagents for affinity chromatography purification of antibodies and non-immunoglobulin proteins.* J Chromatogr A, 2016. **1441**: p. 44-51.

# 4 Cumulative Section

## 4.1 Dual Function pH Responsive Bispecific Antibodies for Tumor Targeting and Antigen Depletion in Plasma

Title:

Dual Function pH Responsive Bispecific Antibodies for Tumor Targeting and Antigen Depletion in Plasma

Authors:

Jan P. Bogen*, **Steffen C. Hinz***, Julius Grzeschik, Aileen Ebenig, Simon Krah, Stefan Zielonka, Harald Kolmar

* Authors contributed equally

Bibliographic data:

*Frontiers in Immunology*

Volume 10, Issue 1892

Article first published online: 09.08.2018 | DOI: 10.3389/fimmu.2019.01892



Contribution by S. C. Hinz:

- Performed literature research
- Performed experiments
- Involved in writing and revising the manuscript
- Scientific supervision of J. P. Bogen's master thesis conducted in this context

frontiers in Immunology

ORIGINAL RESEARCH
published: 09 August 2019
doi: 10.3389/fimmu.2019.01892

# Dual Function pH Responsive Bispecific Antibodies for Tumor Targeting and Antigen Depletion in Plasma

*Jan P. Bogen[1†], Steffen C. Hinz[1†], Julius Grzeschik[1], Aileen Ebenig[1], Simon Krah[2], Stefan Zielonka[2] and Harald Kolmar[1*]*

[1] Department of Applied Biochemistry, Institute for Organic Chemistry and Biochemistry, Technische Universität Darmstadt, Darmstadt, Germany, [2] Protein Engineering and Antibody Technologies, Merck KGaA, Darmstadt, Germany

OPEN ACCESS

**Edited by:**
Ignacio Melero,
University of Navarra, Spain

**Reviewed by:**
Laura Sanz,
Hospital Universitario Puerta de Hierro Majadahonda, Spain
Christian Klein,
Roche Innovation Center Zurich, Switzerland

***Correspondence:**
Harald Kolmar
kolmar@biochemie-tud.de

[†] These authors have contributed equally to this work as first authors

**Specialty section:**
This article was submitted to Cancer Immunity and Immunotherapy, a section of the journal Frontiers in Immunology

**Received:** 05 June 2019
**Accepted:** 26 July 2019
**Published:** 09 August 2019

**Citation:**
Bogen JP, Hinz SC, Grzeschik J, Ebenig A, Krah S, Zielonka S and Kolmar H (2019) Dual Function pH Responsive Bispecific Antibodies for Tumor Targeting and Antigen Depletion in Plasma. Front. Immunol. 10:1892. doi: 10.3389/fimmu.2019.01892

Shedding of membrane-bound cell surface proteins, where the extracellular domain is released and found in the circulation is a common phenomenon. A prominent example is CEACAM5 (CEA, CD66e), where the shed domain plays a pivotal role in tumor progression and metastasis. For treatment of solid tumors, the presence of the tumor-specific antigen in the plasma can be problematic since tumor-specific antibodies might be intercepted by the soluble antigen before invading their desired tumor target area. To overcome this problem, we developed a generic procedure to generate bispecific antibodies, where one arm binds the antigen in a pH-dependent manner thereby enhancing antigen clearance upon endosomal uptake, while the other arm is able to target tumor cells pH-independently. This was achieved by incorporating pH-sensitive binding modalities in the common light chain IGKV3-15*01 of a CEACAM5 binding heavy chain only antibody. Screening of a histidine-doped light chain library using yeast surface display enabled the isolation of pH-dependent binders. When such a light chain was utilized as a common light chain in a bispecific antibody format, only the respective heavy/light chain combination, identified during selections, displayed pH-responsive binding. In addition, we found that the altered common light chain does not negatively impact the affinity of other heavy chain only binders toward their respective antigen. Our strategy may open new avenues for the generation of bispecifics, where one arm efficiently removes a shed antigen from the circulation while the other arm targets a tumor marker in a pH-independent manner.

**Keywords: antibody discovery, bispecific antibodies, common light chain, recycling antibodies, yeast display, CEACAM5**

## INTRODUCTION

Colorectal cancer (CRC) is the third most diagnosed cancer with approximately 10% of all diagnosed cancers. A specific and sensitive marker for colorectal and gastric carcinomas is the carcinoembryonic antigen-related cell adhesion molecule 5 (CEACAM5, CEA, CD66e) which is a membrane protein found on the surface of columnar epithelial and goblet cells of the colon (1). Detached tumor cells can survive the integrin-mediated anoikis by direct interaction of cell-bound

CEACAM5 with Death Receptor 5, increasing the risk of metastatic development (2). During tumor progression, CEACAM5 is shed off the tumor cell surface and can be detected in the serum, where it is a clinically reliable marker for CRC diagnosis (3). Studies imply that the soluble CEACAM5 is a driving factor for metastatic development in the liver by stimulating kupffer cells to secret proinflammatory cytokines such as IL-10, IL-6, and TNF-α into the hepatic sinusoid (4–6). This in turn leads to the upregulation of cell adhesions proteins, which facilitate the arrest of circulating tumor cells. Liver metastasis is the main reason for CRC-related deaths (7).

Besides its pro-metastatic function, CEACAM5 in the blood stream can trap anti-CEACAM5 antibodies and thereby impede the direct targeting of the tumor (3). To circumvent that problem, recent developments aimed at generating CEACAM5 targeting antibodies that exclusively recognize CEACAM5 in its membrane-bound form but not the shed protein (8). Another member of the CEA family of highly related cell surface glycoproteins is CEACAM6, which is also a tumor target since aberrant expression leads to the development of human malignancies (9–11). A hallmark of some tumors is the simultaneous overexpression of both proteins (9, 10).

Even though monoclonal antibodies are a very important drug class, they can be limited in their efficiency and selectivity. As a consequence, numerous next generation antibody formats have been developed including those, where two different epitopes can be addressed by one single molecule. Bispecific antibodies (bsAbs) harbor two antigen binding sites and can therefore bind a single target biparatopically or different targets simultaneously aimed at mediating superior efficacy compared to the combination of two individual monospecific IgGs (12–14). In addition, bsAbs have been designed to bring different cell types in close proximity leading to the formation of immunological synapses, which is not possible with conventional IgGs (15).

A strategy, often pursued in recent decades to generate bispecific antibodies relies on protein engineering of the Fc part by incorporating an asymmetrical CH3:CH3 interface to force heterodimer formation. To this end, already in the 90ths of the last century the knob-into-holes technology was developed, where engineering of several residues within the CH3:CH3 interface forces heavy chain heterodimer formation thus allowing for the arrangement of two different antigen binding VH domains on a single antibody scaffold (16, 17). A plethora of alternative strategies for the generation of heavy chain heterodimers was developed over the years (18–20). These strategies successfully promoted pairing of cognate heavy chains but they do not address the light chain pairing problem. A straightforward solution of this problem is the use of common light chains, where the same light chain is used for pairing of the two different heavy chains (21). In this class of common light chain bispecifics, antigen binding is mainly or exclusively mediated by the heavy chain. Several strategies were described for the isolation of common light chain bsAbs that rely on synthetic human antibody libraries based on common light chains (22), immunization of transgenic rodents expressing a single common light chain (23) or the combination of a heavy chain repertoire with a predefined light chain followed by high throughput screening for binders (24).

Another next generation format is antibodies with pH-responsive binding modalities. For the efficient removal of target proteins from the blood stream, Igawa et al. proposed antibody engineering toward pH-dependent binding (25). Antibodies undergo a permanent recycling through endothelial cells via endocytosis and pinocytosis. Through binding to endosomal FcRn, the antibody is recycled and returned to the blood stream, even if the antigen is bound to the antibody. This process can prolong the half-life of the antigen *in vivo* and is known as antibody buffering (26). An elegant way to get rid of the antigen during this recycling process makes use of the fact that slightly acidic conditions prevail in the endosome. A pH-dependent antibody that has low affinity to its target antigen at acidic pH can release the bound antigen in the endosome which is eventually transported to the lysosome and degraded, while the antibody is recycled back to the circulation due to FcRn-binding (27) (**Figure 1A**). The cyclic process of antigen removal can be further enhanced by engineering the FcRn binding site of antibody Fc (28). To obtain pH-dependent binders, antibodies are generated that contain several histidine residues in their complementary determining regions (CDRs). Histidine is an uncharged amino acid at neutral pH but becomes positively charged at slightly acidic conditions. As a consequence, repulsive electrostatic forces may lower affinity to the target significantly (25, 29).

In this work, we describe a modular workflow with which we generated histidine-doped common light chain variants that are capable of pairing with CEACAM5-binding heavy chains and enable the pH-responsive binding to the antigen. To this end, we generated a histidine-doped light chain library paired it with the CEACAM5-binding heavy chain C5A (24) and enriched pH-responsive, CEACAM5-specific Fabs utilizing yeast surface display and fluorescence activated cell sorting (FACS). Exemplary proof of concept reformatting into an anti-CEACAM5/CEACAM6 bispecific format revealed an antibody, where one arm was binding its target in a pH-dependent manner, while the other remained pH-independent (**Figure 1B**).

## MATERIALS AND METHODS

### Plasmids

The vectors used for yeast surface display of the heavy chain and the secretion of the common light chain were based on the pYD1 plasmid backbone (Yeast Display Vector Kit, version D, #V835-01, Thermo Fisher Scientific). The heavy chain encoding plasmid contained an ampicillin resistance marker, a tryptophan auxotrophic marker, the AGA2 signal peptide as well as the genes for the variable heavy chain domain (VH) and the constant CH1 domain of human $IgG_1$. Besides a kanamycin resistance marker and a leucine auxotrophic marker, the light chain plasmid encoded the αMFpp8 signal sequence for soluble secretion of the VL and the CL domain (30). Gene expression of either plasmid was controlled via the galactose inducible promotor (*GAL1*). The His-doped light chain repertoire was integrated via homologous recombination into the light chain bearing plasmid after digestion with the restriction

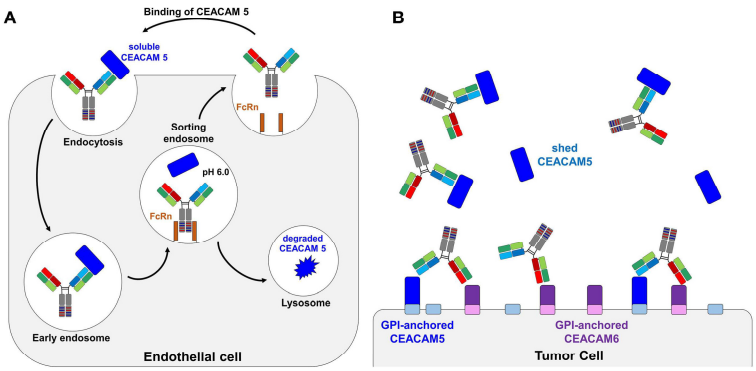


**FIGURE 1 |** Schematic representation of a bispecific pH-responsive anti-CEACAM5 antibody that binds pH-independently CEACAM6. **(A)** Illustration of the bispecific SEEDbody as a recycling body in the periphery. The antibody together with its antigen is internalized by pinocytosis. In the acidic conditions of the endosome, the antibody releases CEACAM5 (blue) due to the pH-shift and gets recycled by the neonatal Fc receptor (orange). The antigen is degraded in the lysosome. **(B)** Depiction of the binding behavior of CEACAM5/CEACAM6 bispecific antibodies. The CEACAM5-specific heavy chain (CH1 and VH illustrated in blue) is binding to shed CEACAM5 (blue boxes). The CEACAM5-attached GPI anchor is depicted as a small box on the tumor cell surface in light blue. The CEACAM6-specific CH1-VH are depicted in red/orange and solely bind to the tumor surface attached CEACAM6 (depicted in violet, GPI-anchor in light violet).

endonucleases *Pst*I-HF and *Sac*I-HF (NEB). For the expression of the Fab-constructs as one-armed SEEDbodies (oaSEEDbodies) or bispecific SEEDbodies, the genes for the light chain were subcloned into a pTT5 plasmid backbone (Expresso CMV based system, Lucigen) with ampicillin resistance and transfected into mammalian cells together with the respective heavy chain containing plasmids.

## Yeast Strains and Media

The *Saccharomyces cerevisiae* strain EBY100 [*MATa URA3-52 trp1 leu2Δ1 his3Δ200 pep4::HIS3 prb1Δ1.6R can1 GAL (pIU211:URA3)*] (Thermo Fisher Scientific) was transformed with the heavy chain containing plasmid. For the construction of the light chain library, the *S. cerevisiae* strain BJ5464 (*MATα URA3-52 trp1 leu2Δ1his3Δ200 pep4::HIS3 prb1Δ1.6R can1 GAL*) (American Type Culture Collection) was utilized. Initially, strains were cultivated in YPD medium composed of 20 g/L peptone/casein, 20 g/L glucose and 10 g/L yeast extract supplemented with appropriate antibiotics (ampicillin 100 mg/L, kanamycin sulfate 75 mg/L or chloramphenicol 25 mg/L). The SD-CAA media for HC plasmid containing cells comprised 5.4 g/L $Na_2HPO_4$ and 8.6 g/L $NaH_2PO_4 \times H_2O$, 20 g/L glucose, 5 g/L ammonium sulfate, 1.7 g/L yeast nitrogen base (without amino acids), and 5 g/L bacto casamino acids. Since the heavy chain encoding plasmid contained a tryptophan auxotrophic marker whereas the light chain plasmid contained a leucine auxotrophic marker, the cultivation media for haploid or diploid cells was supplemented accordingly. Cultivating yeast cells on agar plates was performed in SD-CAA medium with the respective drop-out mix (**Supplementary Table 1**) supplemented with 7% agar-agar. For induction of Fab surface presentation, the diploidic yeast cells were cultivated in SG-CAA medium (composition same as for SD-CAA medium but instead of glucose galactose was used).

## Library Construction and Yeast Mating

The C5A and C6B heavy chain sequences as well as the IGKV3-15*01 common light chain coding sequence were described recently (24). Proceeding from the IGKV3-15*01 common light chain in the pYD plasmid, the CDR-L1 and CDR-L3 together with surrounding framework regions were PCR amplified utilizing primers encoding for two histidines in all possible CDR-L1 or CDR-L3 positions (**Supplementary Tables 2, 3**) in separate PCR reactions. In the subsequent SOE-PCR, these His-doped gene fragments were fused with wild type gene fragments, generating full-length light chain genes with incorporated histidines in the CDR-L1 or CDR-L3, respectively. In additional reactions, the CDR-L1 His-doped gene fragments were fused with CDR-L3 fragments carrying additional histidines utilizing SOE-PCR resulting in light chain genes encoding for two histidines in both CDRs (four histidines in total; **Supplementary Figure 1**). PCRs were performed utilizing Q5® High-Fidelity polymerase (NEB): 98°C 30 s, 30 cycles of 98°C for 10 s, 68°C for 15 s and 72°C for 20 s, followed by a final elongation at 72°C for 20 s. The PCR products were cleaned up using the Promega Wizard® SV Gel and PCR Clean-Up System and subsequently pooled for library generation according to the protocol of Benatuil and coworkers (31). The pYD vector encoding the original IGKV3-15*01 light chain was digested utilizing the restriction enzymes *Pst*I-HF and *Sac*I-HF (NEB) and further purified form a 1% agarose gel utilizing Promega Wizard® SV Gel and PCR Clean-Up System kit. Overall 12 μg of DNA was utilized for electroporation and the resulting haploid yeast cell library was grown in SD-CAA-Leu medium.

In order to generate a diploid yeast library and to generate clones that are able to display a complete Fab molecule, EBY100 was transformed with the heavy chain vector encoding the C5A heavy chain and cultured in SD-CAA-Trp. $3 \times 10^8$ cells of the light chain library and the equal number of heavy chain carrying

yeast cells were mixed, centrifuged and resuspended in 150 µL YPD medium. Subsequently, 50 µL of the cell suspension was put on a pre-warmed YPD agar plate and incubated at 30°C over night. The next day, cells were washed of the agar plate and the resulting diploid library was grown in SD-CAA-Leu/-Trp medium.

## Library Sorting

For library sorting, the diploid yeast library was grown overnight in tryptophan and leucine deficient SD-CAA medium at 30°C and 180 rpm. Afterwards, cells were transferred to SG-CAA medium with a corresponding dropout mix at $10^7$ cells/ml followed by an incubation period of 1 day at 30°C. Cells were harvested by centrifugation and washed once in 1 mL PBS-B pH 7.4 [PBS + 0.1% (w/v) BSA]. The presentation of the Fab fragments on the yeast cell surface was verified utilizing the anti-human κ R-phycoerythrin (R-PE) goat $F(ab')_2$ conjugate (Southern Biotech, diluted 1:75 in PBS-B pH 7.4). Cells were subsequently washed once with PBS-B at pH 7.4 and a second time either with PBS-B at pH 7.4 or pH 6.0, respectively. For target binding, yeast cells were incubated with recombinant human His-tagged CEACAM5 (R&D systems; 62.5 nM in PBS pH 7.4 or 6.0, respectively or phosphate-citrate buffer at pH 5.0). After a wash step with PBS-B at pH 7.4 or pH 6.0, cells were washed a second time at pH 7.4. All subsequent staining steps were performed at pH 7.4. For detection of target binding an anti-penta-His antibody (Qiagen, dilution 1:50) and an anti-mouse APC antibody (Invitrogen, diluted 1:50) were utilized (**Supplementary Figure 2**). All staining steps were performed on ice for 30 min (CEACAM5) or 15 min (labeling reagents), respectively, with a staining volume of 20 µL per $1 \times 10^7$ yeast cells. After the final wash step in PBS-B, the cells were resuspended in PBS-B and analyzed in the BD Influx FACS Cell sorter (sortware 1.0.0.650). Yeast cells that were collected during the sorting process were transferred into SD-CAA medium and were incubated at 30°C and 180 rpm for 48 h before inoculating SG-CAA medium for subsequent sorting.

## Cloning, Expression, Purification of oaSEEDbodies and Bispecific SEEDbodies

After the identification of single clones displaying a pH-responsive Fab fragment, the plasmids were isolated utilizing the Zymoprep Yeast Plasmid Miniprep kit (Zymoresearch). The light chain genes were amplified using primers adding a 5' *EcoR*I site (*I CLC to pTT5*, *II CLC to pTT5*) and a 3' *BamH*I site (CLC to pTT5 rev) of the gene, as well as internal primers substituting an *EcoR*I site (*Fr3 EcoRI mut for/rev*) by a silent mutation (all oligonucleotides for cloning and reformatting are listed in **Supplementary Table 3**). The resulting PCR products were fused in a PCR resulting in a full-length light chain gene with overhangs for restriction. Amplifications were performed utilizing Phusion polymerase (NEB) at 98°C for 30 s, 30 cycles at 98°C for 10 s, 57°C for 15 s and 72°C for 45 s, followed by a final elongation at 72°C for 2 min. After subsequent restriction of the PCR products as well as the pTT5 destination vector with *EcoR*I-HF and *BamH*I-HF (NEB) inserts and the plasmid were ligated utilizing T4 DNA Ligase (NEB) over night at 16°C. The reaction mixture was directly transformed into *E. coli* DH5α and cells were subsequently plated on ampicillin containing LYT agar (16 g/L trypton/casein, 10 g/L yeast extract, 5 g/L NaCl, 7.5 g/L agar-agar). The plasmids from the resulting clones were sequenced at Microsynth Seqlab and positive single clones were picked and inoculated for plasmid preparation using Promega Midi Prep Kit (Promega).

For the determination of $k_{on}$, $k_{off}$, $K_D$ values as well as the melting temperature, the constructs were expressed as one-armed SEEDbodies (oaSEEDbodies) as described recently (24). These antibodies consisted of three chains: a VH-CH1-CH2-SEED-AG chain, a CH2-SEED-GA chain and a light chain comprising VL and CL domains. IMAC purification was performed utilizing the C-terminal His6-tag of the AG-fragment to exclude GA homodimers (24).

For the soluble production of pH-responsive one-armed SEEDbodies, Expi293F cells were cultivated in 30 mL Expi293™ Expression Medium (ThermoFisher) and grown for 2 days at 37°C and 8.0% $CO_2$ at 110 rpm. Transient transfections of Expi293F cells were performed at a cell density of approx. $2.7 \times 10^6$ cells/mL, utilizing 15 µg of each plasmid with 120 µg polyethylenimine (PEI). To this end, plasmid and PEI were mixed and incubated in Expi293™ Expression Medium (Thermo Fisher) for 15 min before adding it dropwise to the cell suspension. After 24 h, the cell suspension was supplemented with 825 µL of aqueous 20% tryptone/casein solution. After 5 days of protein production, the cells were harvested at 3000 rpm for 3 min and the supernatant was filtrated with a 0.45 µm syringe filter and mixed 3:2 (v/v) with IMAC Binding Buffer (50 mM Tris/HCl pH 7.5). Protein purification was performed with an ÄKTA Start FPLC system in combination with a HisTrap HP column (GE Healthcare). After a 5 CV wash step with IMAC Binding Buffer, the POI was eluted with a linear gradient to 100% IMAC Elution Buffer (50 mM Tris/HCl pH 7.5, 500 mM imidazole). Fractions with the POI were pooled and used for subsequent purification via Protein A chromatography. To this end, 500 µL up to 5 ml of Protein A Binding Buffer (20 mM sodium phosphate, pH 7.0) were added and the sample was applied to an equilibrated Protein A HP column (GE Healthcare). Bound protein was eluted with 100% Protein A Elution Buffer (100 mM citrate, pH 3.0). 250 µL of Protein A Neutralization Buffer (1 M Tris/HCl, pH 9.0) was instantly added to 1 mL of Protein A eluate. The fractions were either dialyzed against PBS or buffer exchange was performed utilizing Amicon Ultra Centrifuge Filters (Amicon® Ultra-15 Centrifugal Filter Units, Merck Millipore, 3 kDa MWCO).

## Biolayer Interferometry

The binding kinetics were determined utilizing the Octet RED96 system (FortéBio, Pall Life Science). Measurements were performed at 30°C and 1000 rpm. All biosensors were incubated in PBS prior to utilization for at least 10 min. After determination of the baseline in PBS buffer for 10 s, the anti-human Fc biosensors or anti-human CH1 biosensors, respectively, were loaded with SEEDbodies at a concentration of 5 µg/ml in PBS for 120 s. Quenching of the biosensors was performed for 60 s in kinetic buffer (KB; PBS pH 7.4 or pH 6.0, respectively, or

phosphate-citrate buffer pH5.0 + 0.1% Tween 20 + 1% BSA) prior to incubation of the sensors with 100 nM CEACAM5 or CEACAM6 in KB for 180 s. The dissociation of the antigen was measured for 300 s in KB at the respective pH. For each BLI experiment, a negative control was measured where the biosensor was incubated in KB instead of the respective antigen solution. This negative control was subtracted from all antigen containing samples. Data analysis was performed with FortéBio data analysis software 8.0 using a 1:1 binding model with Savitzky-Golay filtering. To ensure the stability of the pH-responsive light chains over multiple binding and release periods, anti-human CH1 biosensors were loaded with the C5A + CV2 oaSEEDbody and subsequently loaded with CEACAM5 at pH 7.4 in KB for 180 s. Afterwards, the dissociation at pH 5.0 was measured for 300 s. The association and dissociation steps were repeated six times.

## Thermal Stability Assay

The melting temperature of the purified protein was determined utilizing SyproOrange dye fluorescence. Therefore, the protein solution was diluted to 100 µg/ml with a 1:1,000 dilution of SyproOrange in a total volume of 40 µL and a temperature gradient was applied from 30 to 100°C with a gradient of 1°C/min. The measurement was performed with the BioRad 96CFX RT-PCR detection system. The calculation of the TM values was performed with the BioRad 96CTX RT-PCR software.

# RESULTS

Davis and coworkers recently described a strategy for the generation of bispecific antibodies, where heavy chain heterodimerization is achieved by co-expression of Fc-engineered heavy chains that contain mutual exchanges of IgG/IgA segments (SEEDbody technology) (18, 32). These antibodies share a common light chain on both binding arms. One variant, C5A, was reported to bind CEACAM5 with subnanomolar affinity when paired with the germline-derived IGKV3-15*01 light chain (24).

To investigate, whether the common light chain that originally is not involved in target binding can be functionalized to mediate pH-dependent target binding, a subset of common light chain VL domains was generated, where CDR-L1 and CDR-L3 contain two histidines in all positional combinations. Since CDR-L2 is located further away from the heavy chain CDRs in comparison to CDR-L1 and CDR-L3, it was neglected for His-doping. CDR-L1 and CDR-L3 of the IGKV3-15*01 VL domain encoding sequence were His-doped separately by VL gene PCR amplification, in which 91 unique primers, each bearing two histidine codons were used (**Supplementary Table 2**). This resulted in 55 CDR-L3 and 36 CDR-L1 double His combinations. Finally, random combination of CDR-L1 and CDR-L3 variants resulted in 1980 light chain variants each of which containing two histidines at random positions of both CDR-L1 and CDR-L3. This led to a total of 2071 His-doped light chain variants. The His-doped gene fragments were inserted into a pYD1-derived yeast secretion vector via homologous recombination (strain BJ5464), resulting in a library of $7.5 \times 10^5$ clones, indicating high coverage of all possible His combinations.

In the next step, $3 \times 10^8$ cells of the light chain library were mated with $3 \times 10^8$ EBY100 cells containing the CEACAM5 binding heavy chain variant C5A, resulting in diploid yeast cells capable of displaying the Fab fragment on the yeast cell surface via fusion to Aga2p (**Supplementary Figure 2**). With a mating efficiency of 17.2%, the final diploid library was subjected to FACS screening. To this end, CEACAM5 variants displaying yeast cells were incubated with His-tagged CEACAM5 and stained with an anti-penta-His antibody and an anti-mouse APC antibody. A control stain of the initial library in the absence of CEACAM5 showed no APC fluorescence, indicating that the anti-penta-His antibody does not recognize the His-doped CDR sequences (data not shown). To observe surface presentation of the full-length Fab construct, anti-Kappa PE $F(ab')_2$ was utilized. In the first sorting round, 3.82% of double positive yeast cells for display and CEACAM5 binding were enriched aimed at depleting light chain variants, where the His doping disrupted antigen binding (**Figure 2A**). In order to isolate pH responsive binders, the CEACAM5 stainings for the second and the third round were performed at pH 6.0. Gating for those rounds were applied to isolate yeast cells that showed surface presentation but lacked CEACAM5 binding. The final sorting round was performed at pH 7.4 to isolate pH-responsive single clones. All sorting rounds were performed with 62.5 nM CEACAM5.

50 isolated yeast clones were analyzed for CEACAM5 binding at pH 6.0 compared to pH 7.4. While all clones showed strong binding to CEACAM5 at neutral conditions, 3 clones displayed reduced affinity at acidic pH (**Figure 2B**). Subsequent sequence analysis of the pH-dependent binders resulted in two unique pH-responsive variants, referred to as K39 and K40. Both variants showed significantly reduced binding signal at pH 6.0 and pH 5.0 (**Figure 2B**). K39 contained two histidines in the CDR-L1 and no His in CDR-L3, whereas K40 contained three histidines, two in CDR-L1 and unexpectedly only one in the CDR-L3 (**Figure 3A**). The absence of a second histidine within the CDR-L3 probably originates from homologous recombination events during library generation by gap repair. Both clones shared an N32H exchange within the CDR-L1 and displayed moderate pH-dependent binding (**Figure 3B**). To further improve the pH-dependence in antigen binding, the histidine patterns of both isolated single clones were combined, resulting in the combinatory variants (CV) CV1, CV2, and CV3 (**Figure 3A**).

FACS analysis confirmed the pH-responsive binding behavior of the permutation variants, since incubation at pH 5.0 completely abolished the binding signal (**Figure 3B**). Incubation of CEACAM5-bound cells at pH 6.0 showed similar results. As expected, the original IGKV3-15*01 common light chain domain that lacked any His residues in CDR-L1 and CDR-L3 showed no differences in CEACAM5 release at pH 6.0 in comparison with pH 7.4 and only a slightly decreased binding at pH 5.0.

All five variants together with wildtype VL sequence were reformatted as one-armed SEEDbodies (oaSEEDbodies) to determine the binding characteristics to CEACAM5 as a soluble protein. To this end, the respective light chain gene was cloned into the recipient pTT5-VL-CL plasmid. For expression, $8.1 \times 10^7$ Expi293F cells were transfected with 15 µg of pTT5-VL-CL, pTT5-VH-CH1-CH2-CH3(SEED-AG)

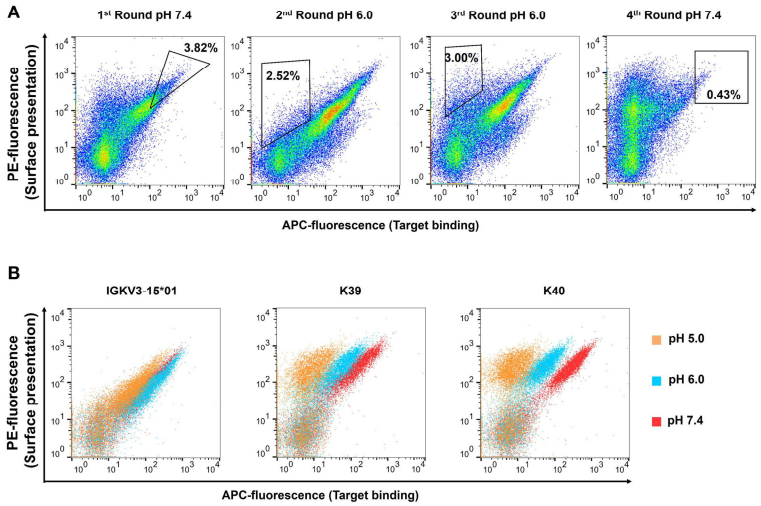


**FIGURE 2 |** Consecutive FACS sortings for the enrichment of **(A)** pH-responsive CEACAM 5 binding Fab-fragments and **(B)** resulting single clones. Target binding is plotted on the x-axis (APC-fluorescence), surface presentation on the y-axis (PE-fluorescence). Each plot contains 50,000 events. Surface presentation was confirmed utilizing the anti-κ PE-antibody. Target staining was performed utilizing 62.5 nM CEACAM5, a anti-His mouse antibody and a anti-mouse APC-antibody. **(A)** In the first round, CEACAM5 binding Fab-fragments were enriched to deplete variants that were not able to bind CEACAM5 due to the histidine incorporation into the CDRs of the light chain. In the second and the third round, target staining was performed at pH 6.0 and yeast cells were sorted that displayed a Fab-fragment that does not bind to CEACAM5. For the fourth round, yeast cells were isolated that were able to display a CEACAM5 binding Fab at neutral conditions. Single clones were picked after this sorting round. **(B)** Overlay of plots from isolated pH-responsive single clones. The single clones were incubated with CEACAM5 at pH 5.0 (orange), 6.0 (blue), or 7.4 (red), respectively.

and pTT5-CH2-CH3(SEED-GA), respectively. The purification was performed in a two step workflow. First, the supernatant was purified after 5 days of protein production via IMAC utilizing the C-terminal His6-tag on the SEED-AG chain to ensure the purification of heterodimeric SEEDbodies. After dialysis, the SEED-containing solution was subjected to Protein A chromatography.

The binding kinetics of the different CEACAM5 binding variants were determined using the FortéBio Octet96red BLI system. To this end, the oaSEEDbodies were loaded onto anti-human-Fc biosensors (AHC tips), quenched in kinetics buffer and the association was measured in 100 nM CEACAM5 solution at pH 7.4, as it resembles the pH value of serum. The dissociation was performed at pH 7.4, pH 6.0, pH 5.5 and pH 5.0 in KB buffer, respectively to simulate the pH-shift of the antibody-antigen complex within the sorting endosome (**Figure 4**). Similar approaches were performed by Schröter et al. (29) and Igawa et al. (27).

The association rates of the engineered variants were nearly identical with the parental antibody, demonstrating that the histidines in the CDRs do not interfere with target binding at neutral conditions (**Table 1**). Nevertheless, the His-doped variants exhibited a lower $K_D$ value at physiological conditions due the slightly accelerated dissociation. This phenomenon was also observed by Schröter and coworkers, where pH-responsive Adalimumab variants showed a 10 to 24-fold reduced $K_D$ value compared to the parental antibody (29). The pH-responsive light chain variants from this work displayed a reduced the $K_D$ in a range between 2.8- and 4.6-fold at pH 7.4 compared to the IGKV3-15*01 light chain.

At pH 6.0 all engineered variants showed a 10–15-times elevated dissociation rate compared to the IGKV3-15*01 wild type light chain. When the dissociation was performed at pH 5.5, the dissociation was accelerated by the factor 18–27 and at pH 5.0 by the factor 41–52, clearly demonstrating the pH-responsive binding modalities of all variants that were in the range of previously published pH-responsive antibodies (27). In contrast, the parental antibody only exhibited a 4-times faster dissociation at pH 5.0 compared to neutral conditions (**Figure 4**, **Table 1**).

To exclude the possibility that the dissociation of CEACAM5 is due to pH-induced denaturation of the Fab-fragment, thermostability of all constructs was measured at neutral and acidic conditions. The resulting $T_M$ values showed no significant difference between neutral and acidic conditions, indicating that the stabilities of the antibodies are pH-independent (**Table 1**).

Since CV2 exhibited the strongest change in the dissociation rates compared to the parental antibody, it was chosen for further experiments. To effectively reduce the concentration of an antigen in serum, a recycling antibody must be able to bind and release its antigen multiple times throughout its lifetime. To investigate whether the variant CV2 is suitable for the usage as a recycling antibody, its mode of action was simulated

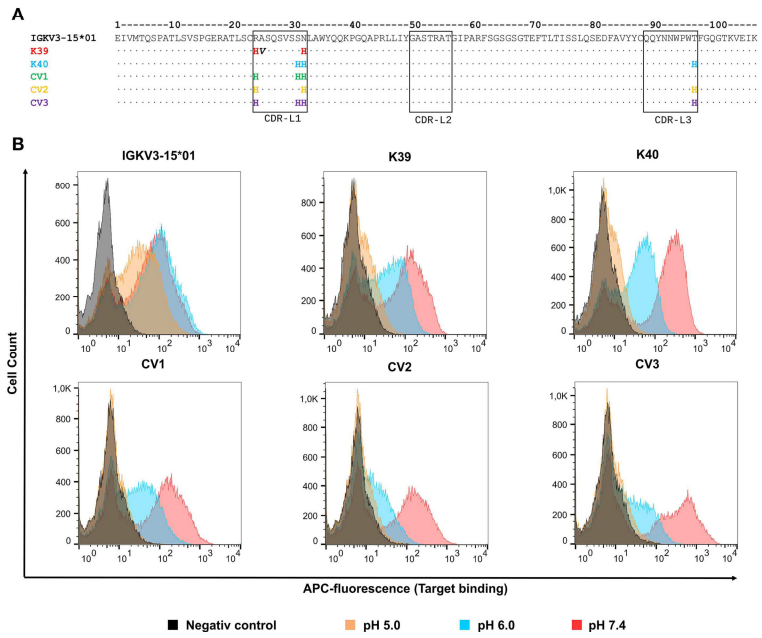


**FIGURE 3 |** Sequences and FACS analysis of the pH-responsive, His-doped common light chains. **(A)** Sequence alignment of the parental IGKV3-15*01 common light chains with the isolated pH-responsive light chains K39, and K40 as well as the permutated light chain variants CV1, CV2, and CV3. Histidines in CDR3 and CDR1 are highlighted in the respective light chain color. Non-histidine mutations are highlighted in bold black. The numbering refers to the Chothia numbering scheme. **(B)** Histograms of yeast cell single clone carrying the respective light chain in combination with the C5A heavy chain on the yeast surface. All cells, except the negative control which was incubated in PBS, were incubated with 62.5 nM CEACAM5 at their respective pH-value, and subsequently all cells were washed with PBSB at pH 7.4, and further labeled with anti-His and anti-mouse-APC. For each experiment 50,000 yeast cells were recorded.

by performing consecutive association and dissociation cycles. Therefore, the antibody was loaded onto anti-Fab biosensor tips. Association of CEACAM5 was again performed at pH 7.4, which would correspond to serum pH. The dissociation was either performed at pH 5.0 to simulate the cellular uptake and undergoing the transportation to the sorting endosome, or at pH 7.4 (**Figure 5**). As a control, the parental antibody was treated identically. The IGKV3-15*01 comprising antibody bound tightly to the antigen and only a minor dissociation was observed at pH 7.4 within the measurement time frame of 5 min, which was only slightly increased at pH 5.0. In contrast, the CV2 displayed strong binding to CEACAM5 at pH 7.4 slow dissociation at pH 7.4 but fast dissociation at pH 5.0 over six repeated cycles of association and dissociation, although the binding capacity decreased over time, likely due to dissociation of the CV2 antibody from the anti-Fab biosensor (**Figure 5**). Nevertheless, these experiments showed that the modular approach of His-doping the common light chain that is not directly involved in the antigen binding can lead to highly pH-responsive variants, suitable for the usage as a recycling antibody.

To verify that the one arm CV2 SEEDbody retains its ability for tumor cell binding, we analyzed binding on COLO 205 cells by FACS (24, **Supplementary Figure 3**). High affinity binding was observed at pH 7.4 and reduced binding at pH 5.0. Unexpectedly, tumor cell binding was retained at pH 6.0 despite the fact that CV2 releases the soluble shed target already at this pH (**Figure 4**) which indicates that the microenvironment on the cell surface influences pH-dependent SEEDbody binding.

For use as bispecifics, it would be required that the His-doped light chain variant retains its capability to act as a common light chain when paired with other heavy-chain only binders. To investigate this aspect, the CEACAM6 binding C6B heavy chain was further investigated for CV2 pairing (24). BLI measurements of a C6B/CV2 oaSEEDbody showed antigen binding with a negligible difference in $K_D$ (8.8 vs. 7.7 nM) compared to C6B/IGKV3-15*01 (**Figure 6**, **Table 2**).

Finally, a bispecific SEEDbody was generated containing the C5A heavy chain in one arm and the C6B heavy chain in the other, both paired with the CV2 light chain. BLI measurements were performed to investigate the ability of the bispecific molecule to bind both antigens. After the loading step with biotinylated CEACAM 5 onto streptavidin tips, the SEEDbody was loaded and subsequently, CEACAM6 was added in the last association

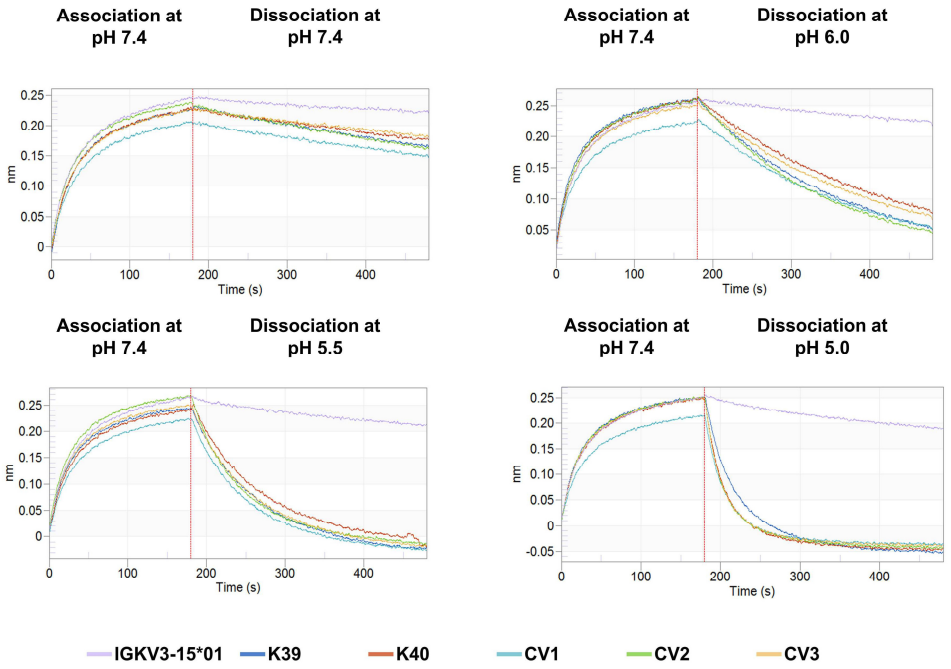


**FIGURE 4 |** BLI sensorgrams of CEACAM5 binding to the pH-responsive clones K39, K40, CV1, CV2, and CV3 as well as for the parental non-pH-responsive IGKV3-15*01 immobilized on AHC tips. The association was performed with 100 nM CEACAM5 at pH 7.4 in KB. The dissociation was performed in KB at the respective pH value. The depicted lines are colored according to the respective light chain data.

**TABLE 1 |** Binding kinetic parameters and $T_M$ of IGKV3-15*01 and all pH-responsive light chain variants binding to CEACAM5.

| Antibody | pH 7.4 | | | pH 6.0 | pH 5.5 | pH 5.0 | $K_{dis}$ ratio (pH 6.0) vs. IGKV3-15 | $K_{dis}$ ratio (pH 5.5) vs. IGKV3-15 | $K_{dis}$ ratio (pH 5.0) vs. IGKV3-15 | Tm (°C) pH 7.4 | Tm (°C) pH 6.0 |
|---|---|---|---|---|---|---|---|---|---|---|---|
| | $K_D$ nM | $K_{on}$ ($\times 10^{-6}$) $M^{-1}$ $s^{-1}$ | $K_{dis}$ ($\times 10^{-4}$) $s^{-1}$ | $K_{dis}$ ($\times 10^{-4}$) $s^{-1}$ | $K_{dis}$ ($\times 10^{-4}$) $s^{-1}$ | $K_{dis}$ ($\times 10^{-4}$) $s^{-1}$ | | | | | |
| IGKV3-15*01 | 0.90 | 0.264 | 2.38 | 3.68 | 6.63 | 8.71 | 1 | 1 | 1 | 66.5 ± 0.7 | 65.0 ± 0.5 |
| K39 | 4.16 | 0.238 | 9.89 | 50.7 | 156 | 353 | 14 | 24 | 41 | 66.7 ± 0.3 | 65.3 ± 0.3 |
| K40 | 3.12 | 0.245 | 7.65 | 37.6 | 121 | 437 | 10 | 18 | 50 | 66.5 ± 0.0 | 65.3 ± 0.8 |
| CV1 | 4.11 | 0.235 | 9.68 | 45.4 | 176 | 416 | 12 | 27 | 48 | 66.5 ± 0.5 | 65.0 ± 0.5 |
| CV2 | 4.14 | 0.279 | 11.5 | 55.5 | 167 | 450 | 15 | 25 | 52 | 66.5 ± 0.5 | 64.8 ± 0.4 |
| CV3 | 2.55 | 0.249 | 6.36 | 40.4 | 152 | 447 | 11 | 23 | 51 | 66.8 ± 0.3 | 65.3 ± 0.3 |

*The binding affinity is listed for association and dissociation at pH 7.4 with both $k_{on}$ and $k_{off}$. The $k_{off}$ values for the different dissociation pH-values are also listed. The ratios of the dissociation constant at pH values <7.4 in comparison to $k_{dis}$ at pH 7.4 are shown on the right together with the dissociation ratios under the same conditions.*

step. The bispecific antibody was able to bind both antigens specifically. As control, a C5A based oaSEEDbodies was utilized in order to exclude nonspecific interactions with CEACAM6 (**Figure 7**).

## DISCUSSION

Most membrane-bound proteins shed their ectodomains to some degree (33). Wang and coworkers divided the therapeutic monoclonal antibodies (mAbs) into three categories based on the characteristics of their targets: (I) membrane bound cell surface target protein with minimal shedding; (II) membrane-bound cell surface target protein that sheds its extracellular domain, and (III) circulating soluble targets, as e.g., growth factors and cytokines (34). Shedding of a pharmacological target from the surface of tumor cells, thus resulting in a soluble target that can also bind a therapeutic antibody, is a common phenomenon that may complicate cancer therapy (35). Whether

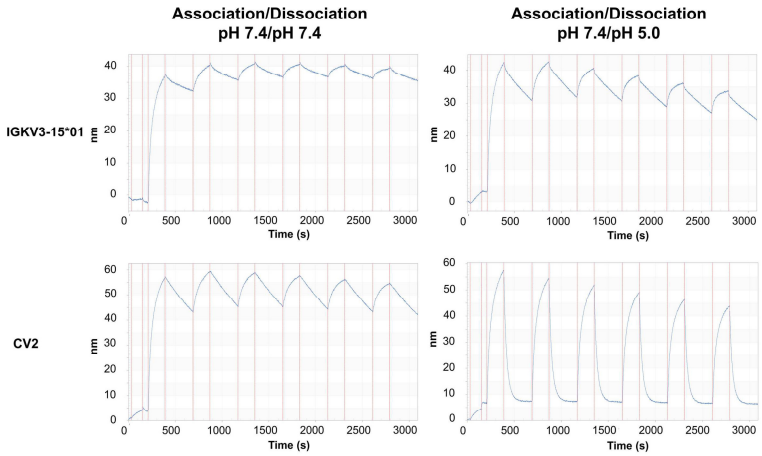


**FIGURE 5 |** Sensorgrams of the periodic association and dissociation of CEACAM5 to immobilized oaSEEDbody comprising C5A and either IGKV3-15 or CV2. On the left panel, association and dissociation of CEACAM5 to the immobilized oaSEEDbodies was performed at pH 7.4. On the right, the dissociation was performed at pH 5.0. Each association step is immediately followed by a dissociation step. All experiments were performed with 100 nM CEACAM5.

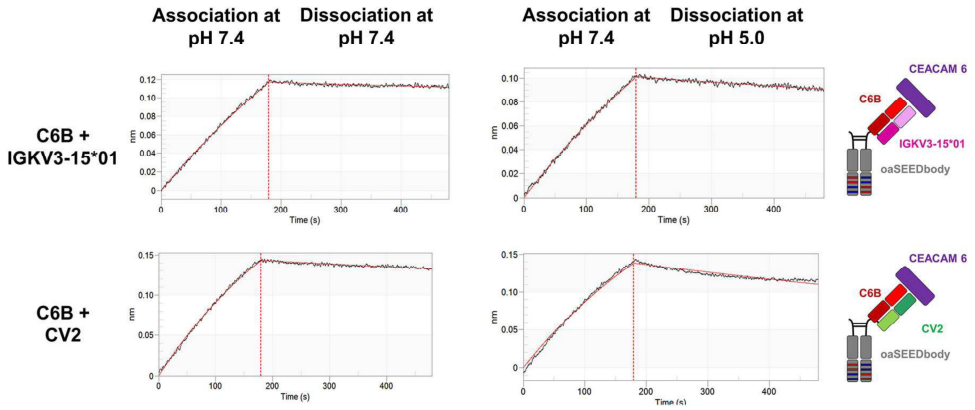


**FIGURE 6 |** Biolayer interferometric measurements of the CEACAM6-binding C6B VH paired with CV2. C6B-derived oaSEEDbodies were loaded onto anti-Fab tips. The association of CEACAM6 was performed at pH 7.4 with a CEACAM6 concentration of 100 nM, the dissociation at pH 7.4 or pH 5.0, respectively, (black line). The fit (1:1 binding model with Savitzky-Golay filtering) for the $K_D$ determination is depicted in red.

target shedding positively or negatively affects the potency of a targeting molecule within a solid tumor remains a matter of debate (35, 36).

For shed targets, antibody-mediated antigen accumulation was observed (28) due to the fact that clearance of tight-binding antibody-antigen complexes is much slower than that of the free antigen. This problem has recently been overcome by recycling and sweeping antibodies, which can actively eliminate soluble antigens from circulation via pH-responsive endosomal target release followed by FcRn mediated recycling (27, 28). No efforts were made yet to use pH-responsive recycling antibodies for therapy of solid tumors, since it might be expected that due to extracellular acidification of the tumor tissue with pH values of 6.5 and lower antibody affinity is drastically reduced in the tumor microenvironment (37–39). Conceptually, this problem can be overcome using bispecific antibodies, where one arm targets tumor cells pH-independently, while the other arm mediates binding and removal of shed antigen via FcRn recycling in combination with receptor-mediated endocytosis (**Figure 1B**). To the best of our knowledge, no bispecific recycling antibodies were described, where one arm is engineered to enable the antibody to bind to an antigen in plasma and dissociate from the antigen in the endosome (after which the antigen undergoes

**TABLE 2 |** Binding kinetic parameters of the C6B heavy chain in combination with IGKV3-15*01 and CV2.

| Antibody | | pH 7.4 | | | pH 6.0 | pH 5.0 | $K_{dis}$ ratio pH 6.0/7.4 | $K_{dis}$ ratio pH 5.0/7.4 | $K_{dis}$ ratio (pH 5.0) vs. IGKV3-15*01 |
|---|---|---|---|---|---|---|---|---|---|
| | | $K_D$ nM | $K_{on}$ ($\times 10^{-4}$) $s^{-1}$ | $K_{dis}$ ($\times 10^{-4}$) $s^{-1}$ | $K_{dis}$ ($\times 10^{-4}$) $s^{-1}$ | $K_{dis}$ ($\times 10^{-4}$) $s^{-1}$ | | | |
| C6B | IGKV3-15*01 | 8.77 | 0.02 | 1.58 | 1.90 | 3.61 | 1.2 | 2.3 | 1.0 |
| | CV2 | 7.73 | 0.03 | 2.62 | 1.42 | 7.68 | 0.5 | 2.9 | 2.1 |

*The binding affinity $K_D$ is shown for association and dissociation at pH 7.4, the $k_{dis}$ is also listed for the dissociation at pH 6.0 and pH 5.0. The ratios of the dissociation constant at pH values <7.4 in comparison to $k_{dis}$ at pH 7.4 are shown on the right together with the dissociation rates under the same conditions.*

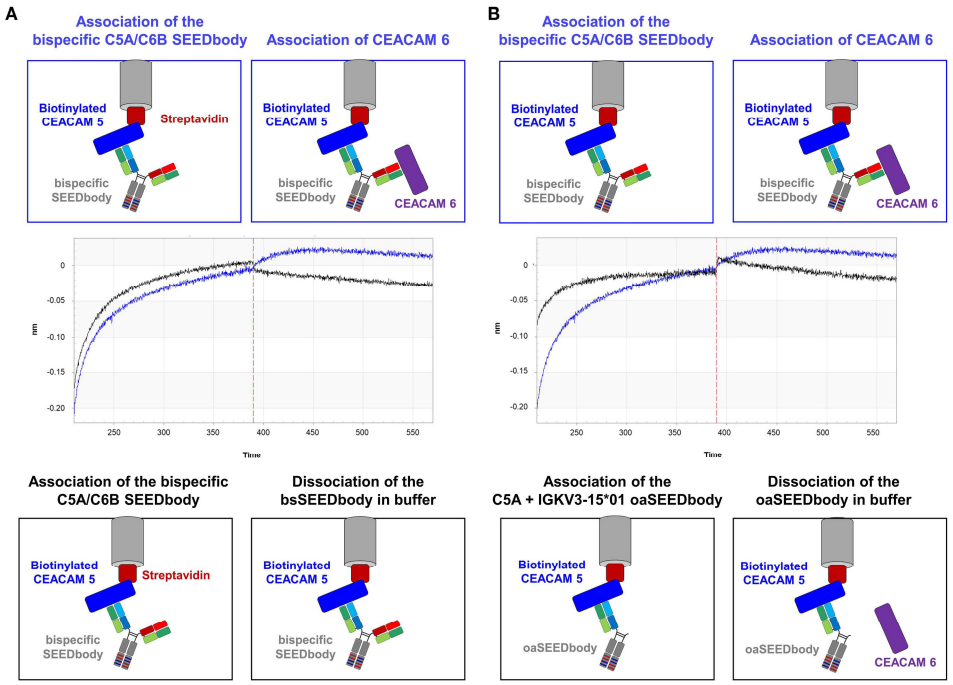


**FIGURE 7 |** Validation of simultaneous binding of CEACAM5 and CEACAM6 by the bispecific C5A/C6B SEEDbody comprising the CV2 light chain. **(A)** Immobilization of biotinylated CEACAM5 on streptavidin tips and subsequent association of the bispecific C5A/C6B SEEDbody. In an additional step, CEACAM6 is associated (blue sensorgram), or the tip is incubated in PBS buffer (black sensorgram). **(B)** After the immobilization of biotinylated CEACAM5 on streptavidin tips, the bispecific C5A/C6B SEEDbody (blue sensorgram) or the C5A oaSEEDbody (black sensorgram) was added. Both tips were transferred to a CEACAM6 containing solution in an additional association step. Association steps are separated via a vertical red dashed line in the sensorgrams.

lysosomal degradation), and the other mediates pH-independent target binding.

In recent years, a plethora of bispecific antibodies has been developed for various disease indications. Prominent applications are the recruitment of specific effectors of the immune system to target tumor cells or adjustment of binding specificity due to interaction with two different surface antigens (40, 41). To overcome the platform-associated issue of light chain pairing, the concept of common light chain bispecifics was developed thus facilitating antibody generation and purification (22, 23).

To obtain pH-responsive common light chain antibodies, we started from C5A, a human heavy chain that is able to bind CEACAM5 when paired with the IGKV3-15*01 light chain (24). We generated a light chain sublibrary that contained two histidines in either CDR-L1, CDR-L3, or in both. After four FACS-assisted sorting rounds, it was possible to identify clones K39 and K40 showing a pH-responsive binding behavior. Interestingly, K39 showed an additional A25V mutation besides

the two histidines in CDR-L1 which was likely a result of PCR mutagenesis. The sequence of K40 also differed from the designed library composition by comprising only one histidine in CDR-L3 instead of two or none. These findings were not considered crucial for compromising the initial library quality since sequence analysis after library construction revealed the desired mutation pattern (data not shown).

In comparison with the IGKV3-15*01 light chain, where only a minor decrease of binding was detectable at pH 5.0, K39 and K40 showed significant reduced binding to CEACAM5 at pH 5.0 and also pH 6.0. Based on K39 and K40, permutated variants CV1, CV2 and CV3 were generated with different histidine combinations in order to further enhance the pH-dependence of CEACAM5 binding. Indeed, CV2 and CV3 showed further reduced antigen binding at acidic pH when displayed on the cell surface of yeast. To further elucidate their binding behavior, one-armed SEEDbodies were generated from these five variants. Biolayer interferometry clearly demonstrated that the association at neutral conditions is not negatively influenced by the histidine substitutions in the light chain CDRs. This is most probably due to the fact, that the IGKV3-15*01 light chain is not involved in the antigen binding (24).

In line with FACS analysis, K39 showed the least binding difference at different pH values whilst also comprising the least number of histidines (2 histidines in CDR-L1). The variants CV2 (3 histidines in total) and CV3 (4 histidines in total) showed the strongest pH-responses. These observations corroborate the finding of Murtaught and coworkers who reasoned, that the pH-dependency is elevated with increasing the number of ionizable groups (42). Interestingly, the CV2 variant showed a slightly higher $k_{dis}$-value compared to the CV3 variant at pH 6.0 and pH 5.0, where the only difference is a single histidine at position 31. This indicates that the "dual histidine" motif might not be as favorable as supposed earlier (42). The variant CV3 showed higher $k_{dis}$-values compared to CV1, which differs in the presence of His97 in CDR-L3. These findings hint to the importance of His97 for the pH-responsive binding modalities.

Since the CV2 variant showed the strongest pH-dependence in antigen binding, multiple bind and release cycles were performed using this CLC to investigate its suitability for the usage as a recycling antibody. The dissociation was performed at pH 5.0 to simulate the conditions in the sorting endosome over a course of 5 min. *In vivo* the sorting endosome takes about 8–15 min to recycle the cargo back into the plasma, underlining the suitability of CV2 as a recycling antibody (43).

As a proof of concept, it was verified that a His-doped common light chain can be utilized for the generation of bispecific antibodies able to bind one antigen pH-independently, while the second target is bound in a pH-responsive manner. In a first step, it was shown that the CV2 light chain can pair with the C6B heavy chain and bind pH-independently to CEACAM6. Following the generation of a C5A/C6B bispecific SEEDbody comprising the CV2 light chain, we demonstrated that this bsAb is able to bind both targets simultaneously. This further underlines the suitability of the concept of His-doped common light chains as a platform to engineer pH-responsive antibodies for mono- and bispecific antibody formats.

## CONCLUDING REMARKS

Several bispecific formats for CEACAM5 targeting were reported for cancer immunotherapy over the years such as an anti CEACAM5/CD3 BITE (MEDI-565/AMG 211) (44) or the head-to-tail 2:1 T cell bispecific antibody for treatment of CEA-positive solid tumors (45, 46) and others (47–49). pH-responsive binding has not been implemented yet in CEACAM5 targeting antibodies. Moreover, this type of bispecifics may be particularly useful for efficient removal of soluble targets that act as growth factors or suppress the induction of antitumor immunity such as TGF-β or IL10 (50) in combination with tumor cell binding or checkpoint inhibition. In conclusion, bispecific sweeping antibodies open new avenues for cancer treatment but will require sophisticated animal models to investigate their advantage over conventional formats. With the simple strategy described here, technical hurdles have been overcome on the road to novel sweeping antibody formats, but there is a long way to go for an in-depth examination of their potency in animals and eventually in humans.

## DATA AVAILABILITY

The raw data supporting the conclusions of this manuscript will be made available by the authors, without undue reservation, to any qualified researcher.

## AUTHOR CONTRIBUTIONS

JB, SH, and HK conceived and designed the experiments. JB, SH, and SK performed the experiments. JB, SH, JG, SK, and HK analyzed the data. JG, AE, and SZ gave scientific advice. JB, SH, SK, and HK wrote the paper.

## FUNDING

The authors declare that this study received funding from Merck KGaA and Merck Lab @ Technische Universität Darmstadt. The funders had no role in study design, data collection and analysis, decision to publish, or preparation of the manuscript.

## ACKNOWLEDGMENTS

We would like to thank the Departments of Protein Engineering and Antibody Technologies at Merck KGaA for material and technical support on plasmids, clones, and BLI measurements.

## SUPPLEMENTARY MATERIAL

The Supplementary Material for this article can be found online at: https://www.frontiersin.org/articles/10.3389/fimmu.2019.01892/full#supplementary-material

## REFERENCES


1. Hammarstrom S. The carcinoembryonic antigen (CEA) family: structures, suggested functions and expression in normal and malignant tissues. *Semin Cancer Biol.* (1999) 9:67–81. doi: 10.1006/scbi.1998.0119
2. Samara RN, Laguinge LM, Jessup JM. Carcinoembryonic antigen inhibits anoikis in colorectal carcinoma cells by interfering with TRAIL-R2 (DR5) signaling. *Cancer Res.* (2007) 67:4774–82. doi: 10.1158/0008-5472.Can-06-4315
3. Lee JH, Lee SW. The roles of carcinoembryonic antigen in liver metastasis and therapeutic approaches. *Gastroenterol Res Pract.* (2017) 2017:7521987. doi: 10.1155/2017/7521987
4. Gangopadhyay A, Bajenova O, Kelly TM, Thomas P. Carcinoembryonic antigen induces cytokine expression in kuppfer cells: implications for hepatic metastasis from colorectal cancer. *Cancer Res.* (1996) 56:4805–10.
5. Edmiston KH, Gangopadhyay A, Shoji Y, Nachman AP, Thomas P, Jessup JM. *In vivo* induction of murine cytokine production by carcinoembryonic antigen. *Cancer Res.* (1997) 57:4432–6.
6. Jessup JM, Laguinge L, Lin S, Samara R, Aufman K, Battle P, et al. Carcinoembryonic antigen induction of IL-10 and IL-6 inhibits hepatic ischemic/reperfusion injury to colorectal carcinoma cells. *Int J Cancer.* (2004) 111:332–7. doi: 10.1002/ijc.20264
7. Shibayama M, Maak M, Nitsche U, Gotoh K, Rosenberg R, Janssen KP. Prediction of metastasis and recurrence in colorectal cancer based on gene expression analysis: ready for the clinic? *Cancers.* (2011) 3:2858–69. doi: 10.3390/cancers3032858
8. Klein C, Waldhauer I, Nicolini VG, Freimoser-Grundschober A, Nayak T, Vugts DJ, et al. Cergutuzumab amunaleukin (CEA-IL2v), a CEA-targeted IL-2 variant-based immunocytokine for combination cancer immunotherapy: overcoming limitations of aldesleukin and conventional IL-2-based immunocytokines. *Oncoimmunology.* (2017) 6:e1277306. doi: 10.1080/2162402x.2016.1277306
9. Blumenthal RD, Hansen HJ, Goldenberg DM. Inhibition of adhesion, invasion, and metastasis by antibodies targeting CEACAM6 (NCA-90) and CEACAM5 (Carcinoembryonic Antigen). *Cancer Res.* (2005) 65:8809–17. doi: 10.1158/0008-5472.Can-05-0420
10. Blumenthal RD, Leon E, Hansen HJ, Goldenberg DM. Expression patterns of CEACAM5 and CEACAM6 in primary and metastatic cancers. *BMC Cancer.* (2007) 7:2. doi: 10.1186/1471-2407-7-2
11. Johnson B, Mahadevan D. Emerging role and targeting of carcinoembryonic antigen-related cell adhesion molecule 6 (CEACAM6) in human malignancies. *Clin Cancer Drugs.* (2015) 2:100–11. doi: 10.2174/2212697X02666150602215823
12. Dahlen E, Veitonmaki N, Norlen P. Bispecific antibodies in cancer immunotherapy. *Ther Adv Vaccines Immunother.* (2018) 6:3–17. doi: 10.1177/2515135518763280
13. Thakur A, Huang M, Lum LG. Bispecific antibody based therapeutics: strengths and challenges. *Blood Rev.* (2018) 32:339–47. doi: 10.1016/j.blre.2018.02.004
14. Suurs FV, Lub-de Hooge MN, de Vries EGE, de Groot DJA. A review of bispecific antibodies and antibody constructs in oncology and clinical challenges. *Pharmacol Ther.* (2019) doi: 10.1016/j.pharmthera.2019.04.006. [Epub ahead of print].
15. Loffler A, Kufer P, Lutterbuse R, Zettl F, Daniel PT, Schwenkenbecher JM, et al. A recombinant bispecific single-chain antibody, CD19 x CD3, induces rapid and high lymphoma-directed cytotoxicity by unstimulated T lymphocytes. *Blood.* (2000) 95:2098–103.
16. Ridgway JB, Presta LG, Carter P. 'Knobs-into-holes' engineering of antibody CH3 domains for heavy chain heterodimerization. *Protein Eng.* (1996) 9:617–21.
17. Atwell S, Ridgway JB, Wells JA, Carter P. Stable heterodimers from remodeling the domain interface of a homodimer using a phage display library. *J Mol Biol.* (1997) 270:26 35. doi: 10.1006/jmbi.1997.1116
18. Davis JH, Aperlo C, Li Y, Kurosawa E, Lan Y, Lo KM, et al. SEEDbodies: fusion proteins based on strand-exchange engineered domain (SEED) CH3 heterodimers in an Fc analogue platform for asymmetric binders or immunofusions and bispecific antibodies. *Protein Eng Des Sel.* (2010) 23:195–202. doi: 10.1093/protein/gzp094
19. Gunasekaran K, Pentony M, Shen M, Garrett L, Forte C, Woodward A, et al. Enhancing antibody Fc heterodimer formation through electrostatic steering effects: applications to bispecific molecules and monovalent IgG. *J Biol Chem.* (2010) 285:19637–46. doi: 10.1074/jbc.M110.117382
20. Von Kreudenstein TS, Escobar-Carbrera E, Lario PI, D'Angelo I, Brault K, Kelly J, et al. Improving biophysical properties of a bispecific antibody scaffold to aid developability: quality by molecular design. *MAbs.* (2013) 5:646–54. doi: 10.4161/mabs.25632
21. Merchant AM, Zhu Z, Yuan JQ, Goddard A, Adams CW, Presta LG, et al. An efficient route to human bispecific IgG. *Nat Biotechnol.* (1998) 16:677–81. doi: 10.1038/nbt0798-677
22. Van Blarcom T, Lindquist K, Melton Z, Cheung WL, Wagstrom C, McDonough D, et al. Productive common light chain libraries yield diverse panels of high affinity bispecific antibodies. *mAbs.* (2018) 10:256–68. doi: 10.1080/19420862.2017.1406570
23. Harris KE, Aldred SF, Davison LM, Ogana HAN, Boudreau A, Brüggemann M, et al. Sequence-based discovery demonstrates that fixed light chain human transgenic rats produce a diverse repertoire of antigen-specific antibodies. *Front Immunol.* (2018) 9:989. doi: 10.3389/fimmu.2018.00889
24. Krah S, Schröter C, Eller C, Rhiel L, Rasche N, Beck J, et al. Generation of human bispecific common light chain antibodies by combining animal immunization and yeast display. *Protein Eng Des Sel.* (2017) 30:291–301. doi: 10.1093/protein/gzw077
25. Igawa T, Mimoto F, Hattori K. pH-dependent antigen-binding antibodies as a novel therapeutic modality. *Biochim Biophys Acta.* (2014) 1844:1943–50. doi: 10.1016/j.bbapap.2014.08.003
26. O'Hear CE, Foote J. Antibody buffering of a ligand *in vivo*. *Proc Natl Acad Sci USA.* (2005) 102:40–4. doi: 10.1073/pnas.0405797102
27. Igawa T, Ishii S, Tachibana T, Maeda A, Higuchi Y, Shimaoka S, et al. Antibody recycling by engineered pH-dependent antigen binding improves the duration of antigen neutralization. *Nat Biotechnol.* (2010) 28:1203–7. doi: 10.1038/nbt.1691
28. Igawa T, Maeda A, Haraya K, Tachibana T, Iwayanagi Y, Mimoto F, et al. Engineered monoclonal antibody with novel antigen-sweeping activity *in vivo*. *PLoS ONE.* (2013) 8:e63236. doi: 10.1371/journal.pone.0063236
29. Schröter C, Günther R, Rhiel L, Becker S, Toleikis L, Doerner A, et al. A generic approach to engineer antibody pH-switches using combinatorial histidine scanning libraries and yeast display. *MAbs.* (2015) 7:138–51. doi: 10.4161/19420862.2014.985993
30. Rakestraw JA, Sazinsky SL, Piatesi A, Antipov E, Wittrup KD. Directed evolution of a secretory leader for the improved expression of heterologous proteins and full-length antibodies in *Saccharomyces cerevisiae*. *Biotechnol Bioeng.* (2009) 103:1192–201. doi: 10.1002/bit.22338
31. Benatuil L, Perez JM, Belk J, Hsieh CM. An improved yeast transformation method for the generation of very large human antibody libraries. *Protein Eng Des Sel.* (2010) 23:155–9. doi: 10.1093/protein/gzq002
32. Muda M, Gross AW, Dawson JP, He C, Kurosawa E, Schweickhardt R, et al. Therapeutic assessment of SEED: a new engineered antibody platform designed to generate mono- and bispecific antibodies. *Protein Eng Des Sel.* (2011) 24:447–54. doi: 10.1093/protein/gzq123
33. Arribas J, Borroto A. Protein ectodomain shedding. *Chem Rev.* (2002) 102:4627–38. doi: 10.1021/cr010202t
34. Kuang B, King L, Wang HF. Therapeutic monoclonal antibody concentration monitoring: free or total? *Bioanalysis.* (2010) 2:1125–40. doi: 10.4155/bio.10.64
35. Li L, Gardner I, Rose R, Jamei M. Incorporating target shedding into a minimal PBPK-TMDD model for monoclonal antibodies. *CPT Pharmacometrics Syst Pharmacol.* (2014) 3:e96. doi: 10.1038/psp.2013.73
36. Pak Y, Zhang Y, Pastan I, Lee B. Antigen shedding may improve efficiencies for delivery of antibody-based anticancer agents in solid tumors. *Cancer Res.* (2012) 72:3143–52. doi: 10.1158/0008-5472.CAN-11-3925
37. Vaupel P, Kallinowski F, Okunieff P. Blood flow, oxygen and nutrient supply, and metabolic microenvironment of human tumors: a review. *Cancer Res.* (1989) 49:6449–65.
38. Helmlinger G, Yuan F, Dellian M, Jain RK. Interstitial pH and pO2 gradients in solid tumors *in vivo*: high-resolution measurements reveal a lack of correlation. *Nat Med.* (1997) 3:177–82. doi: 10.1038/nm0297-177

39. Webb BA, Chimenti M, Jacobson MP, Barber DL. Dysregulated pH: a perfect storm for cancer progression. *Nat Rev Cancer.* (2011) 11:671. doi: 10.1038/nrc3110
40. Kontermann RE, Brinkmann U. Bispecific antibodies. *Drug Discov Today.* (2015) 20:838–47. doi: 10.1016/j.drudis.2015.02.008
41. Sedykh SE, Prinz VV, Buneva VN, Nevinsky GA. Bispecific antibodies: design, therapy, perspectives. *Drug Design Develop Ther.* (2018) 12:195–208. doi: 10.2147/DDDT.S151282
42. Murtaugh ML, Fanning SW, Sharma TM, Terry AM, Horn JR. A combinatorial histidine scanning library approach to engineer highly pH-dependent protein switches. *Protein Sci.* (2011) 20:1619–31. doi: 10.1002/pro.696
43. Huotari J, Helenius A. Endosome maturation. *Embo J.* (2011) 30:3481–500. doi: 10.1038/emboj.2011.286
44. Peng L, Oberst MD, Huang J, Brohawn P, Morehouse C, Lekstrom K, et al. The CEA/CD3-bispecific antibody MEDI-565 (MT111) binds a nonlinear epitope in the full-length but not a short splice variant of CEA. *PLoS ONE.* (2012) 7:e36412. doi: 10.1371/journal.pone.0036412
45. Bacac M, Fauti T, Sam J, Colombetti S, Weinzierl T, Ouaret D, et al. A novel carcinoembryonic antigen T-cell bispecific antibody (CEA TCB) for the treatment of solid tumors. *Clin Cancer Res.* (2016) 22:3286–97. doi: 10.1158/1078-0432.Ccr-15-1696
46. Bacac M, Klein C, Umana P. CEA TCB: a novel head-to-tail 2:1 T cell bispecific antibody for treatment of CEA-positive solid tumors. *Oncoimmunology.* (2016) 5:e1203498–e98. doi: 10.1080/2162402X.2016.1203498
47. Rozan C, Cornillon A, Petiard C, Chartier M, Behar G, Boix C, et al. Single-domain antibody-based and linker-free bispecific antibodies targeting FcgammaRIII induce potent antitumor activity without recruiting regulatory T cells. *Mol Cancer Ther.* (2013) 12:1481–91. doi: 10.1158/1535-7163.Mct-12-1012
48. Li L, He P, Zhou C, Jing L, Dong B, Chen S, et al. A novel bispecific antibody, S-Fab, induces potent cancer cell killing. *J Immunother.* (2015) 38:350–6. doi: 10.1097/cji.0000000000000099
49. Dong B, Zhou C, He P, Li J, Chen S, Miao J, et al. A novel bispecific antibody, BiSS, with potent anti-cancer activities. *Cancer Biol Ther.* (2016) 17:364–70. doi: 10.1080/15384047.2016.1139266
50. Jarnicki AG, Lysaght J, Todryk S, Mills KHG. Suppression of antitumor immunity by IL-10 and TGF-β-producing T cells infiltrating the growing tumor: influence of tumor environment on the induction of $CD4^+$ and $CD8^+$ regulatory T cells. *J. Immunol.* (2006) 177:896–904. doi: 10.4049/jimmunol.177.2.896


**Conflict of Interest Statement:** SK and SZ were employed by Merck KGaA.

The remaining authors declare that the research was conducted in the absence of any commercial or financial relationships that could be construed as a potential conflict of interest.

# *Supplementary Material*

## 1 Supplementary Figures

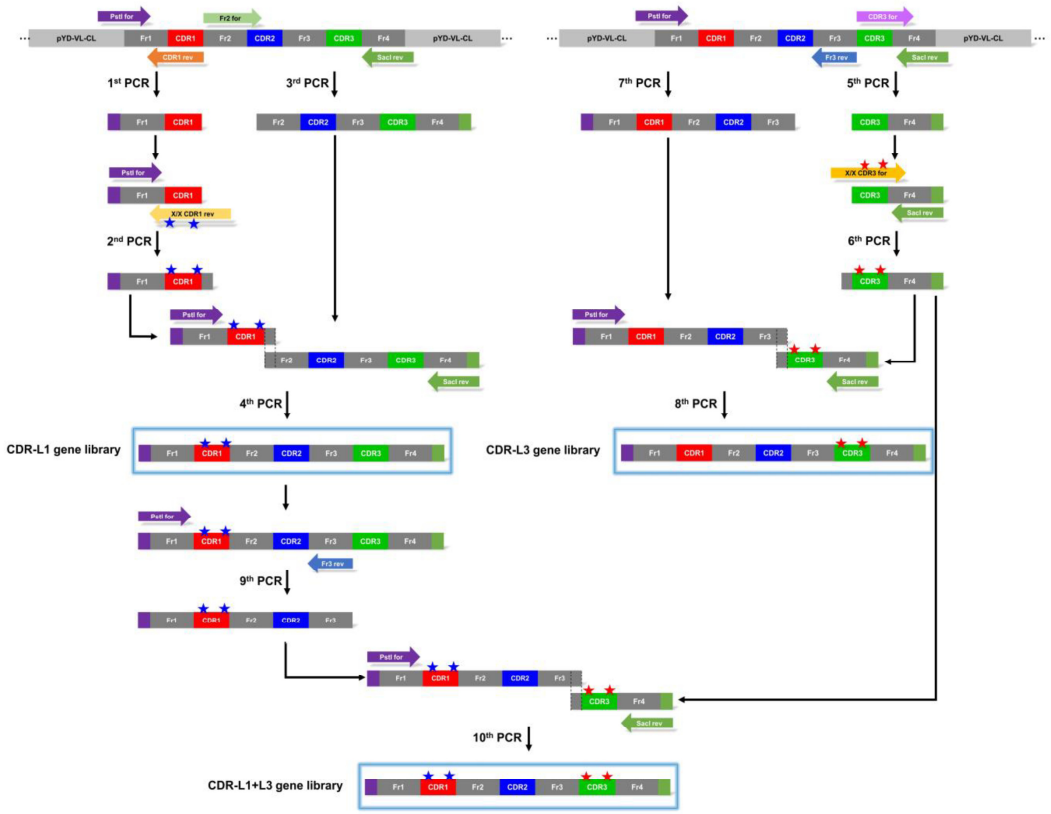


**SUPPLEMENTARY FIGURE S1 | Schematic illustration of the cloning strategy to generate a common light chain library in yeast with an elevated content of histidines**. The backbone of the pYD-VL-CL plasmid is shown in light gray, the sequences of the framework regions in dark gray, the CDR L1 in red, the CDR L2 in blue and the CDR L3 in green. Primers and their respective orientation are illustrated as arrows. Histidine substitutions in the CDR-L1 are shown as blue asterisks, in the CDR-L3 as red asterisks. PCR reactions are numbered. The amplified full-length genes (illustrated in blue frames) carry purple overhangs at the 5' end and dark green overhangs at the 3' overhang for

subsequent gap-repair. Overhangs for SOE-PCRs are illustrated as dotted lines. All sequences are orientated 5'→3'.

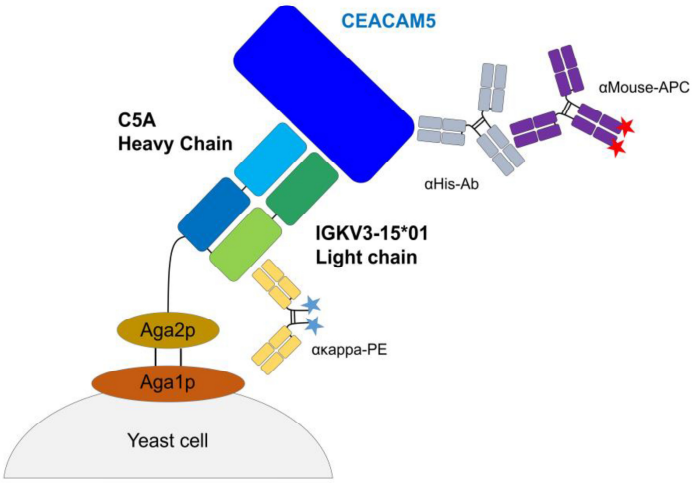


**SUPPLEMENTARY FIGURE S2 | Schematic depiction of yeast surface display for the isolation of pH-responsive, CEACAM5 specific Fab variants**. The VH-CH1 domains (bright or dark blue, respectively) were N-terminally fused to the Aga2p protein (brown) via a $(GGGS)_4$ linker, while the Λga2p protein was connected to the Λga1p membrane protein (orange) via two disulfide bridges. The corresponding light chain (bright or dark green, respectively) was covalently bound to the heavy chain via a cystine. The surface presentation of the Fab was verified by staining with a ακappe-PE $F(ab')_2$ antibody (yellow). The binding to CEACAM5 (royal blue) was detected via an αHis antibody (grey) and a secondary αMouse-APC antibody (violet).

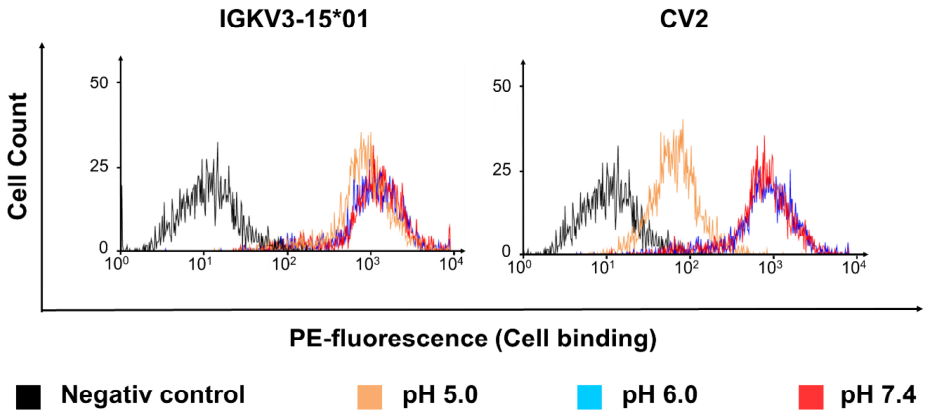


**SUPPLEMENTARY FIGURE S3 | Cell binding of oaSEEDbodies comprising C5A and IGKV3-15*01 or CV2 at different pH-values.** Around 4 × $10^5$ COLO 205 cells in 20 µl were stained with 3 µg of C5A-based oaSEEDbodies at different pH-values. For pH 7.4 and pH 6.0 PBS was used, while phosphate-citrate buffer was utilized at pH 5.0. Cell staining was performed as previously described by Krah and coworkers (24). Binding of the oaSEEDbodies was verified utilizing an anti-human Fc PE-antibody. Target binding is plotted on the x-axis (PE-fluorescence), cell count on the y-axis.

## 2 Supplementary Tables

**SUPPLEMENTARY TABLE S1** | Amino acid composition of drop-out media.

| Substance | Concentration in media (mg/mL) |
|---|---|
| L-Adenine hemisulfate | 40 |
| L-Arginine | 20 |
| L-Aspartic acid | 100 |
| L-Glutamic acid | 100 |
| L-Histidine | 20 |
| L-Lysine | 30 |
| L-Methionine | 20 |
| L-Phenylalanine | 50 |
| L-Serine | 375 |
| L-Threonine | 200 |
| L-Tryptophan | 40 |
| L-Tyrosine | 30 |
| L-Valine | 150 |
| Uracil | 20 |

3

**SUPPLEMENTARY TABLE S2** | Oligonucleotides for the incorporation of histidines into the IGKV3-15*01 light chain. Mutations were incorporated either in the CDR-L1 or CDR-L3, respectively. The numbering refers to the Chothia numbering scheme. Mutagenesis sites are highlighted.

| Name | | | | Nucleotide sequence (5' --> 3') |
|---|---|---|---|---|
| Position of histidine incorporation | Orientation | CDR | Template | |
| **24/25** | rev | CDR1 | pYD-VL-CL | GTTTTTGTTGATACCAAGCCAAGTTAGAAGAAACGGATTGAGA **ATGATG**ACAAGACAATGTAGC |
| **24/26** | rev | CDR1 | pYD-VL-CL | GTTTTTGTTGATACCAAGCCAAGTTAGAAGAAACGGATTG**ATG** AGC**ATG**ACAAGACAATGTAGC |
| **24/27** | rev | CDR1 | pYD-VL-CL | GTTTTTGTTGATACCAAGCCAAGTTAGAAGAAACGGA**ATG**AGA AGC**ATG**ACAAGACAATGTAGC |
| **24/28** | rev | CDR1 | pYD-VL-CL | GTTTTTGTTGATACCAAGCCAAGTTAGAAGAAAC**ATG**TTGAGA AGC **ATG**ACAAGACAATGTAGC |
| **24/29** | rev | CDR1 | pYD-VL-CL | GTTTTTGTTGATACCAAGCCAAGTTAGAAGA**ATG**GGATTGAGA AGC**ATG**ACAAGACAATGTAGC |
| **24/30** | rev | CDR1 | pYD-VL-CL | GTTTTTGTTGATACCAAGCCAAGTTAGA**ATG**AACGGATTGAGA AGC**ATG**ACAAGACAATGTAGC |
| **24/31** | rev | CDR1 | pYD-VL-CL | GTTTTTGTTGATACCAAGCCAAGTT**ATG**AGAAACGGATTGAGA AGC**ATG**ACAAGACAATGTAGC |
| **24/32** | rev | CDR1 | pYD-VL-CL | GTTTTTGTTGATACCAAGCCAA**ATG**AGAAGAAACGGATTGAGA AGC**ATG**ACAAGACAATGTAGC |
| **24/33** | rev | CDR1 | pYD-VL-CL | GTTTTTGTTGATACCAAGC**ATG**GTTAGAAGAAACGGATTGAGA AGC**ATG**ACAAGACAATGTAGC |
| **24/34** | rev | CDR1 | pYD-VL-CL | GTTTTTGTTGATACCA**ATG**CAAGTTAGAAGAAACGGATTGAGA AGC**ATG**ACAAGACAATGTAGC |
| **25/26** | rev | CDR1 | pYD-VL-CL | GTTTTTGTTGATACCAAGCCAAGTTAGAAGAAACGGATTG**ATG** **ATG** TCTACAAGACAATGTAGC |
| **25/27** | rev | CDR1 | pYD-VL-CL | GTTTTTGTTGATACCAAGCCAAGTTAGAAGAAACGGA**ATG**AGA **ATG**TCTACAAGACAATGTAGC |
| **25/28** | rev | CDR1 | pYD-VL-CL | GTTTTTGTTGATACCAAGCCAAGTTAGAAGAAAC**ATG**TTGAGA **ATG** TCTACAAGACAATGTAGC |
| **25/29** | rev | CDR1 | pYD-VL-CL | GTTTTTGTTGATACCAAGCCAAGTTAGAAGA**ATG**GGATTGAGA **ATG** TCTACAAGACAATGTAGC |
| **25/30** | rev | CDR1 | pYD-VL-CL | GTTTTTGTTGATACCAAGCCAAGTTAGA**ATG**AACGGATTGAGA **ATG** TCTACAAGACAATGTAGC |
| **25/31** | rev | CDR1 | pYD-VL-CL | GTTTTTGTTGATACCAAGCCAAGTT**ATG**AGAAACGGATTGAGA **ATG** TCTACAAGACAATGTAGC |
| **25/32** | rev | CDR1 | pYD-VL-CL | GTTTTTGTTGATACCAAGCCAA**ATG**AGAAGAAACGGATTGAGA **ATG**TCTACAAGACAATGTAGC |
| **25/33** | rev | CDR1 | pYD-VL-CL | GTTTTTGTTGATACCAAGC**ATG**GTTAGAAGAAACGGATTGAGA **ATG** TCTACAAGACAATGTAGC |
| **25/34** | rev | CDR1 | pYD-VL-CL | GTTTTTGTTGATACCA**ATG**CAAGTTAGAAGAAACGGATTGAGA **ATG**TCTACAAGACAATGTAGC |
| **26/27** | rev | CDR1 | pYD-VL-CL | GTTTTTGTTGATACCAAGCCAAGTTAGAAGAAACGGA**ATGATG** AGCTCTACAAGACAATGTAGC |
| **26/28** | rev | CDR1 | pYD-VL-CL | GTTTTTGTTGATACCAAGCCAAGTTAGAAGAAAC**ATG**TTG**ATG** AGC TCTACAAGACAATGTAGC |

| | | | | |
|---|---|---|---|---|
| **26/29** | rev | CDR1 | pYD-VL-CL | GTTTTTGTTGATACCAAGCCAAGTTAGAAGAATGGGATTGATG AGCTCTACAAGACAATGTAGC |
| **26/30** | rev | CDR1 | pYD-VL-CL | GTTTTTGTTGATACCAAGCCAAGTTAGAATGAACGGATTGATG AGC TCTACAAGACAATGTAGC |
| **26/31** | rev | CDR1 | pYD-VL-CL | GTTTTTGTTGATACCAAGCCAAGTTATGAGAAACGGATTGATG AGC TCTACAAGACAATGTAGC |
| **26/32** | rev | CDR1 | pYD-VL-CL | GTTTTTGTTGATACCAAGCCAAATGAGAAGAAACGGATTGATG AGCTCTACAAGACAATGTAGC |
| **26/33** | rev | CDR1 | pYD-VL-CL | GTTTTTGTTGATACCAAGCATGGTTAGAAGAAACGGATTGATG AGC TCTACAAGACAATGTAGC |
| **26/34** | rev | CDR1 | pYD-VL-CL | GTTTTTGTTGATACCAATGCAAGTTAGAAGAAACGGATTGATG AGC TCTACAAGACAATGTAGC |
| **27/28** | rev | CDR1 | pYD-VL-CL | GTTTTTGTTGATACCAAGCCAAGTTAGAAGAAACATGATGAGA AGC TCTACAAGACAATGTAGC |
| **27/29** | rev | CDR1 | pYD-VL-CL | GTTTTTGTTGATACCAAGCCAAGTTAGAAGAATGGGAATGAGA AGCTCTACAAGACAATGTAGC |
| **27/30** | rev | CDR1 | pYD-VL-CL | GTTTTTGTTGATACCAAGCCAAGTTAGAATGAACGGAATGAGA AGCTCTACAAGACAATGTAGC |
| **27/31** | rev | CDR1 | pYD-VL-CL | GTTTTTGTTGATACCAAGCCAAGTTATGAGAAACGGAATGAGA AGCTCTACAAGACAATGTAGC |
| **27/32** | rev | CDR1 | pYD-VL-CL | GTTTTTGTTGATACCAAGCCAAATGAGAAGAAACGGAATGAGA AGCTCTACAAGACAATGTAGC |
| **27/33** | rev | CDR1 | pYD-VL-CL | GTTTTTGTTGATACCAAGCATGGTTAGAAGAAACGGAATGAGA AGCTCTACAAGACAATGTAGC |
| **27/34** | rev | CDR1 | pYD-VL-CL | GTTTTTGTTGATACCAATGCAAGTTAGAAGAAACGGAATGAGA AGCTCTACAAGACAATGTAGC |
| **28/29** | rev | CDR1 | pYD-VL-CL | GTTTTTGTTGATACCAAGCCAAGTTAGAAGAATGATGTTGAGA AGC TCTACAAGACAATGTAGC |
| **28/30** | rev | CDR1 | pYD-VL-CL | GTTTTTGTTGATACCAAGCCAAGTTAGAATGAACATGTTGAGA AGC TCTACAAGACAATGTAGC |
| **28/31** | rev | CDR1 | pYD-VL-CL | GTTTTTGTTGATACCAAGCCAAGTTATGAGAAACATGTTGAGA AGC TCTACAAGACAATGTAGC |
| **28/32** | rev | CDR1 | pYD-VL-CL | GTTTTTGTTGATACCAAGCCAAATGAGAAGAAACATGTTGAGA AGCTCTACAAGACAATGTAGC |
| **28/33** | rev | CDR1 | pYD-VL-CL | GTTTTTGTTGATACCAAGCATGGTTAGAAGAAACATGTTGAGA AGC TCTACAAGACAATGTAGC |
| **28/34** | rev | CDR1 | pYD-VL-CL | GTTTTTGTTGATACCAATGCAAGTTAGAAGAAACATGTTGAGA AGC TCTACAAGACAATGTAGC |
| **29/30** | rev | CDR1 | pYD-VL-CL | GTTTTTGTTGATACCAAGCCAAGTTAGAATGATGGGATTGAGA AGC TCTACAAGACAATGTAGC |
| **29/31** | rev | CDR1 | pYD-VL-CL | GTTTTTGTTGATACCAAGCCAAGTTATGAGAATGGGATTGAGA AGCTCTACAAGACAATGTAGC |
| **29/32** | rev | CDR1 | pYD-VL-CL | GTTTTTGTTGATACCAAGCCAAATGAGAAGAATGGGATTGAGA AGCTCTACAAGACAATGTAGC |
| **29/33** | rev | CDR1 | pYD-VL-CL | GTTTTTGTTGATACCAAGCATGGTTAGAAGAATGGGATTGAGA AGCTCTACAAGACAATGTAGC |
| **29/34** | rev | CDR1 | pYD-VL-CL | GTTTTTGTTGATACCAATGCAAGTTAGAAGAATGGGATTGAGA AGCTCTACAAGACAATGTAGC |
| **30/31** | rev | CDR1 | pYD-VL-CL | GTTTTTGTTGATACCAAGCCAAGTTATGATGAACGGATTGAGA AGC TCTACAAGACAATGTAGC |
| **30/32** | rev | CDR1 | pYD-VL-CL | GTTTTTGTTGATACCAAGCCAAATGAGAATGAACGGATTGAGA AGCTCTACAAGACAATGTAGC |

5

| | | | | |
|---|---|---|---|---|
| **30/33** | rev | CDR1 | pYD-VL-CL | GTTTTTGTTGATACCAAGC**ATG**GTTAGA**ATG**AACGGATTGAGA AGCTCTACAAGACAATGTAGC |
| **30/34** | rev | CDR1 | pYD-VL-CL | GTTTTTGTTGATACCA**ATG**CAAGTTAGA**ATG**AACGGATTGAGA AGCTCTACAAGACAATGTAGC |
| **31/32** | rev | CDR1 | pYD-VL-CL | GTTTTTGTTGATACCAAGCCAA**ATGATG**AGAAACGGATTGAGA AGCTCTACAAGACAATGTAGC |
| **31/33** | rev | CDR1 | pYD-VL-CL | GTTTTTGTTGATACCAAGC**ATG**GTT**ATG**AGAAACGGATTGAGA AGCTCTACAAGACAATGTAGC |
| **31/34** | rev | CDR1 | pYD-VL-CL | GTTTTTGTTGATACCA**ATG**CAAGTT**ATG**AGAAACGGATTGAGA AGCTCTACAAGACAATGTAGC |
| **32/33** | rev | CDR1 | pYD-VL-CL | GTTTTTGTTGATACCAAGC**ATGATG**AGAAGAAACGGATTGAGA AGCTCTACAAGACAATGTAGC |
| **32/34** | rev | CDR1 | pYD-VL-CL | GTTTTTGTTGATACCA**ATG**CAA**ATG**AGAAGAAACGGATTGAGA AGCTCTACAAGACAATGTAGC |
| **33/34** | rev | CDR1 | pYD-VL-CL | GTTTTTGTTGATACCA**ATGATG**GTTAGAAGAAACGGATTGAGA AGCTCTACAAGACAATGTAGC |
| **24/31/32** | rev | CDR1 | pYD-VL-CL | GTTTTTGTTGATACCAAGCCAA**ATGATG**AGAAACGGATTGAGA AGC**ATG**ACAAGACAATGTAGCTCTTTC |
| **89/90** | for | CDR3 | pYD-VL-CL | GCTGTTTACTACTGC**CATCAT**TACAACAATTGGCCATGGACTTT TGGTCAAG |
| **89/91** | for | CDR3 | pYD-VL-CL | GCTGTTTACTACTGC**CAT**CAA**CAT**AACAATTGGCCATGGACTTT TGGTCAAG |
| **89/92** | for | CDR3 | pYD-VL-CL | GCTGTTTACTACTGC**CAT**CAATAC**CAT**AATTGGCCATGGACTTT TGGTCAAG |
| **89/93** | for | CDR3 | pYD-VL-CL | GCTGTTTACTACTGC**CAT**CAATACAAC**CAT**TGGCCATGGACTTT TGGTCAAG |
| **89/94** | for | CDR3 | pYD-VL-CL | GCTGTTTACTACTGC**CAT**CAATACAACAAT**CAT**CCATGGACTTT TGGTCAAG |
| **89/95** | for | CDR3 | pYD-VL-CL | GCTGTTTACTACTGC**CAT**CAATACAACAATTGG**CAT**TGGACTTT TGGTCAAG |
| **89/96** | for | CDR3 | pYD-VL-CL | GCTGTTTACTACTGC**CAT**CAATACAACAATTGGCCA**CAT**ACTTT TGGTCAAG |
| **89/97** | for | CDR3 | pYD-VL-CL | GCTGTTTACTACTGC**CAT**CAATACAACAATTGGCCATGG**CAT**TT TGGTCAAG |
| **90/91** | for | CDR3 | pYD-VL-CL | GCTGTTTACTACTGCCAA**CATCAT**AACAATTGGCCATGGACTTT TGGTCAAG |
| **90/92** | for | CDR3 | pYD-VL-CL | GCTGTTTACTACTGCCAA**CAT**TAC**CAT**AATTGGCCATGGACTTT TGGTCAAG |
| **90/93** | for | CDR3 | pYD-VL-CL | GCTGTTTACTACTGCCAA**CAT**TACAAC**CAT**TGGCCATGGACTTT TGGTCAAG |
| **90/94** | for | CDR3 | pYD-VL-CL | GCTGTTTACTACTGCCAA**CAT**TACAACAAT**CAT**CCATGGACTTT TGGTCAAG |
| **90/95** | for | CDR3 | pYD-VL-CL | GCTGTTTACTACTGCCAA**CAT**TACAACAATTGG**CAT**TGGACTTT TGGTCAAG |
| **90/96** | for | CDR3 | pYD-VL-CL | GCTGTTTACTACTGCCAA**CAT**TACAACAATTGGCCA**CAT**ACTTT TGGTCAAG |
| **90/97** | for | CDR3 | pYD-VL-CL | GCTGTTTACTACTGCCAA**CAT**TACAACAATTGGCCATGG**CAT**TT TGGTCAAG |
| **91/92** | for | CDR3 | pYD-VL-CL | GCTGTTTACTACTGCCAACAA**CATCAT**AATTGGCCATGGACTTT TGGTCAAG |
| **91/93** | for | CDR3 | pYD-VL-CL | GCTGTTTACTACTGCCAACAA**CAT**AAC**CAT**TGGCCATGGACTTT TGGTCAAG |
| **91/94** | for | CDR3 | pYD-VL-CL | GCTGTTTACTACTGCCAACAA**CAT**AACAAT**CAT**CCATGGACTTT TGGTCAAG |
| **91/95** | for | CDR3 | pYD-VL-CL | GCTGTTTACTACTGCCAACAA**CAT**AACAATTGG**CAT**TGGACTTT TGGTCAAG |
| **91/96** | for | CDR3 | pYD-VL-CL | GCTGTTTACTACTGCCAACAA**CAT**AACAATTGGCCA**CAT**ACTTT TGGTCAAG |
| **91/97** | for | CDR3 | pYD-VL-CL | GCTGTTTACTACTGCCAACAA**CAT**AACAATTGGCCATGG**CAT**TT TGGTCAAG |
| **92/93** | for | CDR3 | pYD-VL-CL | GCTGTTTACTACTGCCAACAATAC**CATCAT**TGGCCATGGACTTT TGGTCAAG |

| | | | | |
|---|---|---|---|---|
| **92/94** | for | CDR3 | pYD-VL-CL | GCTGTTTACTACTGCCAACAATAC**CAT**AAT**CAT**CCATGGACTTT TGGTCAAG |
| **92/95** | for | CDR3 | pYD-VL-CL | GCTGTTTACTACTGCCAACAATAC**CAT**AATTGG**CAT**TGGACTTT TGGTCAAG |
| **92/96** | for | CDR3 | pYD-VL-CL | GCTGTTTACTACTGCCAACAATAC**CAT**AATTGGCCA**CAT**ACTTT TGGTCAAG |
| **92/97** | for | CDR3 | pYD-VL-CL | GCTGTTTACTACTGCCAACAATAC**CAT**AATTGGCCATGG**CAT**TT TGGTCAAG |
| **93/94** | for | CDR3 | pYD-VL-CL | GCTGTTTACTACTGCCAACAATACAAC**CATCAT**CCATGGACTTT TGGTCAAG |
| **93/95** | for | CDR3 | pYD-VL-CL | GCTGTTTACTACTGCCAACAATACAAC**CAT**TGG**CAT**TGGACTTT TGGTCAAG |
| **93/96** | for | CDR3 | pYD-VL-CL | GCTGTTTACTACTGCCAACAATACAAC**CAT**TGGCCA**CAT**ACTTT TGGTCAAG |
| **93/97** | for | CDR3 | pYD-VL-CL | GCTGTTTACTACTGCCAACAATACAAC**CAT**TGGCCATGG**CAT**TT TGGTCAAG |
| **94/95** | for | CDR3 | pYD-VL-CL | GCTGTTTACTACTGCCAACAATACAACAAT**CATCAT**TGGACTTT TGGTCAAG |
| **94/96** | for | CDR3 | pYD-VL-CL | GCTGTTTACTACTGCCAACAATACAACAAT**CAT**CCA**CAT**ACTTT TGGTCAAG |
| **94/97** | for | CDR3 | pYD-VL-CL | GCTGTTTACTACTGCCAACAATACAACAAT**CAT**CCATGG**CAT**TT TGGTCAAG |
| **95/96** | for | CDR3 | pYD-VL-CL | GCTGTTTACTACTGCCAACAATACAACAATTGG**CATCAT**ACTTT TGGTCAAG |
| **95/97** | for | CDR3 | pYD-VL-CL | GCTGTTTACTACTGCCAACAATACAACAATTGG**CAT**TGG**CAT**TT TGGTCAAG |
| **96/97** | for | CDR3 | pYD-VL-CL | GCTGTTTACTACTGCCAACAATACAACAATTGGCCA**CATCAT**TT TGGTCAAG |
| **97** | for | CDR3 | pYD-VL-CL | GCTGTTTACTACTGCCAACAATACAACAATTGGCCATGG**CAT**TT TGGTCAAGGTACTAAGG |

**SUPPLEMENTARY TABLE 3** | Primer sequences for cloning.

| Name | | | Nucleotide sequence (5' --> 3') |
|---|---|---|---|
| **PstI** | for | pYD-VL-CL | CATTTTCAATTAAGACCATGAGATTTCCTTCAATTTTTACTGCAGTTTTA TTC |
| **SacI** | rev | pYD-VL-CL | CTATTAACACTCTCCCCTGTTGAAGCTCTTTGTGACGGGCGAG |
| **Fr2** | for | pYD-VL-CL | TGGTATCAACAAAAACCAGGTCAAGCTCCAAGATTATTG |
| **CDR1** | rev | pYD-VL-CL | AGCCAAGTTAGAAGAAACGGATTGAGAAGCTCTACAAGAC |
| **Fr3** | rev | pYD-VL-CL | GCAGTAGTAAACAGCGAAATCTTCGGATTGCAATG |
| **CDR3** | for | pYD-VL-CL | CAACAATACAACAATTGGCCATGGACTTTTGGTCAAGG |
| **pTT5 seq** | for | pTT5-VL-CL | CTGCGCTAAGATTGTCAGT |
| **I CLC to pTT5** | for | pTT5-VL-CL | GCTGCCTGTCAGACTGCTGGTGCTGATGTTCTGGATTCCCGCCAGCCTG AGCGAAATCGTCATGACTCAATC |
| **II CLC to pTT5** | for | pTT5-VL-CL | GTTTAAACGGATCTCTAGCGAATTCGCGGTCGCCACCATGAAGCTGCC TGTCAGACTGC |
| **Fr3 EcoRI mut** | for | pTT5-VL-CL | CTGGTTCAGGTACTGAGTTCACCTTGACTATC |
| **Fr3 EcoRI mut** | rev | pTT5-VL-CL | GATAGTCAAGGTGAACTCAGTACCTGAACCAG |
| **CLC to pTT5** | rev | pTT5-VL-CL | AGAGGTCGAGGTCGGGGGATCCTCATCAACACTCTCCCCTGTTGAAGC |

## 4.2 Simplifying the Detection of Surface Presentation Levels in Yeast Surface Display by Intracellular tGFP Expression

Title:

Simplifying the Detection of Surface Presentation Levels in Yeast Surface Display by Intracellular tGFP Expression

Authors:

**Steffen C. Hinz***, Adrian Elter*, Julius Grzeschik, Jan Habermann, Bastian Becker, Harald Kolmar

* Authors contributed equally

Bibliographic data:

*Methods in Molecular Biology*

Volume 2070, Pages: 211-222.

Article first published online: 18.10.2019 | DOI: 10.1007/978-1-4939-9853-1_12



Contribution by S. C. Hinz:

- Performed experiments for validating the presented protocols
- Involved in writing and revising the manuscript

# Chapter 12

# Simplifying the Detection of Surface Presentation Levels in Yeast Surface Display by Intracellular tGFP Expression

**Steffen C. Hinz, Adrian Elter, Julius Grzeschik, Jan Habermann, Bastian Becker, and Harald Kolmar**

## Abstract

Yeast surface display (YSD) is an ultra-high throughput method used in protein engineering. Protein-protein interactions as well as surface presentation on the yeast cell surface are verified through fluorophore-conjugated labeling agents.

In this chapter we describe an improved setup for full-length surface presentation detection. To this end, we used a single open reading frame (ORF) encoding for the protein to be displayed and a 2A sequence and tGFP for an intracellular fluorescence signal. The 2A sequence allows the simultaneous generation of two separate proteins from the same ORF through ribosomal skipping. The entangled expression of the POI on the yeast surface and intracellular tGFP obviates the need for fluorescent staining steps.

**Key words** T2A, 2A peptide, Yeast surface display, GFP, Ribosomal skipping

## 1 Introduction

Yeast surface display is a commonly used technology for ultra-high throughput screenings in protein engineering [1, 2]. It relies on the genotype-phenotype coupling of yeast cells with every yeast cell expressing one defined protein variant on the cell surface [3]. Successful usage of yeast surface display is reported for proteases, antibody fragments, and other proteins [4]. The surface presentation is usually detected by fluorescence staining of peptide tags (FLAG, HA, c-Myc) combined with detection of antigen binding. Since the staining of different peptide-epitopes requires orthogonal labeling agents, the staining can be time-consuming and requires the production or purchase of labeling agents.

2A peptides are virus-derived polypeptide sequences described for different virus strains. They are located between virus proteins

Steffen C. Hinz and Adrian Elter contributed equally to this work.

Stefan Zielonka and Simon Krah (eds.), *Genotype Phenotype Coupling: Methods and Protocols*, Methods in Molecular Biology, vol. 2070, https://doi.org/10.1007/978-1-4939-9853-1_12, © Springer Science+Business Media, LLC, part of Springer Nature 2020

and enable the "cleavage" of these proteins during translation utilizing a unique "skipping" mechanism. This mechanism comprises the formation of a helical structure of the nascent polypeptide chain during the ribosomal translation and the nucleophilic attack of a water molecule resulting in an interruption of the polypeptide chain elongation without stopping the translation itself. The 18–22 amino acid-containing 2A peptides derived from different virus strains differ in their skipping efficiency while comprising a preserved C-terminal "GDVEXNPGP" motif [5]. Skipping occurs between the glycine and proline located at the C-terminus of the 2A peptide preventing the glycyl-prolyl peptide bond from forming [6, 7]. Chng et al. identified the 2A peptide derived from the *thosea asigna* virus (abbreviated T2A) to have nearly 100% cleaving efficiency in CHO cells [8].

In this chapter, we describe the coupling of the expression of a protein of interest (POI) with tGFP via utilization of the T2A peptide. According to the gene sequence (5′-POI-T2A-tGFP-3′), translation of the T2A gene is necessary for tGFP expression. This allows to identify POI-presenting yeast cells through microscopy or flow cytometry. The bicistronic construct allows tGFP to accumulate intracellular, whereas the POI is presented on the yeast cell surface [9, 10]. This enables the circumvention of labeling for surface presentation, saving time and labeling agents (Fig. 2).

In more detail, we describe the construction of a T2A-tGFP-containing plasmid for yeast surface display which allows the detection of full-length expression and surface presentation through intracellular tGFP fluorescence. Herein, we elaborate on the generation of a single clone construct, but this cloning strategy can be adjusted for the generation of large YSD libraries (Fig. 2).

## 2 Materials

All buffers and solutions were prepared with MilliQ $H_2O$ unless declared otherwise.

### 2.1 Single Clone Construction for Yeast Surface Display

1. *Bam*HI-HF (New England Biolabs).
2. *Xho*I-HF (New England Biolabs).
3. 10× CutSmart buffer (New England Biolabs).
4. *pCT* plasmid [3].
5. Yeast strain: EBY100.
6. YPD media: 20 g/L D(+)-glucose, 20 g/L tryptone, 10 g/L yeast extract.

7. *Buffer* A: 1 M Tris–HCl, 2.5 M dithiothreitol (DTT).
8. *Buffer* E: 10 mM Tris–HCl, 270 mM sucrose 1 mM $MgCl_2$.
9. Electroporator Gene Pulser Xcell™ (Bio-Rad, Dreieich, Germany).
10. 0.2 cm electroporation cuvettes (Bio-Rad).
11. Bacto™ Casamino acids (BD Biosciences, San Jose, USA).
12. SD-CAA: 8.6 g/L $NaH_2PO_4$ $H_2O$, 5.4 g/L $Na_2HPO_4$, 20 g/L D(+)-galactose, 6.7 g/L yeast nitrogen base without amino acids, 5 g/L Bacto™ casamino acids.
13. SD-CAA agar plates: 8.6 g/L $NaH_2PO_4{\cdot}H_2O$, 5.4 g/L $Na_2HPO_4$, 20 g/L D(+)-galactose, 6.7 g/L yeast nitrogen base without amino acids, 5 g/L Bacto™ casamino acids, 5–10 g/L agar–agar.
14. 9 cm Petri dishes.

### 2.2 Oligonucleotides

The utilized oligonucleotides are listed in Table 1.

**Table 1**
**Oligonucleotides for the construction of the tGFP containing pCT-based plasmid and the randomization of a vNAR fragment**

| Primer | Sequence |
|---|---|
| *c-myc-T2A_up* | CACTGTGACTGTGAAAGGATCCGAGCAAAAGCTTATTTCTGAAGAGGACTTGGAGGGCCGCGG |
| *T2A_tGFP_lo* | GGTAATACGACATTCAATTTCCATTGGGCC |
| *tGFP_up* | GGCCCAATGGAAATTGAATGTCGTATTACC |
| *Term_lo* | TTTGTTACATCTACACTGTTGTTATCAGATCTCGAGCTATTATTCTTCACC |
| *CDR1rand_up* | ACCATCAATTGCGTCCTAAAA$(XXX)_5$TTGGGTAGCACGTACTGGTATTTCACAAAGAAG |
| *H3_Mat_lo* | GCTGCCGCGGCCCTCGGATCCWTTCACAGTCASARKGGTSCCSCCNCC |
| *FR1_up* | ATGGCCGCACGGCTTGAACAAACACCGACAACGACAACAAAGGAGGCAGGCGAATCACTGACCATCAATTGCGTCCTAA |
| *H3_gr2_up* | GTGGTGGTGGTTCTGGTGGTGGTGGTTCTGCTAGCATGGCCGCACGGCTTGAACA |
| *H3_Mat_2A_lo* | CCTCCACGTCGCCGCAGGTCAGCAGGCTGCCGCGGCCCTCGGATCCWTTC |
| *pCT_seq_up* | TACGACGTTCCAGACTACGCTCTGCAGGCT |
| *pCT_seq_lo* | AGTTGGTAACGGAACGAAAAATAGAAA |

## 3 Methods

Herein we describe the construction and implementation of a T2A-tGFP gene string into a yeast surface display plasmid (pCT) and subsequent flow cytometry analysis.

### 3.1 Single Clone Construction: Insert

Starting with the T2A genestring and the already amplified tGFP gene, the first PCR is necessary to fuse the T2A with the fluorescent protein (tGFP in this case) which is later used as an indicator for full-length expression. The T2A gene is complemented with the c-Myc-tag at 5′ for yeast homologous recombination, whereas the tGFP is complemented 3′ with the first 30 nucleotides of the terminator (Fig. 1).

1. Amplify the T2A gene using the primers *c-myc_T2A_up* and *T2A_tGFP_lo* to incorporate the 5′ c-Myc-Tag and a tGFP compatible overhang for fusion PCR. The detailed PCR protocol is listed in Table 2 (PCR 1).
2. Utilize the primers *tGFP_up* and *term_lo* for amplification (Table 2, PCR 2) of the tGFP gene including the 3′ overhang for homologous recombination and the 5′ end for gene fusion with the T2A gene.
3. Prepare a PCR reaction mixture with the purified T2A gene amplicon and the purified tGFP amplicon in an equimolar ratio. After 10 cycles with an annealing temperature of 72 °C and an elongation time of 30 s, add 1 µL of 1 µM *c-myc-T2A_up* and 1 µL of 1 µM *term_lo* primers, and continue the PCR for 20 cycles with given properties. The incubation times and temperatures are listed in Table 2 (PCR 3). Verify the presence of a 792 bp fragment by agarose gel electrophoresis with a 1% (w/v) agarose gel. Purify the amplicons with a PCR purification kit and determine the concentration and the total amount of insert DNA.

### 3.2 Single Clone Construction: Backbone

1. Digest 5 µg of pCT plasmid with 5 U *Xho*I-HF® and 5 U *Bam*HI-HF® overnight at 37 °C. Perform the digestion in a reaction volume of 50 µL. Supplement the solution with 5 µL of CutSmart (10×) buffer and complement nuclease-free water to a total volume of 50 µL.
2. Verify the digestion via agarose gel analysis with a 1% (w/v) agarose gel and purify the digested plasmid. Use a PCR cleanup kit (we use the Wizard® SV Gel and PCR Clean-Up System manufactured by Promega) to purify the plasmid according to the kit's manual. Determine the plasmid concentration after the cleanup.

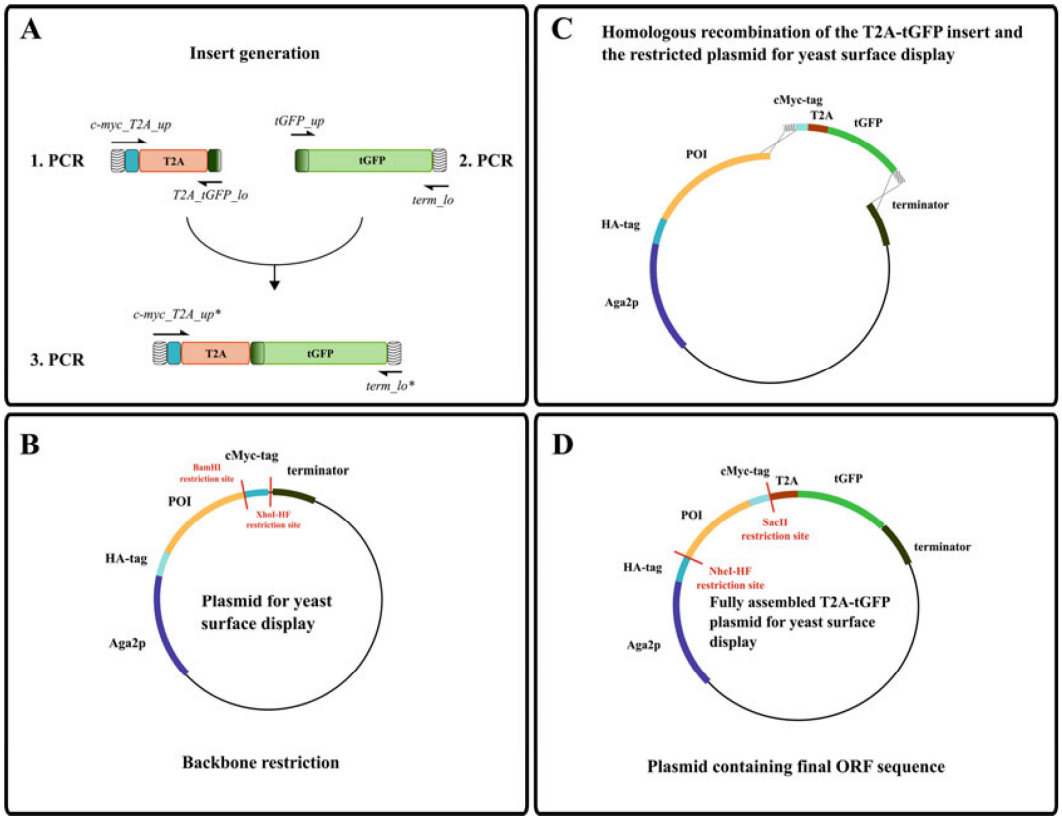


**Fig. 1** PCR strategy and plasmid preparation for the implementation of a T2A-tGFP-containing plasmid for yeast surface display. (**a**) The insert is generated in three consecutive PCRs. The c-Myc-T2A gene fragment is amplified with the 5′ overhangs for homologous recombination in yeast. The tGFP gene is amplified in parallel with overhangs for homologous recombination at the 3′ site. Both gene fragments are fused by fusion PCR through shared nucleotide sequences between the T2A and the tGFP gene and subsequent amplification with the primers *c-myc_T2A_up* and *term_lo* after the first 10 PCR cycles without additional primers. Asterisks indicate the time-displaced additions of both primers. (**b**) The plasmid for yeast surface display is restricted with *Bam*HI and *Xho*I and subsequently purified for the gapping procedure. (**c**) The T2A-tGFP containing plasmid is assembled through homologous recombination in yeast. The necessary nucleotide overhangs are depicted black-striped at the end of the insert. (**d**) Fully assembled plasmid with the T2A and tGFP genes with the endonuclease restriction sites for further cloning experiments depicted in red with the respective endonuclease

### *3.3 Single Clone Construction: Transformation*

1. It is necessary to start with an overnight culture of EBY100, preferably inoculated from an agar–agar plate ensuring the yeasts are not contaminated. The pre-culture is cultivated at 30 °C and medium agitation (140–180 rpm) in YPD medium.

**Table 2**
**Thermocycler protocol for PCRs performed with Q5® High-Fidelity DNA Polymerase**

| Step | Temperature (°C) | Duration (s) |
|---|---|---|
| Initial denaturation | 98 | 30 |
| 30 cycles | 98<br>66 (1. PCR)<br>58 (2. PCR)<br>60 (3. PCR)<br>72 | 30<br>30<br><br><br>30/kb |
| Final elongation | 72 | 300 |
| Hold | 4 | – |

2. The pre-culture is utilized to inoculate 50 mL of YPD under the same cultivation conditions as the pre-culture with a starting $OD_{600}$ of 0.5.
3. The cultivation is continued until an $OD_{600}$ of 1.3–1.5 which should take approx. 3 h.
4. Treat the yeast cells with 500 µL of Tris-DTT stock solution 10–15 min prior to harvest during the cultivation period (*see* **Note 1**).
5. Harvest yeast cells by centrifugation (3 min at 4 °C and 3500 × *g*). All the following steps are performed on ice unless declared otherwise.
6. Wash EBY100 cells thrice with ice-cold Buffer E (*see* **Note 2**). To this end, resuspend the cell pellet in 25 mL Buffer E and centrifuge the cell suspension afterwards at 4 °C and 3500 × *g* for 3 min and discard the supernatant. Repeat this step subsequently with 10 mL and 1 mL, respectively.
7. Resuspend the cell pellet in ice-cold 1 mL Buffer E and transfer 100 µL of the cell suspension into an ice-prechilled electroporation cuvette. The solution is supplemented with 0.5–1 µg of linearized plasmid DNA and threefold molar excess of the DNA insert and incubated for 1–2 min (*see* **Note 3**).
8. Perform the electroporation with the following conditions: 2.5 kV, 200 Ω, and 25 µF. Immediately after the transformation, mix the cells with 1 mL YPD and incubate at 30 °C for 1 h.
9. Centrifuge the cells after regeneration at 10,000 × *g* for 2 min, aspirate the supernatant, and wash the cells once with 1 mL of PBS and repeat the centrifugation.

**Table 3**
**Thermocycler protocol for colony PCRs performed with *Taq* Polymerase**

| Step | Temperature (°C) | Duration (s) |
|---|---|---|
| Initial denaturation | 98 | 30 |
| 30 cycles | 98<br>55<br>68 | 30<br>30<br>60/kb |
| Final elongation | 68 | 300 |
| Hold | 4 | – |

10. Resuspend the yeast cells in 100 µL PBS and plate the cell suspension on SD-CAA plates. Yeast colonies should be visible after 2–3 days of incubation at 30 °C.
11. Pick 10 single clones and resuspend each single clone in 20 µL 20 mM NaOH, respectively. Incubate the cell suspension at 98 °C for 15 min. Utilize 1 µL of the suspension as a colony PCR template. Perform the colony PCR with the *pCT_seq_up* and *pCT_seq_lo* primers and an annealing temperature of 55 °C (PCR protocol summarized in Table 3). Analyze the PCR amplicons via a 1% (w/v) agarose gel. Amplicons with a length of ~1300 bp are considered to be correct. Sequence putative positive PCR to confirm the sequence prior to further utilization of the single clones (*see* **Note 4**).

### *3.4 Single Clone Flow Cytometry Analysis*

1. Inoculate 2 mL SD-CAA with a yeast single clone comprising the plasmid with the correct sequence and cultivate it overnight at 30 °C and 180 rpm. Supplement the cell suspension with 3 mL of SG-CAA medium and continue to cultivate the suspension for at least 8 h at 30 °C and 180 rpm.
2. Determine the $OD_{600}$ of the grown yeast cells (use SD-CAA or PBS as a blank) and harvest $1 \times 10^7$ cells by centrifugation (13,000 × *g*, 1 min).
3. Aspirate the supernatant and resuspend the cell pellet in 20 µL PBSB (PBS buffer supplemented with 0.1 % BSA (w/v)) buffer supplemented with an anti-c-Myc-biotin antibody (diluted 1:30), and incubate the cells for 20 min on ice. As negative control, incubate $1 \times 10^7$ cells in 20 µL PBSB without the anti-c-Myc antibody in parallel. Use both aliquots in the subsequent staining steps.

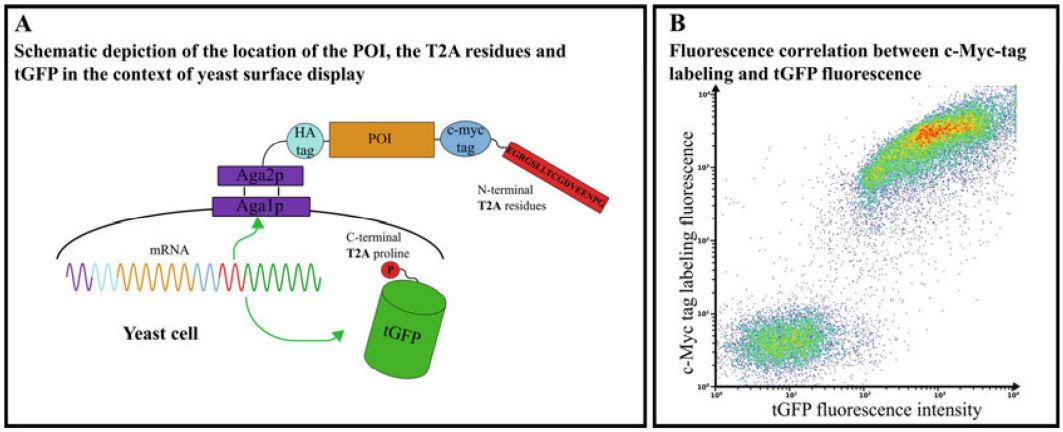


**Fig. 2** Schematic depiction of yeast surface display in combination with T2A and intracellular tGFP readout. (**a**) The different proteins are displayed in different colors according to the respective mRNA section. The T2A residues are located on the yeast cell surface at the C-terminus of the c-Myc-tag (highlighted in red). The C-terminal proline of the T2A protein is N-terminally fused to the intracellular tGFP (also highlighted in red). The ribosomal translation is depicted as green arrows. (**b**) Correlation between c-Myc-tag labeling and intracellular tGFP fluorescence as reported by flow cytometry. 50,000 yeast cells are displayed. The c-Myc-tag is labeled in a two-step procedure with an anti-c-Myc-biotin antibody and streptavidin-APC

4. Add 1 mL of ice-cold PBSB to the cell suspension, mix thoroughly, and centrifuge at 13,000 × *g* for 1 min. Remove the supernatant.
5. Resuspend the cells in 20 μL PBSB in the presence of a 1:75 dilution of streptavidin APC and incubate the suspension for 15 min on ice.
6. Wash the cells with 1 mL of ice-cold PBSB and harvest the cells through centrifugation (13,000 × *g*, 4 °C). Aspirate the supernatant and resuspend the cells in 300–500 μL of ice-cold PBSB.

Depict the tGFP fluorescence and the APC fluorescence in a two-dimensional plot in the cell sorter software. The yeast cells of the negative control should show two distinct populations differing in their tGFP fluorescence intensity; neither population should show APC fluorescence. The anti-c-Myc-biotin-labeled sample will have the entire tGFP-positive population shifted towards APC fluorescence indicating an entangled expression of surface-presented POI and intracellular accumulation tGFP (*see* **Note 5**; Fig. 2B). If the yeast cells do not show sufficient surface presentation levels, increase the incubation time in galactose-containing medium according to your needs (*see* **Note 6**).

## 4 Notes

1. It is recommended to make a new Tris–DTT solution prior to every transformation.
2. After autoclaving, the sorbitol containing solution tends to have a concentration gradient of sorbitol from top to bottom. Short shaking of the bottle solves this problem.
3. To estimate the number of yeast cells that do not carry the desired insert but the parental plasmid instead, at least one negative control has to be carried along (1 μg of backbone DNA, 0 μg of insert DNA).
4. Even though the labeling of surface presented tags like HA- and c-Myc-tag located at the N-/C-terminus of your protein of interest will give you an impression how many full-length constructs are displayed on the yeast cell surface in comparison to truncated variants, particular in case of large YSD libraries, this is not sufficient to determine your library quality. Especially the degree of randomization is an important characteristic which can be determined by deep sequencing. In a quick-and-dirty approach, you can sequence yeast single clones (the more the better, we recommend at least 10 single clone sequences) of your initial library which will indicate if you have some degree of randomization in your POI.
5. Observing the tGFP fluorescence via FACS alone will not give you the possibility to determine if the T2A skipping was successful since the tGFP could also be displayed on the yeast cells. Utilizing a fluorescence microscope—or even better a confocal microscope—will help you to conclude if the tGFP is accumulated in the cytoplasm [10].
6. In library generation approaches, we utilized the T2A-peptide gene as a homologous overhang for gap repair depleting the C-terminal c-Myc-Tag reducing the C-terminal peptide length. However, you can also generate the library with the c-Myc-Tag at the C-terminus. The utilized primers need to be adjusted accordingly and the plasmid restriction is performed with *Nhe*I and *Bam*HI. For the construction of YSD libraries, the transformation protocol should be adjusted according to the protocol of Bernatuil et al. [11]. Libraries can be checked for truncated POIs on the yeast cell surface with HA-tag labeling as described elsewhere [10] (Table 4).

**Table 4**
**Nucleotide sequences used in this study**

| Construct | DNA sequence |
|---|---|
| Full-length construct | AGTTACTTCGCTGTTTTTCAATATTTTCTGTTATTGCTTCAG<br>TTTTAGCACAGGAACTGACAACTATATGCGAGCAAATCCCCTCACCAAC<br>TTTAGAATCGACGCCGTACTCTTTGTCAACGACTACTA<br>TTTTGGCCAACGGGAAGGCAATGCAAGGAGTTTTTGAATATTACAAA<br>TCAGTAACGTTTGTCAGTAATTGCGGTTCTCACCCCTCAACAAC<br>TAGCAAAGGCAGCCCCATAAACACACAGTATGTTTTTAAGGACAATAGC<br>TCGACGATTGAAGGTAGATACCCATACGACGTTCCAGACTACGCTC<br>TGCAGGCTAGTGGTGTGGTGGTTCTGGTGGTGGTGGTTCTGGTGGTGG<br>TGGTTCTGCTAGCATGGCCGCACGGC<br>TTGAACAAACACCGACAACGACAACAAAGGAGGCAGGCGAATCAC<br>TGACCATCAATTGCGTCCTAAAACCGGAATGGACTATCTTGGGTAGGACG<br>TACTGGTATTTCACAAAGAAGGGCGCAACAAAGAAGGCGAGGTTATCAAC<br>TGGCGGACGATACTCGGACACAAAGAATACGGCATCAAAGTCCCTTTCC<br>TTGCGAATTAGTGACCTAAGAGTTGAAGACAGTGGTACATATCACTG<br>TGAAGCGTTGATTTATAGCGATATGGGCATGATTATGTGGAAAA<br>TTGAAGGGGGGGGGACCACTGTGACTGTGAAAGGATCCGAGCAAAAGC<br>TTATTTCTGAAGAGGACTTGGAGGGCCGCGGCAGCCTGCTGACC<br>TGCGGCGACGTGGAGGAAAACCCAGGCCCAATGGAAATTGAATGTCGTA<br>TTACCGGCACCCTGAATGGTGTTGAATTTGAACTGGTTGGTGGTGG<br>TGAAGGTACACCGGAACAGGGTCGTATGACCAATAAAA<br>TGAAAAGCACCAAAGGTGCACTGACCTTTAGCCCGTATCTGCTGTCTCA<br>TGTTATGGGCTATGGCTTTTATCATTTTGGCACCTATCCGAGCGGTTA<br>TGAAAATCCGTTTCTGCATGCCATAATAATGGTGGCTATACCAA<br>TACCCGCATTGAAAAATATGAAGATGGTGGTGTTCTGCATGTTAGC<br>TTTAGCTATCGTTATGAAGCCGGTCGTGTGATTGGTGATTTTAAAGTTA<br>TGGGCACCGGTTTTCCGGAAGATAGCGTGATTTTTACCGATAAAATTA<br>TTCGCAGCAATGCCACCGTTGAACATCTGCACCCGATGGGTGATAATGA<br>TCTGGATGGTAGCTTTACCCGTACCTTTAGCCTGCGTGATGGTGGTTA<br>TTATAGCAGCGTTGTGGATAGCCATATGCATTTTAAAAGCGCCATTCA<br>TCCGAGCATTCTGCAGAACGGTGGTCCGATGTTTGCATTTCGTCGTG<br>TGGAAGAAGATCATAGCAATACCGAACTGGGCATTGTTGAATATCAGCA<br>TGCCTTTAAAACACCGGATGCAGATGCCGGTGAAGAATAATAGCTCGAG |
| Aga2p | ATGCAGTTACTTCGCTGTTTTTCAATATTTTCTGTTATTGCTTCAG<br>TTTTAGCACAGGAACTGACAACTATATGCGAGCAAATCCCCTCACCAAC<br>TTTAGAATCGACGCCGTACTCTTTGTCAACGACTACTA<br>TTTTGGCCAACGGGAAGGCAATGCAAGGAGTTTTTGAATATTACAAA<br>TCAGTAACGTTTGTCAGTAATTGCGGTTCTCACCCCTCAACAAC<br>TAGCAAAGGCAGCCCCATAAACACACAGTATGTTTTTAAGGACAATAGC<br>TCGACGATTGAAGGTAGATACCCA |
| HA-tag | TACGACGTTCCAGACTACGCTCTGCAGGCT |
| $Gly_4Ser$ linker | AGTGGTGGTGGTGGTTCTGGTGGTGGTGGTTCTGGTGGTGGTGGTTC<br>TGCTAGC |
| vNAR | ATGGCCGCACGGC<br>TTGAACAAACACCGACAACGACAACAAAGGAGGCAGGCGAATCAC<br>TGACCATCAATTGCGTCCTAAAACCGGAATGGACTATCTTGGGTAGGACG |

(continued)

**Table 4**
**(continued)**

| Construct | DNA sequence |
|---|---|
| | TACTGGTATTTCACAAAGAAGGGCGCAACAAAGAAGGCGAGGTTATCAAC<br>TGGCGGACGATACTCGGACACAAAGAATACGGCATCAAAGTCCCTTTCC<br>TTGCGAATTAGTGACCTAAGAGTTGAAGACAGTGGTACATATCACTG<br>TGAAGCGTTGATTTATAGCGATATGGGCATGATTATGTGGAAAA<br>TTGAAGGGGGGGGGACCACTGTGACTGTGAAA |
| BamHI site | GGATCC |
| c Myc tag | GAGCAAAAGCTTATTTCTGAAGAGGACTTG |
| T2A | GAGGGCCGCGGCAGCCTGCTGACCTGCGGCGACG<br>TGGAGGAAAACCCAGGCCCA |
| tGFP | ATGGAAATTGAATGTCGTATTACCGGCACCCTGAATGGTGTTGAA<br>TTTGAACTGGTTGGTGGTGGTGAAGGTACACCGGAACAGGGTCGTA<br>TGACCAATAAAATGAAAAGCACCAAAGGTGCACTGACCTTTAGCCCGTA<br>TCTGCTGTCTCATGTTATGGGCTATGGCTTTTATCATTTTGGCACCTA<br>TCCGAGCGGTTATGAAAATCCGTTTCTGCATGCCATTAATAATGGTGGC<br>TATACCAATACCCGCATTGAAAAATATGAAGATGGTGGTGTTCTGCATG<br>TTAGCTTTAGCTATCGTTATGAAGCCGGTCGTGTGATTGGTGA<br>TTTTAAAGTTATGGGCACCGGTTTTCCGGAAGATAGCGTGA<br>TTTTTACCGATAAAATTATTCGCAGCAATGCCACCGTTGAACATC<br>TGCACCCGATGGGTGATAATGATCTGGATGGTAGCTTTACCCGTACC<br>TTTAGCCTGCGTGATGGTGGTTATTATAGCAGCGTTGTGGATAGCCATA<br>TGCATTTTAAAAGCGCCATTCATCCGAGCATTCTGCAGAACGGTGG<br>TCCGATGTTTGCATTTCGTCGTGTGGAAGAAGATCATAGCAATACCGAAC<br>TGGGCATTGTTGAATATCAGCATGCCTTTAAAACACCGGATGCAGA<br>TGCCGGTGAAGAATAATAG |
| XhoI site | CTCGAG |

## References


1. Cherf GM, Cochran JR (2015) Applications of yeast surface display for protein engineering. Methods Mol Biol 1319:155–175
2. Angelini A, Chen TF, de Picciotto S et al (2015) Protein engineering and selection using yeast surface display. Methods Mol Biol 1319:3–36
3. Boder ET, Wittrup KD (1997) Yeast surface display for screening combinatorial polypeptide libraries. Nat Biotechnol 15:553–557. https://doi.org/10.1038/nbt0697-553
4. Könning D, Zielonka S, Grzeschik J et al (2017) Camelid and shark single domain antibodies: structural features and therapeutic potential. Curr Opin Struct Biol 45:10–16. https://doi.org/10.1016/j.sbi.2016.10.019
5. Liu Z, Chen O, Wall JBJ et al (2017) Systematic comparison of 2A peptides for cloning multi-genes in a polycistronic vector. Sci Rep 7:2193. https://doi.org/10.1038/s41598-017-02460-2
6. Ryan MD, Mehrotra A, Gani D et al (2001) Analysis of the aphthovirus 2A/2B polyprotein 'cleavage' mechanism indicates not a proteolytic reaction, but a novel translational effect: a putative ribosomal 'skip. J Gen Virol 82:1013–1025. https://doi.org/10.1099/0022-1317-82-5-1013
7. Ryan MD, Donnelly M, Lewis A et al (1999) A model for nonstoichiometric, Cotranslational protein scission in eukaryotic ribosomes. Bioorg Chem 27:55–79. https://doi.org/10.1006/bioo.1998.1119

8. Chng J, Wang T, Nian R et al (2015) Cleavage efficient 2A peptides for high level monoclonal antibody expression in CHO cells. MAbs 7:403–412. https://doi.org/10.1080/19420862.2015.1008351
9. de Felipe P (2004) Skipping the co-expression problem: the new 2A "CHYSEL"technology. Genet Vaccines Ther 2:13. https://doi.org/10.1186/1479-0556-2-13
10. Grzeschik J, Hinz SC, Könning D et al (2017) A simplified procedure for antibody engineering by yeast surface display: coupling display levels and target binding by ribosomal skipping. Biotechnol J 12:1600454. https://doi.org/10.1002/biot.201600454
11. Benatuil L, Perez JM, Belk J, Hsieh C-M (2010) An improved yeast transformation method for the generation of very large human antibody libraries. Protein Eng Des Sel 23:155–159. https://doi.org/10.1093/protein/gzq002

## 4.3 A Generic Procedure for the Isolation of pH- and Magnesium-Responsive Chicken scFvs for Downstream Purification of Human Antibodies

Title:

A Generic Procedure for the Isolation of pH- and Magnesium-Responsive Chicken scFvs for Downstream Purification of Human Antibodies

Authors:

**Steffen C. Hinz***, Adrian Elter*, Oliver Rammo, Achim Schwämmle, Ataurehman Ali, Stefan Zielonka, Thomas Herget, Harald Kolmar

* Authors contributed equally

Bibliographic data:

*Frontiers in Immunology*

Volume 8, Issue 688

Article first published online: 23.06.2020 | DOI: 10.3389/fbioe.2020.00688



Contribution by S. C. Hinz:

- Performed experiments for validating the presented protocols
- Involved in writing and revising the manuscript

Beiträge von S. C. Hinz:

- Performed literature research
- Performed experiments
- Involved in writing and revising the manuscript
- Expansion of the project to include magnesium-responsive antibody fragments

frontiers in Bioengineering and Biotechnology

ORIGINAL RESEARCH
published: 23 June 2020
doi: 10.3389/fbioe.2020.00688

# A Generic Procedure for the Isolation of pH- and Magnesium-Responsive Chicken scFvs for Downstream Purification of Human Antibodies

*Steffen C. Hinz[1,2†], Adrian Elter[1,2†], Oliver Rammo[3], Achim Schwämmle[3], Ataurehman Ali[1], Stefan Zielonka[4], Thomas Herget[5] and Harald Kolmar[1,2*]*

[1] Institute for Organic Chemistry and Biochemistry, Technische Universität Darmstadt, Darmstadt, Germany, [2] Merck Lab @ Technische Universität Darmstadt, Darmstadt, Germany, [3] Life Science Division, Merck KGaA, Darmstadt, Germany, [4] Protein Engineering and Antibody Technologies, Merck KGaA, Darmstadt, Germany, [5] Strategy und Transformation, Merck KGaA, Darmstadt, Germany

OPEN ACCESS

**Edited by:**
Haifeng Zhao,
South China University of Technology, China

**Reviewed by:**
Qi Zhao,
University of Macau, China
Samarthya Bhagia,
Oak Ridge National Laboratory, United States

***Correspondence:**
Harald Kolmar
kolmar@biochemie-tud.de

[†]These authors have contributed equally to this work and share first authorship

**Specialty section:**
This article was submitted to Industrial Biotechnology, a section of the journal Frontiers in Bioengineering and Biotechnology

**Received:** 24 March 2020
**Accepted:** 02 June 2020
**Published:** 23 June 2020

**Citation:**
Hinz SC, Elter A, Rammo O, Schwämmle A, Ali A, Zielonka S, Herget T and Kolmar H (2020) A Generic Procedure for the Isolation of pH- and Magnesium-Responsive Chicken scFvs for Downstream Purification of Human Antibodies. Front. Bioeng. Biotechnol. 8:688. doi: 10.3389/fbioe.2020.00688

Affinity chromatography provides an excellent platform for protein purification, which is a key step in the large scale downstream processing of therapeutic monoclonal antibodies (Mabs). Protein A chromatography constitutes the gold standard for Mab purification. However, the required acidic conditions (2.8–3.5) for elution from the affinity matrix limit their applicability, particularly for next generation antibodies and antibody fusion proteins, since denaturation and irreversible aggregation can occur due to the acidic buffer conditions. Here we describe a generic procedure for the generation of antigen-specific chromatography ligands with tailor-made elution conditions. To this end, we generated a scFv-library based on mRNA from a chicken immunized with human Fc. The antibody repertoire was displayed on yeast *Saccharomyces cerevisiae* screened *via* FACS toward pH- and magnesium-responsive scFvs which specifically recognize human IgG antibodies. Isolated scFvs were reformatted, produced in *Escherichia coli* and immobilized on NHS-agarose columns. Several scFvs were identified that mediated antibody binding at neutral pH and antibody recovery at pH values of 4.5 and higher or even at neutral pH upon $MgCl_2$ exposure. The iterative screening methodology established here is generally amenable to the straightforward isolation of stimulus-responsive antibodies that may become valuable tools for a variety of applications.

**Keywords: affinity chromatography, yeast display, protein purification, immune library, chicken antibody, single chain fragment variable, downstream processing, protein A**

## INTRODUCTION

In the time period of 2014 to 2018 a total of 129 unique biopharmaceuticals were approved for either the US or EU market raising the total number of approved biopharmaceuticals to 316. The category of biopharmaceuticals contains monoclonal antibodies (mAbs), hormones, clotting factors, enzymes and others. This heterogeneous group of molecules is mainly utilized in cancer, inflammation-related, hemophilia and diabetes indications and is responsible for $188 bn sales

in 2017 with expectations to reach nearly $400 bn in 2025 (Grand View Research, 2017). With up to 65.5% of total sales, monoclonal antibodies remain the most interesting protein scaffold. In the recent decade, the market became more congested and multiple molecules are utilized for similar indications. This leads to an increase in competitive pressure, a motivation for research and development of new low-cost production and purification strategies (Walsh, 2018).

In the production process of proteins, downstream processing is one of the major cost driving factors, accountable for 45–90% of the whole manufacturing process costs, making it a promising target for optimization (Straathof, 2011). Affinity chromatography is a powerful tool for efficient purification of the protein of interest (POI) omitting the need for multiple chromatography steps (Harakas, 1994; MacLennan, 1995; Saraswat et al., 2013; Urh et al., 2009). However, the genetic fusion of affinity tags to the POI is a putative origin for immune reactions which should be avoided (Dingman and Balu-Iyer, 2019). In the case of antibodies, natural occurring affinity ligands exist, omitting the need for affinity tags. These bacterial proteins can be found in *Staphylococcus* species (Protein A, Protein G) or *Peptostreptococcus* species (Protein L) and mask the bacteria from the immune system of the host organism and are also known as virulence factors (Ricci et al., 2001; Palmqvist et al., 2002). This strong natural interaction can be exploited for affinity chromatography, where antibodies can be efficiently bound onto a Protein A-agarose column (Duhamel et al., 1979). This natural affinity comes with a drawback. For the interruption of this tight interaction, harsh elution conditions have to be applied. Commonly used Protein A chromatography relies on glycine/citrate buffer compositions with a pH of 2.8–3.5 to achieve high recovery. These acidic conditions are not well tolerated by some antibodies and may lead to protein loss by aggregation (Vázquez-Rey and Lang, 2011; Mazzer et al., 2015; Jin et al., 2019) as well as structural changes such as deamidation and backbone cleavage upon succinimide formation (Linhult et al., 2005; Lu et al., 2019) and therefore result in less economical production conditions. Intensive efforts have been made to improve Protein A/G to overcome this intrinsic drawback. On one hand, the high costs of Protein A/G columns have been countered by improvements toward alkaline stability, allowing more purifications cycles per column (Nilsson et al., 1987; Gulich et al., 2002; Hahn et al., 2006). On the other hand, efforts have been made to establish less acidic elution conditions by Protein A/G engineering and rational design culminating in variants that can be used with elution at pH 4.5 (Gulich et al., 2000; Watanabe et al., 2009, 2019; Pabst et al., 2014; Tsukamoto et al., 2014). Alternative approaches focus on temperature-dependent elution (Koguma et al., 2013) or antibody binding upon calcium supplementation and subsequent elution with EDTA at neutral pH (Kanje et al., 2018; Scheffel et al., 2019).

Several alternative binding proteins have been developed for Fc affinity purification purposes. For example, single-domain antibody domains (VHH) have been isolated from immunized camelids. For their use in downstream processing applications gentle elution conditions should prevail and these antibodies were therefore engineered toward pH- and magnesium-responsive binding behavior (Klooster et al., 2007; Detmers et al., 2010; Hermans et al., 2014). Further developments focus on semi-synthetic protein scaffold libraries based on i.e., a DNA-binding protein derived from a hyperthermophilic crenarchaea called Sso7D ("Affitins") (Gera et al., 2012; Behar et al., 2016), "Affimers" based on cystatin and human stefin A (McPherson and Tomlinson, 2014; Tiede et al., 2017), modular leucine-rich repeat units called "Repebodies" (Heu et al., 2014), and many more as elegantly reviewed by Škrlec et al. (2015) not only limited to affinity chromatography but also for imaging purposes and therapeutic applications (Bedford et al., 2017; Simeon and Chen, 2018).

The goal of this study was to establish a generic screening procedure for pH- and/or magnesium-responsive binders against a given target *via* yeast surface display of a single chain fragment variable (scFv) library obtained from immunized chickens for use in affinity chromatography applications. Here we describe a screening strategy that allows for isolation of high affinity target binding antibodies that release their target at slightly acidic pH or in combination with pH drop and elevated magnesium concentrations. We used chickens for immunization since the phylogenetic distance between avians and humans is significantly increased, enhancing the probability to obtain antibodies against human antigens bypassing antigen self-tolerance related problems (Davies et al., 1995). Also, chicken antibodies tend to be structural more rigid caused by non-canonical disulfide bridges located in the CDRs and elevated body temperature of avians (Prinzinger et al., 1991; Wu et al., 2012). Additionally, the special genetic arrangement of the VH and VL gene of chickens allows the amplification of the whole antibody repertoire with two separate one-step PCRs using defined primer pairs (Reynaud et al., 1985, 1987, 1989, 1991; Thompson and Neiman, 1987; McCormack et al., 1993).

Here we show that the combination of avian immunization, yeast surface display (YSD) and ultra-high throughput screening by FACS results in the isolation of numerous human Fc-specific pH- and magnesium-responsive scFvs. After immobilization they displayed favorable binding and elution profiles and allowed for target antibody purification using mild elution conditions.

## MATERIALS AND METHODS

### Immunization

The immunization of a pathogen-free adult laying hen (*Gallus gallus domesticus*) was performed at Davids Biotechnologie GmbH, Germany. The specimen was intramuscularly injected with 150 µg SEED-Fc-protein (gift from Dr. S. Zielonka, Merck KGaA, Darmstadt) (Davis et al., 2010; Muda et al., 2011) in combination with immune adjuvant AddaVax (InvivoGen). Boosters were given 2, 4, 5, and 8 weeks after the initial injection. Immune response against the Fc-protein was determined after 5 weeks by antigen-specific titer determination using ELISA. The chicken was sacrificed after 9 weeks and the total splenic RNA was subsequently isolated using TriFast reagent (VWR).

Experimental procedures and animal care were in accordance with EU animal welfare protection laws and regulations.

## Yeast Strains and Media

*Saccharomyces cerevisiae* EBY100 [*MATa URA3-52 trp1 leu2Δ1 his3Δ200 pep4::HIS3 prb1Δ1.6R can1 GAL (pIU211:URA3)*] (Thermo Fisher Scientific) cells were utilized for yeast surface display. Prior to library generation, yeast cells were cultivated in YPD medium composed of 20 g/L peptone/casein, 20 g/L glucose and 10 g/L yeast extract supplemented with appropriate antibiotics (ampicillin 100 mg/L, kanamycin sulfate 75 mg/L or chloramphenicol 25 mg/L). The SD-CAA media for yeast cell cultivation after library generation comprised 5.4 g/L $Na_2HPO_4$ and 8.6 g/L $NaH_2PO_4 \times H_2O$, 20 g/L glucose, 5 g/L ammonium sulfate, 1.7 g/L yeast nitrogen base (without amino acids), and 5 g/L bacto casamino acids. For surface presentation induction, SG-CAA medium was used which resembles SD-CAA but instead of glucose, galactose was supplemented.

## Library Construction

The generation of the scFv gene library was performed as described by Grzeschik et al. (2019). Briefly, the VH and VL genes were amplified with *VH_gr_up*/*VH_SOE_lo* and *VL_SOE_up*/*VL_gr_lo*, respectively (**Supplementary Table S3**), after cDNA synthesis and subsequent mRNA digestion. Both fragments were fused in two additional PCR reactions introducing a $(Gly_4Ser)_3$ linker sequence, amplifying the scFv gene while adding overhangs at the 5′ and 3′ end of the scFv gene for homologous recombination in yeast. The PCR amplicon was subsequently purified. The pCT plasmid (Boder and Wittrup, 1997) which was used for surface presentation was digested with *Nhe*I and *BamH*I (New England Biolabs) and purified prior to gap repair cloning. The library generation with scFv insert, pCT backbone and EBY100 yeast cells were performed according to Benatuil et al. (2010).

Twelve transformation reactions were performed each consisting of 4 μg digested pCT plasmid and 12 μg scFv insert. The number of individual transformants was determined by dilution plating after 3 days of cultivation at 30°C.

## Library Sorting

Prior to yeast cell sorting, the yeast library was cultivated overnight in SD-CAA medium at 30°C and 180 rpm. Subsequently, the cell suspension was centrifuged at 4000 rcf and the medium aspirated. The cell pellet was utilized to inoculate SG-CAA medium to a final cell density of $1 \times 10^7$ cells/mL followed by an incubation period of at least 12 h at 30°C. Cells were harvested by centrifugation and washed once in 1 mL PBS-B pH 7.4 [PBS + 0.1% (w/v) BSA] prior to the staining procedure.

The presentation of the scFv molecules on the yeast cell surface was verified either with an anti-c-myc antibody (produced in house) and anti-mouse IgG FITC (Sigma Aldrich) or anti-mouse IgG R-phycoerythrin (PE) (Sigma Aldrich) as secondary labeling agent or anti-c-myc biotin antibody (Miltenyi biotech) and Streptavidin-PE (Fisher Scientific) or Streptavidin-allophycocyanin (APC) (Fisher Scientific), respectively. The detailed staining strategy including working dilution is summarized in **Supplementary Table S1**. The staining steps are summarized in **Supplementary Table S2**.

In the screening process, daratumumab (Janssen-Cilag), pertuzumab (Genentech) and cetuximab (Merck) were utilized. Antibody binding was detected with anti-Human IgG (Fab specific) -FITC (Sigma-Aldrich), Goat $F(ab')_2$ anti-Human Kappa-PE (Southern Biotech) or Goat anti-Human IgG Fc Secondary Antibody PE (Invitrogen) (**Figure 1C**). In the first and second screening round SEED Fc protein (Merck KGaA) was utilized conjugated with DyLight650 (Thermo Fisher Scientific). Conjugation was performed according to the manufacturer's manual with 5-fold molar excess of NHS-DyLight650.

Yeast cells that were collected during the sorting process were transferred into SD-CAA medium and cultivated for 48 h at 30°C and 180 rpm before re-activating surface presentation by inoculating SG-CAA medium for subsequent sorting. In each sorting round, the total number of screened cells exceeded 10-fold the number of cells in the previous sorting process to ensure proper library coverage during sorting.

## Bacterial Strains and Media

*Escherichia coli* Top10 cells [$F^-$ *mcr*A Δ(*mrr-hsd*RMS-*mcr*BC) φ80*lac*ZΔM15 Δ*lac*X74 *rec*A1 *ara*D139 Δ(*ara-leu*) 7697 *gal*U *gal*K *rps*L ($Str^R$) *end*A1 *nup*G λ-] (Thermo Fisher Scientific) were used for transformation of golden gate assembly batches. Cell cultivation was performed in dYT medium (yeast extract 10 g/L; peptone ex casein 16 g/L; NaCl 5 g/L). Correctly assembled plasmids were rescued and subsequently transformed into the SHuffle T7 Express strain (*fhuA2 lacZ::T7 gene1* [lon] *ompT ahpC Etc gal* λ*att*::pNEB3-r1-*cDsbC* ($Spec^R$, $lacI^q$) Δ*trxB sulA11 R(mcr-73::miniTn10*–$Tet^S$) [dcm] *R(zgb-210::Tn10* –$Tet^S$) *endA1* Δ*gor* Δ*(mcrC-mrr)114::IS10*) (New England Biolabs) for expression. SHuffle T7 Express cells were cotransformed with the pLysS Erv1p/DsbC plasmid (Veggiani and de Marco, 2011) and transformants were maintained upon addition of 60 μg/ml kanamycin and 25 μg chloramphenicol. Expression in SHuffle T7 Express was conducted in SB medium (yeast extract 20 g/L; peptone ex casein 32 g/L; NaCl 5 g/L; NaOH 1 N 5 mL).

## Cloning, Expression, Purification of Solitaire scFvs

Single clones with pH-responsive or magnesium-responsive properties were reformatted into a pET30a expression plasmid comprising *Bsa*I-HF®v2 sites for golden gate cloning (GGC). To this end, scFv genes were amplified from the respective pCT plasmid using *scFv_chick_his_GG_up* and *scFv_chick_SII_GG_*lo primers (**Supplementary Table S3**) introducing *Bsa*I restriction sites for golden gate assembly as well as a 5′ His6-tag and 3′ StrepTagII (Johar and Talbert, 2017) for purification. The golden gate assembly was performed with 75 ng pET30a backbone and 25 ng of the purified PCR amplicon. Plasmids with the correct sequence were subsequently transformed into SHuffle T7 Express *E. coli* cells containing a pLysS Erv1p/DsbC plasmid.

The expression of the scFvs was performed according to Veggiani and de Marco (2011) in SB medium with a final

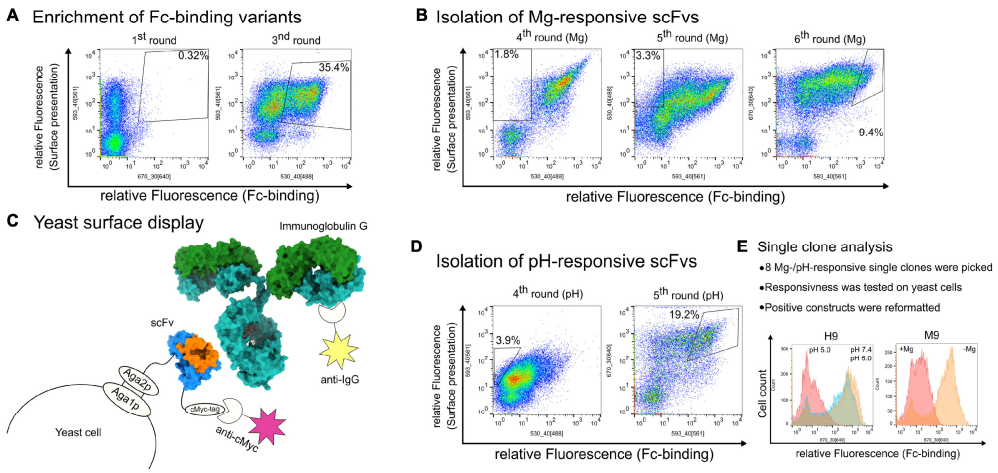


**FIGURE 1 |** Summary of the sorting steps for the isolation of pH- and magnesium-responsive chicken-scFvs. In general, FACS plots show Fc-binding plotted on the *x*-axis and surface presentation on the *y*-axis. Each plot contains 50,000 events. Detailed staining strategy is summarized in **Supplementary Table S1**. **(A)** Enrichment of Fc-specific scFvs *via* YSD and FACS during the 1st and 2nd sorting rounds. **(B)** Summarized screening campaign for the isolation of magnesium-responsive scFvs. The 3rd and 4th sorting rounds were performed to deplete scFv variants that bound regardless of the $MgCl_2$ concentration by sorting non-binding yeast cells after incubating the cells with 2 M $MgCl_2$. The 5th sorting round was conducted in order to enrich IgG binding cells and to isolate single clones. **(C)** Schematic depiction of yeast surface display. The scFv molecule (pdb: 4p48) is displayed on the yeast cell *via* aga2p-fusion. Surface presentation is verified by staining the *C*-terminal c-Myc-tag. The scFv backbone is shown in blue, the CDRs are highlighted in orange. Antibody binding (pdb: 1igt) is verified indirectly by fluorophore staining. The heavy chains are depicted in light blue, the light chains in green. **(D)** Consecutive sorting rounds to enrich pH-responsive scFvs. The 3rd sorting round was conducted with an additional incubation step at pH 5.0 and non-binding yeast cells were isolated. The 4th sorting round was performed in order to isolate yeast single clones. **(E)** General procedure for the analysis of single clones. Exemplarily, H9 and M9 analysis is depicted in a histogram, respectively. Fc-binding is depicted on the *x*-axis and cell count on the *y*-axis. For H9, cells washed at pH 7.4 after target protein incubation are shown in orange, cells washed at pH 6.0 in blue and cells washed at pH 5.0 are shown in red. M9-bearing cells are shown in the red histogram with non-Magnesium exposed cells are shown in orange and cells exposed to 2 M $MgCl_2$ are shown in red.

concentration of 0.1% arabinose and 1 mM IPTG at 18°C, 180 rpm for at least 16 h.

Cells were harvested by centrifugation, lysed by sonication and the soluble fraction was applied onto a HisTrap HP 5 mL column (GE Healthcare) for purification. Chromatography was performed on an ÄKTA Start FPLC system. As binding buffer IMAC Buffer A (Tris/HCl 50 mM pH 7.5, NaCl 150 mM) was utilized. Bound protein was eluted with IMAC Buffer B (Tris/HCl 50 mM pH 7.5, NaCl 150 mM, 1 M imidazole) in a linear gradient. After the IMAC, the protein containing fractions were pooled and diluted 1:2 with Buffer W (Iba Lifescience). As a second purification step, the protein containing solution was applied on a StrepTactin XT high capacity column (Iba Lifescience). Column wash was performed with Buffer W and bound protein was eluted with Buffer E (Iba Lifescience). Buffer exchange was performed with a dialysis hose with a MWCO of 3 kDa with at least 2 dialysis steps.

## Protein Immobilization

Purified scFv protein was coupled to prepacked NHS-agarose columns (GE Healthcare, 1 ml column volume) according to the manufacturers protocol. To this end, 5 mg protein (in PBS buffer) were slowly applied to the column with a contact time of approx. 500 µl/15 min after rinsing the column with 6 ml ice-cold HCl (1 mM) *via* a syringe. The column was cleared from non-immobilized protein by washing the column with 2 ml PBS. Subsequently, the column was washed with 6 ml Buffer Q (500 mM Tris-HCl, 500 mM NaCl, pH 8.3), 6 ml Buffer QB (100 mM sodium acetate, 500 mM NaCl, pH 4.0) and 6 ml Buffer Q. After an incubation time of 60–90 min in Buffer Q to quench unreacted NHS-groups, the column was subsequently washed with 6 ml Buffer QB, 6 ml Buffer Q and 6 ml Buffer QB, respectively. In the last step, the column was purged with coupling buffer (PBS) and stored at 4°C until further utilization.

The coupling efficiency was determined utilizing the Pierce 660 nm Protein Assay Reagent. Briefly, the flowthrough of the coupling solution as well as the 3 ml coupling buffer wash solution were collected after passing through the column. Fifty µL of the solution was mixed with 750 µL assay solution. After 5 min incubation at RT, the absorbance at 660 nm was measured. For each protein, a unique calibration curve was recorded which was utilized to calculate the protein concentration in the flowthrough.

## Nano Differential Scanning Fluorimetry Measurement

Melting point measurements were performed on a Prometheus NT.48 instrument (NanoTemper Technologies). Ten µl of a

1 mg/ml protein solution in PBS was filled into the capillaries and a temperature gradient of 2°C/min was applied from 20 to 95°C. During the gradient, the fluorescence at 330 and 350 nm were measured to determine the melting temperature $T_M$. Data processing was performed using the Prometheus ThermControl v.2.1.2.

## Downstream Processing Test Procedure

ScFv-conjugated columns were analyzed on a Bio-Rad NGC FPLC system. Each column was washed with sample buffer for at least 10 CV prior testing. The testing protocol included the following chromatography steps: (1) 5 CV sample buffer; (2) 5 CV elution buffer; (3) 5 CV sample buffer; (4) Sample application [3 mg Gamunex (Bayer)]. Gamunex is a therapeutic product for patients with an immunoglobulin deficiency. It contains a mixture of 98%-pure IgG-isotypes with a ratio of IgG1 62.8%, IgG2 29.7%, IgG3 4.8%, and IgG4 2.7%. (5) 10 CV sample buffer; (6) 5 CV sample buffer/elution buffer (mixed in variable ratios); (7) 5 CV elution buffer; (8) 5 CV sample buffer. Depending on the performed test series, phosphate citrate pH 7.4 was utilized as sample buffer (pH-test series) or Tris/HCl 50 mM pH 7.0 (magnesium-test series), respectively. As elution buffer, either phosphate citrate pH 3.0 or Tris/HCl 50 mM pH 7.0, $MgCl_2$ 2 M was utilized. To evaluate the recovery at the utilized pH/magnesium concentration, the area under curve for the first elution step was divided by the total area under curve for both peaks multiplied by 100, resulting in percent values. Unless otherwise indicated, pH test series were performed at flowrates of 3 mL/min (except sample application with 1 mL/min) whereas magnesium test series were performed at 1 mL/min.

## Expression of Trastuzumab

For the purification experiments, Trastuzumab was produced according to published procedures (Schneider et al., 2019). The purification was performed either with a Protein A HP 1 mL column (GE Healthcare) or a self-produced column with 15 mL cell culture supernatant (diluted 1:2 with phosphate citrate buffer pH 7.4) with a two-step purification protocol described in the downstream processing test procedure paragraph.

## Biolayer Interferometry

The binding kinetics were determined utilizing the Octet RED96 system (ForteBio, Pall Life Science). Measurements were performed at 30°C and 1000 rpm. All biosensors were incubated in PBS prior to utilization for at least 10 min. After determination of the baseline in PBS buffer for 30 s, the anti-human Fab-sensors (FAB2G) were loaded with daratumumab at a concentration of 1 μg/ml in PBS for 300 s. Quenching of the biosensors was performed for 60 s in kinetic buffer (ForteBio, Pall Life Science) prior to incubation of the sensors with varying concentrations (25–800 nM) of scFv in PBS for 600 s (H9; M9) or 720 s (M2). The dissociation of the antigen was measured for 600 s in phosphate-citrate-buffer at the respective pH (pH 5.0, pH 4.5, or pH 4.0). For each BLI experiment, a negative control was measured in which the biosensor was incubated in PBS instead of the IgG1 antibody. This negative control was subtracted from all antigen containing samples. Data analysis was performed with ForteBio data analysis software 9.0 using a 1:1 binding model with Savitzky–Golay filtering. For $K_D$ determination, at least three different scFv concentrations were used for a global fit. For the dissociation, only the fast dissociation step was considered for calculation (H9: 45 s; M2: 30 s; M9: 30 s) as described by Molecular Devices (Renee and Weilei, 2017). The $K_{dis}$ values in different buffers were measured at single concentrations (H9: 500 nM; M2: 400 nM; M9: 250 nM).

# RESULTS

Our previous immunization campaigns of chickens indicated that a high diversity of antibodies against mammalian antigens can be obtained (Grzeschik et al., 2019). Hence, we reasoned that this repertoire might contain several antibodies that display *per se* pH- and/or magnesium responsive binding. To test this hypothesis, we used a human SEED-Fc fragment as antigen for chicken immunization. A SEED-Fc consists of an IgG CH2 domain and a strand-exchanged IgG CH3. The strand exchanges were made with an CH3 of an IgA (Davies et al., 1995). A serum sample withdrawn 35 days after immunization indicated a strong immune response (data not shown). RNA was isolated from spleen tissue and cDNA was prepared by reverse transcription. The cDNA was amplified by PCR and VL und VH chains were randomly combined into scFv fragments by SOE PCR as described (Grzeschik et al., 2019). After transfer into yeast display vector pCT by gap repair (Benatuil et al., 2010) a yeast display library was generated in 1 day comprising approximately $5.2 \times 10^9$ transformants.

To exclusively obtain Fc binding antibodies, four different antigens [daratumumab (Janssen-Cilag), pertuzumab (Genentech), cetuximab (Merck), Fc-fusion protein] all sharing a common human IgG1-Fc fragment, were used for screening. Starting with $1.6 \times 10^8$ clones of the initial library which displayed a surface presentation level of 37.8% (**Supplementary Figure S1**), obviating the need for a magnetic bead preselection step, two consecutive FACS sorting rounds were performed with 1 μM Fc-fusion in the first sorting round and after cell growth with 1 μM of the human therapeutic antibody daratuzumab in the second sorting round to enrich Fc-binding scFv variants. To this end, yeast cells were sorted that showed fluorescence indicative of target binding and also for yeast surface presentation of the scFv resulting in 0.32% (round 1) and 35.4% (round 3) sorted yeast cells (**Figure 1A**). After the second sorting round, strong enrichment of binders was observed (**Figure 1A**). Afterward, the library was split into two different batches. One batch was further utilized to isolate pH-responsive scFvs whereas the second batch was utilized to screen for Mg-responsive scFvs (from now on called pH-batch and Mg-batch, respectively). In order to isolate pH-responsive scFvs, the yeast cells from the pH-batch were stained with 250 nM pertuzumab and FITC-labeled anti-Fab antibody. Afterward, cells were incubated at pH 5.0 for 5 min and those yeast cells were isolated that showed surface presentation but lacked target binding (**Figure 1D**). Prior to single clone analysis, a 5th sorting round was performed using 150 nM daratumumab to isolate

single clones that showed target binding at pH 7.4 (**Figure 1D**). All FACS plots showing the sorting for pH-responsive scFvs are depicted in **Supplementary Figure S2**.

Magnesium-responsive scFvs were generated within three consecutive FACS rounds after the initial library enrichment. To this end, two consecutive selection rounds were performed by screening for non-binders upon indirect cell staining with 1 μM cetuximab followed by subsequent incubation in Tris/HCl buffer pH 7.0 with 2 M $MgCl_2$. Sorted cells lacking the target binding fluorescence signal under these conditions increased from 1.8 to 3.3%, respectively (**Figure 1B**). The last sorting round prior to single clone analysis was performed *via* screening for binders of 150 nM daratumumab with no $MgCl_2$ added to ensure enrichment of Fc-specific binders after two rounds of sorting for non-binding scFvs. The complete sorting campaign is shown in **Supplementary Figure S3**.

Eight pH- and nine magnesium-responsive single clones were picked and analyzed toward their binding properties in either phosphate-citrate pH 5.0 buffer (Dawson et al., 1987) or Tris/HCl 2 M $MgCl_2$ buffer (pH 7.0), respectively. To this end, $5 \times 10^6$ yeast cells of each putative pH-responsive single clone were collected by centrifugation and stained with 100 nM pertuzumab and APC labeled anti-kappa antibody for target binding and a biotinylated anti-myc-epitope antibody followed by streptavidin R-phycoerythrin (SPE) staining for surface presentation (**Supplementary Figure S4A**). Except for single clone H2, all variants showed pH-responsive behavior and were therefore considered for reformatting and expression. In FACS analysis, H7 and H9 exhibited significant loss of target binding at pH 5.0 (exemplarily shown for H9 in **Figure 1E**). Putative yeast-displayed magnesium responsive variants were tested toward target binding *via* FACS with 150 nM daratumumab (exemplarily shown for M9 in **Figure 1E**, data for all single clones depicted in **Supplementary Figure S4B**). Single clone 1 and 7 showed no or only minor target binding decrease after $MgCl_2$ treatment and were therefore excluded from further experiments. Responsive variants were sequenced and reformatted into a pET30 expression plasmid *via* golden gate cloning with a *N*-terminal His6-tag and a *C*-terminal StrepTagII to be used as purification handles. Seven unique pH-responsive variants were expressed which could be allocated to four different sequence clusters (H1–H9). Likewise, the magnesium-responsive variants showed high diversity with five unique variants out of eight belonging to four different clusters (M2-M9) (**Table 1**).

The melting temperature for every expressed protein was determined by Nano differential scanning fluorimetry. The measurements showed $T_M$ values in line with published melting temperatures for chicken scFvs ranging from 48 and 68°C (**Table 1**) with H1, M3, M9 having melting temperatures exceeding 60°C, comparable to Fab molecules (Orr et al., 2003; Garber and Demarest, 2007; Miller et al., 2010). For some variants, two distinct melting temperatures could be observed. This might be due to different melting temperatures for the VL and the VH domain (Miller et al., 2010).

For the chromatography experiments, 5 mg of each scFv were utilized for coupling to NHS-agarose columns. The coupling efficiency varied between 67 and 96% (**Table 1**). Prepared columns were stored at 4°C until further utilization. All chromatographic procedures were performed on a NGS Bio-Rad system with pH-module calibration between each column experiment set. A column experiment set includes a pH-gradient (pH 3.0–7.4) and up to eight different isocratic elution chromatographies for pH-experiments or a $MgCl_2$-gradient (0–2 M $MgCl_2$) and up to five different isocratic elution chromatographies, respectively.

To determine the recovery, a two-step isocratic elution was performed. The first isocratic step was performed in phosphate-citrate-buffer with variable pH (**Figure 2A** – Elution 1). The second elution step was performed in phosphate-citrate-buffer pH 3.1–3.3 ensuring the elution of remaining IgG on the column (**Figure 2A** – Elution 2). The area under curve (AUC) was determined for each elution step. The AUC ratio of the first elution step and the sum of the first and second elution step resulted in a percentage value which defines the recovery. In comparison with Protein A, all proteins except H4 and H8 showed higher recovery, exceeding 90% at pH values >4.0. The best variants, H7 and H9, displayed recovery of more than 92% above pH 4.5 (**Figure 2B**).

The pH-experiments were also conducted with the magnesium-responsive variants. Interestingly, three out of five scFvs displayed pH-responsive behavior (**Figure 2C**). Particularly M2, M6, and M3 revealed pH- responsive elution behavior even outperforming Protein A at pH 4.0. M8 did not show any elution at pH 3.2.

In the chromatography experiments with $MgCl_2$ as eluant, M8 was the best performing scFv showing quantitative elution at 400 mM $MgCl_2$, closely followed by M9. M2 performed adequately with nearly quantitative elution at 800 mM $MgCl_2$. M3 and M6 only showed mediocre magnesium-responsiveness with only 55 and 65% elution at 1000 mM $MgCl_2$, respectively (**Figure 2D**). As negative control, H7 and H9 were tested toward their magnesium-responsiveness but did not show any protein elution signal at 2 M $MgCl_2$. To see whether the elution was driven by high ionic strength or specifically by $Mg^{2+}$ ions, bound antibody on scFv M9 column was incubated with Tris/HCl buffer pH 7.0 containing either 2 M NaCl, 2 M $CaCl_2$ or 2 $MgCl_2$, respectively. It was apparent, that antibody elution was specific for bivalent cations, with strong preference for $Mg^{2+}$. In direct comparison, $Ca^{2+}$ only lead to a recovery of 80% with very strong tailing, clearly demonstrating $Mg^{2+}$ specificity (**Figure 3**).

An unexpected finding was the pH-dependent elution of M2, M3, and M6. All three variants were examined in combinatorial experiments with phosphate-citrate-buffer (pH 5.5–4.5) and low concentrations of $MgCl_2$ (0, 100, 200 mM). As expected, the addition of $MgCl_2$ significantly improved the recovery for all tested variants (**Figures 4A–C**). As negative control, H7 was also tested toward the combinatorial effects of $MgCl_2$ and pH. The addition of 100 mM $MgCl_2$ was beneficial at pH 5.5 and 5.2 and slightly improved recovery. However, further increasing the $MgCl_2$ concentration did not further improve the elution behavior (**Figure 4D**).

The most pH-responsive affinity ligands H7 and H9 were utilized to investigate, whether the recovery can be further enhanced by lowering the flow rate during elution from 3 ml/min

**TABLE 1 |** Summary of TM values at pH 7.4 and pH 3.0 for all isolated pH- and magnesium-responsive scFvs including the observed yields and determined coupling efficiencies.

| | Cluster | $T_M1$ pH 7.4 | $T_M2$ pH 7.4 | $T_M1$ pH 3.0 | $T_M2$ pH 3.0 | Yield [mg/L] | Coupling [%] |
|---|---|---|---|---|---|---|---|
| H1 | III | 60.5 | 68.4 | 40.55 | 50.00 | 4.7 | n.d. |
| H3 | II | 45.7* | – | n.d. | – | 5.2 | – |
| H4 | I | 55.4 | – | 27.8 | – | 12.7 | 96.5 |
| H6 | I | 58.5 | – | 43.8 | – | 16.9 | 71.1 |
| H7 | I | 57.95 | 70.35 | 43.85 | 56.5 | 4.8 | n.d. |
| H8 | II | 52.3 | – | 49.0 | – | 24.4 | 71.3 |
| H9 | I | 48.7 | 55.8 | 33.3 | 42.15 | 5.38 | n.d. |
| M2 | I | 51.0 | – | 32.5 | – | 10.9 | 78.8 |
| M3 | II | 61.2 | – | 38.1 | – | 8.1 | 67.2 |
| M6 | III | 53.55 | – | 35.3 | – | 3.6 | n.d. |
| M8 | III | 52.45 | – | n.d. | – | 5.14 | 75.1 |
| M9 | III | 69.48 | – | 59.4 | 65.5 | 14.8 | 80.6 |

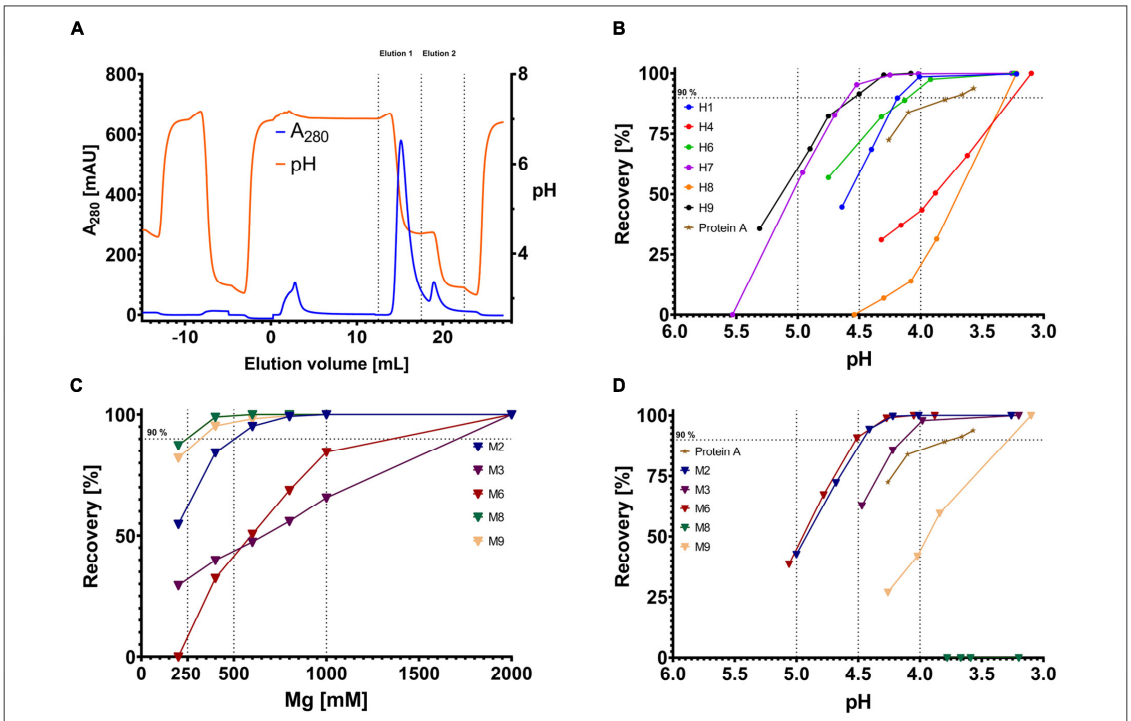


**FIGURE 2 |** Example chromatogram and recovery diagrams. **(A)** Sample chromatogram with the absorbance at 280 nm depicted on the *y*-axis (blue line) and the elution volume on the *x*-axis. Additionally, the recorded pH is shown on the right *y*-axis in orange. Elution 1 and elution 2, which are used for determining the recovery, are indicated by dashed lines on the *x*-axis. **(B,D)** Recovery for pH-responsive scFvs **(B)** and magnesium-responsive scFvs. The recovery is depicted on the *y*-axis, the pH value on the *x*-axis. Each dot represents a single measurement (triangles for magnesium-responsive variants), scFvs are separated by color, Protein A data points are depicted as stars. Vertical dashed lines indicate pH 4.0, pH 4.5 and pH 5.0, respectively, horizontal dashed lines indicate 90% recovery. **(C)** Depiction of the recovery of Magnesium-responsive chicken scFvs. Dashed vertical lines indicate 250 mM, 500 mM, or 1000 mM $MgCl_2$ concentration.

to 1 ml/min. It could be shown, that decreasing flow rate gains 3–5% recovery (**Supplementary Figure S5**). In order to evaluate the specificity of H9, an Expi293F culture was transiently transfected with expression plasmids coding for trastuzumab heavy chain and trastuzumab light chain, respectively. After 5 days of expression, the supernatant was filtered, diluted 1:2 with phosphate citrate buffer pH 7.4 and directly applied onto the column. The elution was performed with phosphate citrate buffer

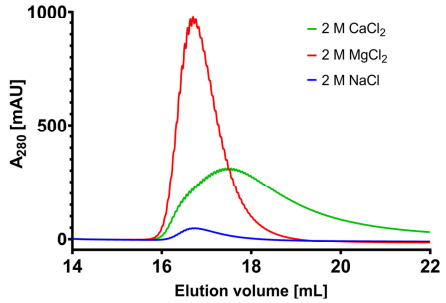


**FIGURE 3 |** Selectivity test of M9 toward $CaCl_2$, NaCl and $MgCl_2$. Depiction of the elution of 2 mg Gamunex bound to immobilized M9 by 2 M NaCl (blue), 2 M $CaCl_2$ (green) or 2 M $MgCl_2$ (red), respectively. Recovery as determined by the AUC was 98.8% for $MgCl_2$, 79.3% for $CaCl_2$ and 8.2% for NaCl, respectively.

at pH 4.6 in the first elution step. As revealed by SDS-PAGE, it was possible to isolate trastuzumab from mammalian cell culture supernatant at high yield and purity with a total recovery of 98.7% (**Figure 5**). A likewise performed purification with a Protein A HP 1 ml column showed no elution at pH 4.6 and the antibody eluted at pH 3.0 off the column (**Supplementary Figure S9**). Both purification procedures showed comparable elution profiles, resulting in antibody recovery either at pH 4.6 (H9 functionalized column) or pH 3.0 (Protein A HP 1 ml column).

For the in depth characterization of the soluble affinity ligands *via* Biolayer Interferometry (BLI), H9, M2 and M9 were chosen to be the most interesting molecules due to their pH-responsive behavior (H9), their magnesium-responsive binding in combination with high $T_M$ (M9), or their combined magnesium and pH-responsive binding (M2). To this end, Daratumumab was immobilized onto anti-Human Fab-CH1 biosensors. The sensors were quenched in kinetics buffer and the association of the respective scFv was measured at different concentrations (**Supplementary Figure S6**). The dissociation was examined at pH 7.4, pH 5.0, and pH 4.5 respectively, as well as at pH 7.0 with 200, 400, and 600 mM $MgCl_2$ added. H9 displayed high affinity binding with a $K_D$ of 35.8 nM (**Table 2**). The dissociation rate increased with lower pH. A 21-, 44-, 161-fold enhanced dissociation was observed when placing the loaded tips in phosphate-citrate-buffer at pH 5.0, pH 4.5, and pH 4.0, respectively. Under similar conditions, M2 showed a 2.8, 5.4-, and

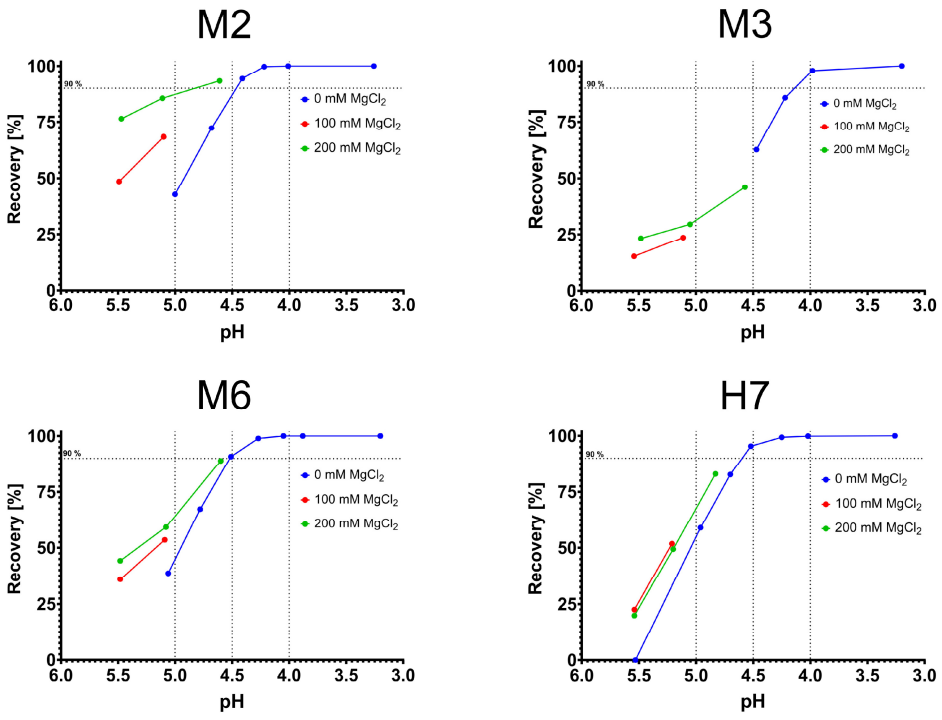


**FIGURE 4 |** Combinatorial experiments with varying magnesium concentration and varying pH values. pH is depicted on the *x*-axis, recovery on the *y*-axis. Blue data points were ascertained in phosphate buffer (0 M $MgCl_2$), red data points in phosphate buffer with 100 mM $MgCl_2$ and green data points in phosphate buffer with 200 mM $MgCl_2$.

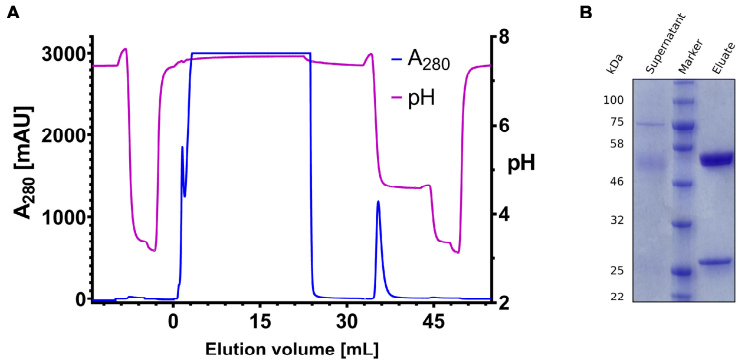


**FIGURE 5 |** Trastuzumab purification from trastuzumab producing Expi293F cell culture supernatant. **(A)** Chromatogram of the purification of trastuzumab from 15 mL Expi293 supernatant. Absorbance at 280 nm is depicted on the left *y*-axis (blue), pH is shown on the right *y*-axis (violet). The elution volume is depicted on the *x*-axis. Elution was performed in two steps with pH 4.6 and pH 3.0, respectively. **(B)** SDS-PAGE gel with the supernatant on the left lane and the purified sample on the right lane, the protein ladder (Blue Prestained Protein Standard, Broad Range; New England Biolabs) is depicted on the middle lane.

**TABLE 2 |** Kinetic data gathered *via* BLI for M2, M9, and H9.

| | $K_D$ [nM] | $K_D$ Error [nM] | $k_{on}$ [$M^{-1}s^{-1}$] | $k_{on}$ Error [$M^{-1}s^{-1}$] | $k_{dis}$ [$s^{-1}$] | $k_{dis}$ Error [$s^{-1}$] |
|---|---|---|---|---|---|---|
| *M2* | 504 | ±20.9 | $6.93 \times 10^4$ | $\pm 2.52 \times 10^3$ | $3.50 \times 10^{-2}$ | $\pm 6.89 \times 10^{-4}$ |
| *M9* | 290 | ±16.1 | $6.01 \times 10^4$ | $\pm 2.89 \times 10^3$ | $1.74 \times 10^{-2}$ | $\pm 4.83 \times 10^{-4}$ |
| *H9* | 35.9 | ±0.55 | $6.41 \times 10^4$ | $\pm 2.53 \times 10^2$ | $2.30 \times 10^{-3}$ | $\pm 3.39 \times 10^{-5}$ |

*Data was obtained on an Octet RED96 system (ForteBio, Pall Life Science) with FAB2G sensors. Fitting was performed with ForteBio Data Analysis 9.0.0.14.*

13-fold enhanced dissociation following the observations from the previous on-column experiments, where H9 was significantly more pH-responsive than M2. M2 and M9 exhibit medium affinity with $K_D$ values in the triple digit nanomolar range of 504 and 290 nM, respectively. Interestingly, M2 and M9 did only display a slightly increased dissociation with increasing magnesium chloride concentrations (**Table 3**). We also checked for cross-reactivity of M2, M9, and I19 toward IgG4 antibodies. M2 and M9 did not show any binding signal toward IgG4, whereas H9 did bind IgG4 with comparable affinity as IgG1 (data not shown). Further cross-reactivity checks have not been performed since IgG1 and IgG4 are the most relevant isotypes in a therapeutic context (Irani et al., 2015).

## DISCUSSION

In this work, we describe the fast and straightforward generation of chicken derived antibody fragments (scFvs) which can be used as ligands in affinity chromatography. By using yeast surface display and FACS it was possible to isolate chicken scFvs with pH-responsive and magnesium-responsive dissociation profiles which kept their responsive behavior upon immobilization on solid phase. Generation of scFv libraries in yeast *S. cerevisiae* is a well-established procedure (Feldhaus et al., 2003; Grzeschik et al., 2019) that routinely allows one to generate more than $10^9$ clones in a single working day. In this experiments, $5.2 \times 10^9$ yeast transformants were obtained from harvested chicken B-cells, where more than 90% of the obtained clones contained a full length scFv encoding gene.

The screening for pH-responsive scFvs was performed according to previously reported screening campaigns for the isolation of pH-responsive antibody fragments (Könning et al., 2016; Bogen et al., 2019). In total, four sorting rounds were necessary to isolate scFvs with desired properties including only one negative sorting step to omit non-responsive binders. Likewise, the isolation of magnesium-responsive scFvs was performed within five sorting rounds including two consecutive negative selection rounds (**Figure 1**).

A small subset of only 10 single clones of each campaign was further analyzed, of which most displayed pH or magnesium-responsive binding, or both which indicates that this FACS-based shuttle-screening is a simple and robust procedure to enrich antibodies with prescribed binding characteristics.

Sequence analysis revealed seven unique pH-responsive and five unique magnesium-responsive scFv variants which could be allocated to three clusters each. No cluster was shared between both families, despite the fact that some of the magnesium-responsive binders also displayed pH-dependent binding. pH-dependent binding is often associated with a higher occurrence of histidine residues in the antibody complementarity determining regions since histidine is the only amino acid that is uncharged at neutral pH and becomes positively charged at acidic pH. The positive charge at lower pH can induce repulsive electrostatic interactions in cases where positive charges of the bound antigen are in close proximity

**TABLE 3 |** Comparison of dissociation constants $k_{dis}$ at pH 7.4, pH 5.0, pH 4.5, pH 4.0 and 200 mM $MgCl_2$, 400 mM $MgCl_2$, 600 mM $MgCl_2$, respectively.

| | *pH 7.4* | | *pH 5.0* | | *pH 4.5* | | *pH 4.0* | | *$MgCl_2$ 200 mM* | | *$MgCl_2$ 400 mM* | | *$MgCl_2$ 600 mM* | |
|---|---|---|---|---|---|---|---|---|---|---|---|---|---|---|
| | $k_{dis}$ [$s^{-1}$] | $k_{dis}$ Error [$s^{-1}$] | $k_{dis}$ [$s^{-1}$] | $k_{dis}$ Error [$s^{-1}$] | $k_{dis}$ [$s^{-1}$] | $k_{dis}$ Error [$s^{-1}$] | $k_{dis}$ [$s^{-1}$] | $k_{dis}$ Error [$s^{-1}$] | $k_{dis}$ [$s^{-1}$] | $k_{dis}$ Error [$s^{-1}$] | $k_{dis}$ [$s^{-1}$] | $k_{dis}$ Error [$s^{-1}$] | $k_{dis}$ [$s^{-1}$] | $k_{dis}$ Error [$s^{-1}$] |
| *M2* | 3.59 × $10^{-2}$ | 9.68 × $10^{-4}$ | 1.32 × $10^{-1}$ | 1.42 × $10^{-3}$ | 1.92 × $10^{-1}$ | 3.65 × $10^{-3}$ | 4.77 × $10^{-1}$ | 1.50 × $10^{-2}$ | 1.06 × $10^{-1}$ | 1.39 × $10^{-3}$ | 1.54 × $10^{-1}$ | 2.45 × $10^{-3}$ | 2.06 × $10^{-1}$ | 3.34 × $10^{-3}$ |
| *Enhancement [x-fold]** | 1 | | 2.8 | | 5.4 | | 13 | | 3.0 | | 4.3 | | 5.7 | |
| *M9* | 2.75 × $10^{-1}$ | 1.78 × $10^{-2}$ | n.d. | n.d. | n.d. | n.d. | n.c. | n.d. | 3.29 × $10^{-1}$ | 2.35 × $10^{-2}$ | 4.10 × $10^{-1}$ | 3.27 × $10^{-2}$ | 4.67 × $10^{-1}$ | 4.59 × $10^{-2}$ |
| *Enhancement [x-fold]** | 1 | | | | | | | | 1.2 | | 1.5 | | 1.7 | |
| *H9* | 2.55 × $10^{-3}$ | 2.41 × $10^{-3}$ | 5.35 × $10^{-2}$ | 9.03 × $10^{-4}$ | 1.13 × $10^{-1}$ | 1.89 × $10^{-3}$ | 4.11 × $10^{-1}$ | 8.07 × $10^{-3}$ | n.d. | n.d. | n.d. | n.d. | n.d. | n.d. |
| *Enhancement [x-fold]** | 1 | | 21 | | 44 | | 161 | | | | | | | |

*Calculations were performed with ForteBio Data Analysis 9.0.0.14. *Enhancement in comparison to the respective dissociation constant $k_{dis}$ at pH 7.4 and 0 mM $MgCl_2$ is shown.*

to the antibody binding site (Murtaugh et al., 2011). We have not observed unusual strong enrichment of histidines in our described clones (data not shown). In addition, the pH-responsive behavior can also be caused by destabilizing the VH/VL interaction as well as the CDR loop arrangement weakening the antigen-binding. Specific framework changes to exploit ionisable groups in order to generate pH/calcium-responsive proteins are described in literature (Gulich et al., 2000; Kellmann et al., 2017; Kanje et al., 2018). Since we have no detailed knowledge of the exact binding epitopes it is currently unclear, which amino acids in the CDRs and the bound target protein epitope and which type of interaction account for the observed pH responsive binding. Aspartate and glutamate are typically involved in magnesium complexation, which could interfere with antigen binding (Dudev and Lim, 2007; Brylinski and Skolnick, 2011; Khrustalev et al., 2016). Since these residues are also amenable to protonation at acidic pH, and the microenvironment of the antigen-antibody complex may occasionally promote a shift to higher pK of these residues, it is tempting to speculate that these effects account for the observed pH-responsive binding of several obtained clones, that have exclusively been screened for reduced binding at elevated magnesium concentration. Notably, the pH- and magnesium-dependent binding is not due to denaturation of the scFv at acidic pH or high magnesium concentrations since melting temperatures were largely unchanged under these conditions (**Table 1**). Furthermore, it was possible to verify that the addition of $MgCl_2$ can stabilize the scFv and therefore elevate the observed melting temperature (**Supplementary Figure S7**).

All scFvs could be expressed in *E. coli* SHuffle T7 Express cells with low to medium expression levels. No efforts were made yet to optimize expression yields, e.g., by codon optimization or using culture media for high density growth. No efforts were made to optimize the scFv loading density and target antibody binding capacity. Coupling onto NHS-agarose columns was performed with 5 mg protein resulting in coupling efficiencies of 67-96%. If a 1:1 interaction is assumed, the column with the least amount of coupled scFv (M3, 67%) should be capable of capturing 18.6 mg antibody which was considered sufficient to evaluate the capturing performance.

Protein A is the gold standard for antibody purification using mild elution conditions requiring a pH less than 4.0 for release of bound antibody. H1, H6, H7, and H9 did show efficient elution up to pH 4.0 with over 95% recovery which exceeds the recovery of Protein A at pH 4.0. H7 and H9 – both originated from the same cluster – appeared to be the most pH-responsive variants with close to quantitative elution at pH 4.5 (**Figure 2B**). The magnesium-responsive variants M2, M3, and M6 also showed more efficient elution than Protein A at pH 4.0. However, the most magnesium-responsive variants M8 and M9 did not show pH-responsive Fc binding. We found that combining pH-changes dependent on $Mg^{2+}$-concentration can significantly increase recovery. Particularly for M2 we found that low $MgCl_2$ concentrations will increase the recovery from 40% to 90% at ~pH 5.0 (**Figure 4**). Also, the flow rate decrease from 3 ml/min to 1 ml/min lead to an increase of approx. 5% at pH

4.6 for H9 (**Supplementary Figure S5**) indicating that elution conditions might be further tuneable if desired.

In recent years, the Capture Select$^{TM}$ strategy was introduced that relies on the isolation of camelid VHH domain that selectively bind various type of antibodies. These have also been developed for antibody affinity purification and elution at acidic pH or using elevated magnesium concentrations (Hermans et al., 2017). Little information is available in literature about the screening procedure, but multiple formats against different antibody formats have been developed upon lama immunization and subsequent phage display screening (Klooster et al., 2007; Detmers et al., 2010; Reinhart et al., 2012). Notably, in comparison to camelid derived VHHs that require a magnesium burst of 1 M $MgCl_2$ in combination with 40% propylene glycol for elution, chicken scFvs isolated in this work showed elution at neutral pH with significantly reduced $MgCl_2$ concentration (400 mM).

The observed $K_D$ values for H9, M2 and M9 ranged from 40 nM to over 500 nM, well in the range of affinities sufficient for affinity chromatography as described by literature (Anspach, 2004; Mondal et al., 2006; Chen et al., 2014). Watanabe et al. (2009) engineered pH-responsive Protein G variants by rational design comprising similar $K_D$ values. Their best variant showed an affinity decrease of 80-fold at 4.0 which is clearly exceeded by H9 with an affinity decrease of 161-fold. The findings for the magnesium-buffer dependency of target release were surprisingly not correlating to the on-column experiments. M9 displayed better recovery but less affinity decrease in the BLI experiments compared to M2. This indicates that the artificial conditions in the BLI setup do not correlate very well to the binding conditions of the scFv and the antigen on column.

Lastly, usability of chicken scFvs for affinity chromatography was underlined by the fact that no decrease in column capacity was observed during the testing period over up to 18 chromatography cycles. Additionally, no decrease in AUC was observed in a repeated cycle experiment were five consecutive chromatography runs were performed with H7 (**Supplementary Figure S8**) after all test runs.

In summary, in this work, we describe as straightforward procedure for the isolation of chicken antibody-based affinity ligands for affinity chromatography. We demonstrated that the immunization of chicken and the subsequent FACS selection process delivers a plethora of different ligands which can be individually optimized for chromatography applications. It is important to note that this generic strategy can also be applied to the purification of proteins with therapeutic relevance other than monoclonal antibodies.

## DATA AVAILABILITY STATEMENT

The raw data supporting the conclusions of this article will be made available by the authors, without undue reservation, to any qualified researcher.

## AUTHOR CONTRIBUTIONS

SH and HK conceived and designed the experiments, and wrote the manuscript. SH, AE, and AA performed the experiments. AE performed the experiments for the revision. SH, AE, OR, AS, and HK analyzed the data. OR, AS, SZ, and TH gave scientific advice. All authors contributed to the article and approved the submitted version.

## FUNDING

The authors declare that this study received funding from Merck KGaA and Merck Lab @ Technische Universität Darmstadt. The funders had no role in study design, data collection and analysis, decision to publish, or preparation of the manuscript.

## ACKNOWLEDGMENTS

We would like to express to our gratitude to Tina Bock and Gerhard Schwall of the Merck Lab @ Technische Universität Darmstadt for discussion and scientific advice. We kindly thank Vanessa Kohl for experimental support. We would also like to thank the Department of Protein Engineering and Antibody Technologies and the Life Science Division at Merck KGaA for material and technical support on protein coupling and chromatography experiments.

## SUPPLEMENTARY MATERIAL

The Supplementary Material for this article can be found online at: https://www.frontiersin.org/articles/10.3389/fbioe.2020.00688/full#supplementary-material

## REFERENCES

Anspach, F. B. (2004). in *Fundamentals and Applications of Chromatography and Related Differential Migration Methods – Part A: Fundamentals and Techniques*, 6 Edn, Vol. 69A, ed. E. Heftmann, (Amsterdam: Elsevier Science).

Bedford, R., Tiede, C., Hughes, R., Curd, A., McPherson, M. J., Peckham, M., et al. (2017). Alternative reagents to antibodies in imaging applications. *Biophys. Rev.* 9, 299–308. doi: 10.1007/s12551-017-0278-2

Behar, G., Renodon-Corniere, A., Mouratou, B., and Pecorari, F. (2016). Affitins as robust tailored reagents for affinity chromatography purification of antibodies and non-immunoglobulin proteins. *J. Chromatogr. A* 1441, 44–51. doi: 10.1016/j.chroma.2016.02.068

Benatuil, L., Perez, J. M., Belk, J., and Hsieh, C. M. (2010). An improved yeast transformation method for the generation of very large human antibody libraries. *Protein Eng. Des. Sel.* 23, 155–159. doi: 10.1093/protein/gzq002

Boder, E. T., and Wittrup, K. D. (1997). Yeast surface display for screening combinatorial polypeptide libraries. *Nat. Biotechnol.* 15, 553–557. doi: 10.1038/nbt0697-553

Bogen, J. P., Hinz, S. C., Grzeschik, J., Ebenig, A., Krah, S., Zielonka, S., et al. (2019). Dual function pH responsive bispecific antibodies for tumor targeting and antigen depletion in plasma. *Front. Immunol.* 10:1892. doi: 10.3389/fimmu.2019.01892

Brylinski, M., and Skolnick, J. (2011). FINDSITE-metal: integrating evolutionary information and machine learning for structure-based metal-binding site prediction at the proteome level. *Proteins* 79, 735–751. doi: 10.1002/prot.22913

Chen, C., Khoury, G. E., and Lowe, C. R. (2014). Affinity ligands for glycoprotein purification based on the multi-component Ugi reaction. *J. Chromatogr. B* 969, 171–180. doi: 10.1016/j.jchromb.2014.07.035

Davies, E. L., Smith, J. S., Birkett, C. R., Manser, J. M., Anderson-Dear, D. V., and Young, J. R. (1995). Selection of specific phage-display antibodies using libraries derived from chicken immunoglobulin genes. *J. Immunol. Methods* 186, 125–135. doi: 10.1016/0022-1759(95)00143-x

Davis, J. H., Aperlo, C., Li, Y., Kurosawa, E., Lan, Y., Lo, K. M., et al. (2010). SEEDbodies: fusion proteins based on strand-exchange engineered domain (SEED) CH3 heterodimers in an Fc analogue platform for asymmetric binders or immunofusions and bispecific antibodies. *Protein Eng. Des. Sel.* 23, 195–202. doi: 10.1093/protein/gzp094

Dawson, R. M. C., Elliott, D. C., Elliott, W. H., and Jones, K. M. (1987). *Data for Biochemical Research*, 3 Edn. Oxford: Oxford Science Publications.

Detmers, F., Hermans, P., Jiao, J.-A., and McCue, J. T. (2010). Novel affinity ligands provide for highly selective primary capture. *BioProcess Int.* 8, 50–54.

Dingman, R., and Balu-Iyer, S. V. (2019). Immunogenicity of protein pharmaceuticals. *J. Pharm. Sci.* 108, 1637–1654. doi: 10.1016/j.xphs.2018.12.014

Dudev, M., and Lim, C. (2007). Discovering structural motifs using a structural alphabet: application to magnesium-binding sites. *BMC Bioinform.* 8:106. doi: 10.1186/1471-2105-8-106

Duhamel, R. C., Schur, P. H., Brendel, K., and Meezan, E. (1979). pH gradient elution of human IgG1, IgG2 and IgG4 from protein A-sepharose. *J. Immunol. Methods* 31, 211–217. doi: 10.1016/0022-1759(79)90133-9

Feldhaus, M. J., Siegel, R. W., Opresko, L. K., Coleman, J. R., Feldhaus, J. M. W., Yeung, Y. A., et al. (2003). Flow-cytometric isolation of human antibodies from a nonimmune Saccharomyces cerevisiae surface display library. *Nat. Biotechnol.* 21, 163–170. doi: 10.1038/nbt785

Garber, E., and Demarest, S. J. (2007). A broad range of Fab stabilities within a host of therapeutic IgGs. *Biochem. Biophys. Res. Commun.* 355, 751–757. doi: 10.1016/j.bbrc.2007.02.042

Gera, N., Hill, A. B., White, D. P., Carbonell, R. G., and Rao, B. M. (2012). Design of pH sensitive binding proteins from the hyperthermophilic Sso7d scaffold. *PLoS One* 7:e48928. doi: 10.1371/journal.pone.0048928

Grand View Research, (2017). *Biologics market size worth $399.5 billion by 2025 | Growth rate: 3.9%*. Available online at: https://www.grandviewresearch.com/press-release/global-biologics-market (accessed January 3, 2020).

Grzeschik, J., Yanakieva, D., Roth, L., Krah, S., Hinz, S. C., Elter, A., et al. (2019). Yeast surface display in combination with fluorescence-activated cell sorting enables the rapid isolation of antibody fragments derived from immunized chickens. *Biotechnol. J.* 14:e1800466. doi: 10.1002/biot.201800466

Gulich, S., Linhult, M., Stahl, S., and Hober, S. (2002). Engineering streptococcal protein G for increased alkaline stability. *Protein Eng.* 15, 835–842. doi: 10.1093/protein/15.10.835

Gulich, S., Uhlen, M., and Hober, S. (2000). Protein engineering of an IgG-binding domain allows milder elution conditions during affinity chromatography. *J. Biotechnol.* 76, 233–244. doi: 10.1016/s0168-1656(99)00197-2

Hahn, R., Shimahara, K., Steindl, F., and Jungbauer, A. (2006). Comparison of protein A affinity sorbents III. Life time study. *J. Chromatogr. A* 1102, 224–231. doi: 10.1016/j.chroma.2005.10.083

Harakas, N. K. (1994). Protein purification process engineering. Biospecific affinity chromatography. *Bioprocess Technol.* 18, 259–316.

Hermans, P., Adams, H., and Detmers, F. (2014). Purification of antibodies and antibody fragments using capture select affinity resins. *Methods Mol. Biol.* 1131, 297–314. doi: 10.1007/978-1-62703-992-5_19

Hermans, W. J. J., Blokland, S., Kesteren, M. A. V., Horrevoets, J. M., and Detmers, F. J. M. (2017). Antigen-binding protein directed against epitope in the CH1 domain of human IgG antibodies. *Google Patents*.

Heu, W., Choi, J. M., Lee, J. J., Jeong, S., and Kim, H. S. (2014). Protein binder for affinity purification of human immunoglobulin antibodies. *Anal. Chem.* 86, 6019–6025. doi: 10.1021/ac501158t

Irani, V., Guy, A. J., Andrew, D., Beeson, J. G., Ramsland, P. A., and Richards, J. S. (2015). Molecular properties of human IgG subclasses and their implications for designing therapeutic monoclonal antibodies against infectious diseases. *Mol. Immunol.* 67, 171–182. doi: 10.1016/j.molimm.2015.03.255

Jin, W., Xing, Z., Song, Y., Huang, C., Xu, X., Ghose, S., et al. (2019). Protein aggregation and mitigation strategy in low pH viral inactivation for monoclonal antibody purification. *MAbs* 11, 1479–1491. doi: 10.1080/19420862.2019.1658493

Johar, S. S., and Talbert, J. N. (2017). Strep-tag II fusion technology for the modification and immobilization of lipase B from Candida antarctica (CALB). *J. Genet. Eng. Biotechnol.* 15, 359–367. doi: 10.1016/j.jgeb.2017.06.011

Kanje, S., Venskutonyte, R., Scheffel, J., Nilvebrant, J., Lindkvist-Petersson, K., and Hober, S. (2018). Protein engineering allows for mild affinity-based elution of therapeutic antibodies. *J. Mol. Biol.* 430, 3427–3438. doi: 10.1016/j.jmb.2018.06.004

Kellmann, S. J., Dubel, S., and Thie, H. (2017). A strategy to identify linker-based modules for the allosteric regulation of antibody-antigen binding affinities of different scFvs. *MAbs* 9, 404–418. doi: 10.1080/19420862.2016.1277302

Khrustalev, V. V., Barkovsky, E. V., and Khrustaleva, T. A. (2016). Magnesium and manganese binding sites on proteins have the same predominant motif of secondary structure. *J. Theor. Biol.* 395, 174–185. doi: 10.1016/j.jtbi.2016.02.006

Klooster, R., Maassen, B. T., Stam, J. C., Hermans, P. W., Ten Haaft, M. R., Detmers, F. J., et al. (2007). Improved anti-IgG and HSA affinity ligands: clinical application of VHH antibody technology. *J. Immunol. Methods* 324, 1–12. doi: 10.1016/j.jim.2007.04.005

Koguma, I., Yamashita, S., Sato, S., Okuyama, K., and Katakura, Y. (2013). Novel purification method of human immunoglobulin by using a thermo-responsive protein A. *J. Chromatogr. A* 1305, 149–153. doi: 10.1016/j.chroma.2013.07.015

Könning, D., Zielonka, S., Sellmann, C., Schröter, C., Grzeschik, J., Becker, S., et al. (2016). Isolation of a pH-sensitive IgNAR variable domain from a yeast-displayed, histidine-doped master library. *Mar. Biotechnol.* 18, 161–167. doi: 10.1007/s10126-016-9690-z

Linhult, M., Gulich, S., and Hober, S. (2005). Affinity ligands for industrial protein purification. *Protein Pept. Lett.* 12, 305–310. doi: 10.2174/0929866053765662

Lu, X., Nobrega, R. P., Lynaugh, H., Jain, T., Barlow, K., Boland, T., et al. (2019). Deamidation and isomerization liability analysis of 131 clinical-stage antibodies. *MAbs* 11, 45–57. doi: 10.1080/19420862.2018.1548233

MacLennan, J. (1995). Engineering microprotein ligands for large-scale affinity purification. *Biotechnology* 13, 1180–1183. doi: 10.1038/nbt1195-1180

Mazzer, A. R., Perraud, X., Halley, J., O'Hara, J., and Bracewell, D. G. (2015). Protein A chromatography increases monoclonal antibody aggregation rate during subsequent low pH virus inactivation hold. *J. Chromatogr. A* 1415, 83–90. doi: 10.1016/j.chroma.2015.08.068

McCormack, W. T., Tjoelker, L. W., and Thompson, C. B. (1993). Immunoglobulin gene diversification by gene conversion. *Prog. Nucleic Acid Res. Mol. Biol.* 45, 27–45. doi: 10.1016/s0079-6603(08)60865-x

McPherson, M., and Tomlinson, D. (2014). Scaffold proteins derived from plant cystatins. *Google Patents*.

Miller, B. R., Demarest, S. J., Lugovskoy, A., Huang, F., Wu, X., Snyder, W. B., et al. (2010). Stability engineering of scFvs for the development of bispecific and multivalent antibodies. *Protein Eng. Des. Sel.* 23, 549–557. doi: 10.1093/protein/gzq028

Mondal, K., Gupta, M. N., and Roy, I. (2006). Affinity-based strategies for protein purification. *Anal. Chem.* 78, 3499–3504. doi: 10.1021/ac069406

Muda, M., Gross, A. W., Dawson, J. P., He, C., Kurosawa, E., Schweickhardt, R., et al. (2011). Therapeutic assessment of SEED: a new engineered antibody platform designed to generate mono- and bispecific antibodies. *Protein Eng. Des. Sel.* 24, 447–454. doi: 10.1093/protein/gzq123

Murtaugh, M. L., Fanning, S. W., Sharma, T. M., Terry, A. M., and Horn, J. R. (2011). A combinatorial histidine scanning library approach to engineer highly pH-dependent protein switches. *Protein Sci.* 20, 1619–1631. doi: 10.1002/pro.696

Nilsson, B., Moks, T., Jansson, B., Abrahmsen, L., Elmblad, A., Holmgren, E., et al. (1987). A synthetic IgG binding domain based on staphylococcal protein A. *Protein Eng.* 1, 107–113. doi: 10.1093/protein/1.2.107

Orr, B. A., Carr, L. M., Wittrup, K. D., Roy, E. J., and Kranz, D. M. (2003). Rapid method for measuring scFv thermal stability by yeast surface display. *Biotechnol. Prog.* 19, 631–638. doi: 10.1021/bp0200797

Pabst, T. M., Palmgren, R., Forss, A., Vasic, J., Fonseca, M., Thompson, C., et al. (2014). Engineering of novel staphylococcal Protein A ligands to enable milder elution pH and high dynamic binding capacity. *J. Chromatogr. A* 1362, 180–185. doi: 10.1016/j.chroma.2014.08.046

Palmqvist, N., Foster, T., Tarkowski, A., and Josefsson, E. (2002). Protein A is a virulence factor in *Staphylococcus aureus* arthritis and septic death. *Microb. Pathog.* 33, 239–249. doi: 10.1006/mpat.2002.0533

Prinzinger, R., Preßmar, A., and Schleucher, E. (1991). Body temperature in birds. *Comp. Biochem. Physiol. Part A Physiol.* 99, 499–506. doi: 10.1016/0300-9629(91)90122-S

Reinhart, D., Weik, R., and Kunert, R. (2012). Recombinant IgA production: single step affinity purification using camelid ligands and product characterization. *J. Immunol. Methods* 378, 95–101. doi: 10.1016/j.jim.2012.02.010

Renee, T., and Weilei, M. (2017). *Analysis of FcRn-Antibody Interactions on the Octet Platform. Application Note 19*. Available online at: https://www.moleculardevices.com/en/assets/app-note/biologics/analysis-of-fcrn-antibody-interactions-on-octet-platform (accessed January 20, 2020).

Reynaud, C. A., Anquez, V., Dahan, A., and Weill, J. C. (1985). A single rearrangement event generates most of the chicken immunoglobulin light chain diversity. *Cell* 40, 283–291. doi: 10.1016/0092-8674(85)90142-4

Reynaud, C. A., Anquez, V., Grimal, H., and Weill, J. C. (1987). A hyperconversion mechanism generates the chicken light chain preimmune repertoire. *Cell* 48, 379–388. doi: 10.1016/0092-8674(87)90189-9

Reynaud, C. A., Anquez, V., and Weill, J. C. (1991). The chicken D locus and its contribution to the immunoglobulin heavy chain repertoire. *Eur. J. Immunol.* 21, 2661–2670. doi: 10.1002/eji.1830211104

Reynaud, C. A., Dahan, A., Anquez, V., and Weill, J. C. (1989). Somatic hyperconversion diversifies the single Vh gene of the chicken with a high incidence in the D region. *Cell* 59, 171–183. doi: 10.1016/0092-8674(89)90879-9

Ricci, S., Medaglini, D., Marcotte, H., Olsen, A., Pozzi, G., and Bjorck, L. (2001). Immunoglobulin-binding domains of peptostreptococcal protein L enhance vaginal colonization of mice by Streptococcus gordonii. *Microb. Pathog.* 30, 229–235. doi: 10.1006/mpat.2000.0427

Saraswat, M., Musante, L., Ravida, A., Shortt, B., Byrne, B., and Holthofer, H. (2013). Preparative purification of recombinant proteins: current status and future trends. *Biomed. Res. Int.* 2013:312709. doi: 10.1155/2013/312709

Scheffel, J., Kanje, S., Borin, J., and Hober, S. (2019). Optimization of a calcium-dependent Protein A-derived domain for mild antibody purification. *MAbs* 11, 1492–1501. doi: 10.1080/19420862.2019.1662690

Schneider, H., Deweid, L., Pirzer, T., Yanakieva, D., Englert, S., Becker, B., et al. (2019). Dextramabs: a novel format of antibody-drug conjugates featuring a multivalent polysaccharide scaffold. *ChemistryOpen* 8, 354–357. doi: 10.1002/open.201900066

Simeon, R., and Chen, Z. (2018). In vitro-engineered non-antibody protein therapeutics. *Protein Cell* 9, 3–14. doi: 10.1007/s13238-017-0386-6

Škrlec, K., Štrukelj, B., and Berlec, A. (2015). Non-immunoglobulin scaffolds: a focus on their targets. *Trends Biotechnol.* 33, 408–418. doi: 10.1016/j.tibtech.2015.03.012

Straathof, A. J. J. (2011). "2.57 – the proportion of downstream costs in fermentative production processes," in *Comprehensive Biotechnology*, 2nd Edn, ed. M. Moo-Young, (Burlington: Academic Press), 811–814. doi: 10.1016/b978-0-08-088504-9.00492-x

Thompson, C. B., and Neiman, P. E. (1987). Somatic diversification of the chicken immunoglobulin light chain gene is limited to the rearranged variable gene segment. *Cell* 48, 369–378. doi: 10.1016/0092-8674(87)90188-7

Tiede, C., Bedford, R., Heseltine, S. J., Smith, G., Wijetunga, I., Ross, R., et al. (2017). Affimer proteins are versatile and renewable affinity reagents. *eLife* 6:e24903. doi: 10.7554/eLife.24903

Tsukamoto, M., Watanabe, H., Ooishi, A., and Honda, S. (2014). Engineered protein A ligands, derived from a histidine-scanning library, facilitate the affinity purification of IgG under mild acidic conditions. *J. Biol. Eng.* 8:15. doi: 10.1186/1754-1611-8-15

Urh, M., Simpson, D., and Zhao, K. (2009). "Chapter 26 affinity chromatography: general methods," in *Methods in Enzymology*, Vol. 463, eds R. R. Burgess, and M. P. Deutscher, (Cambridge, MA: Academic Press), 417–438. doi: 10.1016/s0076-6879(09)63026-3

Vázquez-Rey, M., and Lang, D. A. (2011). Aggregates in monoclonal antibody manufacturing processes. *Biotechnol. Bioeng.* 108, 1494–1508. doi: 10.1002/bit.23155

Veggiani, G., and de Marco, A. (2011). Improved quantitative and qualitative production of single-domain intrabodies mediated by the co-expression of Erv1p sulfhydryl oxidase. *Protein Expr. Purif.* 79, 111–114. doi: 10.1016/j.pep.2011.03.005

Walsh, G. (2018). Biopharmaceutical benchmarks 2018. *Nat. Biotechnol.* 36, 1136–1145. doi: 10.1038/nbt.4305

Watanabe, H., Matsumaru, H., Ooishi, A., Feng, Y., Odahara, T., Suto, K., et al. (2009). Optimizing pH response of affinity between protein G and IgG Fc: how electrostatic modulations affect protein-protein interactions. *J. Biol. Chem.* 284, 12373–12383. doi: 10.1074/jbc.M809236200

Watanabe, H., Yoshida, C., Ooishi, A., Nakai, Y., Ueda, M., Isobe, Y., et al. (2019). Histidine-mediated intramolecular electrostatic repulsion for controlling pH-dependent protein-protein interaction. *ACS Chem. Biol.* 14, 2729–2736. doi: 10.1021/acschembio.9b00652

Wu, L., Oficjalska, K., Lambert, M., Fennell, B. J., Darmanın-Sheehan, A., Ni Shuilleabhain, D., et al. (2012). Fundamental characteristics of the immunoglobulin VH repertoire of chickens in comparison with those of humans, mice, and camelids. *J. Immunol.* 188, 322–333. doi: 10.4049/jimmunol.1102466

**Conflict of Interest:** TH, AS, OR, and SZ were employed by Merck KGaA. Merck KGaA has an interest in and develops resins for affinity chromatography.

The remaining authors declare that the research was conducted in the absence of any commercial or financial relationships that could be construed as a potential conflict of interest.

frontiers

# *Supplementary Material*

## 1 Supplementary Data

**Table S1.** Detailed staining strategy for all sorting rounds including the dilution of working solution for primary and secondary labeling agents.

| | SURFACE PRESENTATION | | TARGET BINDING | |
|---|---|---|---|---|
| Sorting round | Primary labeling agent | Secondary labeling agent | Primary labeling agent | Secondary labeling agent |
| **1.** | anti-c-myc biotin antibody (1:30) | Streptavidin-PE (1:75) | 1 µM Fc-protein-dylight650 | - |
| **2.** | anti-c-myc biotin antibody (1:30) | Streptavidin-PE (1:75) | 1 µM Fc-protein-dylight650 | - |
| **3.** | anti-c-myc antibody (undil.) | anti-mouse IgG R-PE (1:30) | 1 µM Daratumumab | anti-Human IgG (Fab specific) –FITC (1:20) |
| **4. pH** | anti-c-myc antibody (undil.) | anti-mouse IgG R-PE (1:30) | 250 Pertuzumab | anti-Human IgG (Fab specific) –FITC (1:20) |
| **5. pH** | anti-c-myc biotin antibody (1:30) | Streptavidin-APC (1:75) | 150 nM Daratumumab | Goat F(ab')$_2$ anti-Human Kappa-PE (1:80) |
| **4. $MgCl_2$** | anti-c-myc biotin antibody (1:30) | Streptavidin-PE (1:75) | 1 µM Cetuximab | anti-Human IgG (Fab specific) –FITC (1:20) |
| **5. $MgCl_2$** | anti-c-myc antibody (undil.) | anti-mouse IgG FITC (1:20) | 1 µM Cetuximab | Goat anti-Human IgG Fc Secondary Antibody PE (1:80) |
| **6. $MgCl_2$** | anti-c-myc biotin antibody (1:30) | Streptavidin-APC (1:75) | 150 nM Daratumumab | Goat F(ab')$_2$ anti-Human Kappa-PE (1:80) |

**Table S2**. Immuno-staining procedure of yeast cells before cell sorting. Cells were stained in a total volume of 20 µL per 1 × $10^7$ yeast cells. Every incubation step was followed by a wash step (W) using 1 mL PBS-B pH 7.4 (PBS + 0.1% (w/v) BSA) except for the last wash step which was performed twice to reduce background fluorescence. All staining and wash steps were performed at 4 °C.

**INCUBATION STEPS**

| **Sorting round** | Incubation with target protein in PBS-B pH 7.4; 30 min; 4 °C | W | Negative selection step (either 5 min incubation in 1 mL phosphate citrate pH 5.0 or 30 s in Tris/HCl 50 mM pH 7.0, $MgCl_2$ 2 M) | W | Primary labeling agents for surface detection and target binding in PBS-B pH 7.4; 15 min; 4 °C | W | Secondary labeling agents for surface detection and target binding in PBS-B pI1 7.4; 15 min; 4 °C | W |
|---|---|---|---|---|---|---|---|---|
| **Sorting campaign for the isolation of pH-responsive scFvs** | | | | | | | | |
| 1. | + | **1x** | | **1x** | + | **1x** | + | **2x** |
| 2. | + | **1x** | | **1x** | + | **1x** | + | **2x** |
| 3. | + | **1x** | | **1x** | + | **1x** | + | **2x** |
| 4. pH | + | **1x** | phosphate citrate pH 5.0 | **1x** | + | **1x** | + | **2x** |
| 5. pH | + | **1x** | | **1x** | + | **1x** | + | **2x** |
| **Sorting campaign for the isolation of $MgCl_2$-responsive scFvs** | | | | | | | | |
| 1. | + | **1x** | | **1x** | + | **1x** | + | **2x** |
| 2. | + | **1x** | | **1x** | + | **1x** | + | **2x** |
| 3. | + | **1x** | | **1x** | + | **1x** | + | **2x** |
| 4. $MgCl_2$ | + | **1x** | Tris/HCl 50 mM pH 7.0, $MgCl_2$ 2 M | **1x** | + | **1x** | + | **2x** |
| 5. $MgCl_2$ | + | **1x** | Tris/HCl 50 mM pH 7.0, $MgCl_2$ 2 M | **1x** | + | **1x** | + | **2x** |
| 6. $MgCl_2$ | + | **1x** | | **1x** | + | **1x** | + | **2x** |

2

**Table S3.** Primers used for library generation and reformatting into an expression plasmid. Sequences are depicted in 5' to 3' orientation.

| | |
|---|---|
| *VH_gr_up* | GGTGGTGGTGGTTCTGGTGGTGGTGGTTCTGCTAGCGCCGTGACGTTGGACGAG |
| *VH_SOE_lo* | TCCGCCCCCCGACCCGCCGCCGCCTGAGCCGCCTCCCCCGGAGGAGACGATGACTTCGGT |
| *VL_SOE_up* | GGCGGCTCAGGCGGCGGCGGGTCGGGGGGCGGAGGGAGCGCGCTGACTCAGCCGTCCTCG |
| *VL_gr_lo* | CAAGTCCTCTTCAGAAATAAGCTTTTGTTCGGATCCTAGGACGGTCAGGGTTGTCCC |
| *scFv_chick_his_GG_up* | ATATATGGTCTCAATGGCTCACCACCACCACCACCACGGGTCTGCTAGCGCCGTGACGTTGGACGAGTCCG |
| *scFv_chick_SII_GG_*lo | ATATATGGTCTCATCATCATTTTTCGAACTGCGGGTGGCTCCAAGACCCTAGGACGGTCAGGGTTGTCCCGGCC |

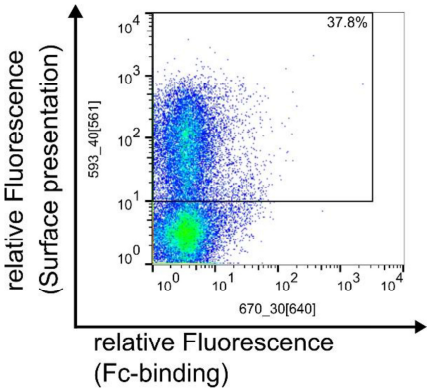


**Figure S1.** Depiction of 50,000 events of the initial, unsorted yeast library with target binding on the x-axis and surface presentation on the y-axis to determine the presentation levels.

3

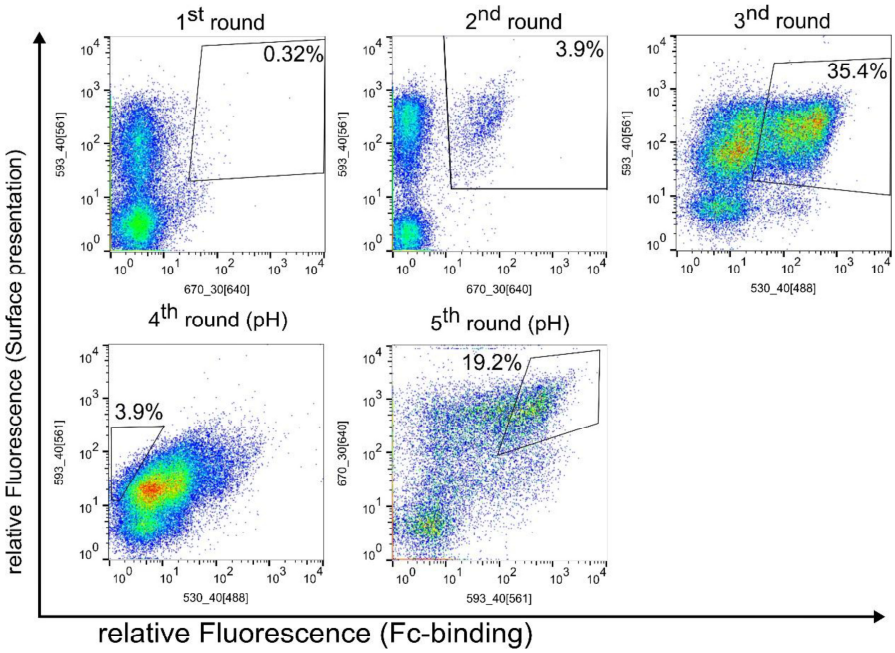


**Figure S2.** Summary of the sorting campaign for the isolation of pH-responsive chicken-scFvs. Each FACS plot shows 50,000 events with Fc-binding plotted on the x-axis and surface presentation on the y-axis. Detailed staining strategy is summarized in Table S1. Enrichment of Fc-specific scFvs *via* YSD and FACS during the 1st, 2nd and 3rd sorting rounds. The 4th sorting round was performed to deplete non-pH-responsive scFvs with an additional washing step with phosphate citrate buffer (Table S2). Last sorting round was conducted to isolate single clones positive for IgG binding at pH 7.4.

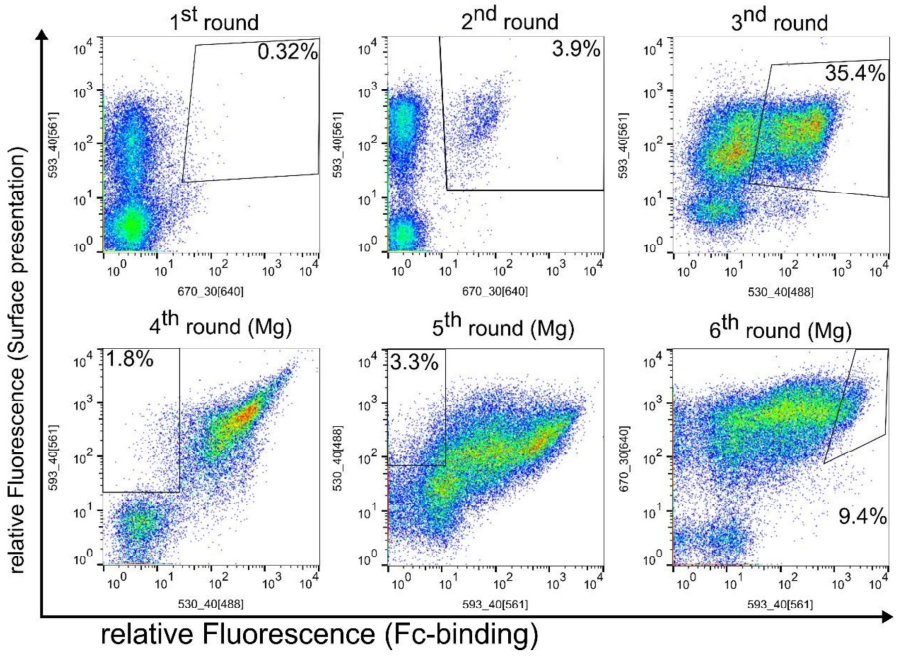


**Figure S3.** Summary of the sorting campaign for the isolation of magnesium-responsive chicken-scFvs. Each FACS plot shows 50,000 events with Fc-binding plotted on the x-axis and surface presentation on the y-axis. Detailed staining strategy is summarized in Table S1. Enrichment of Fc-specific scFvs *via* YSD and FACS during the 1st, 2nd and 3rd sorting rounds. The 4th and 5th sorting rounds were performed to deplete non-magnesium-responsive scFvs with an additional washing step with $MgCl_2$-containing buffer (Table S2). Last sorting round was conducted to isolate single clones positive for IgG binding at pH 7.4.

5

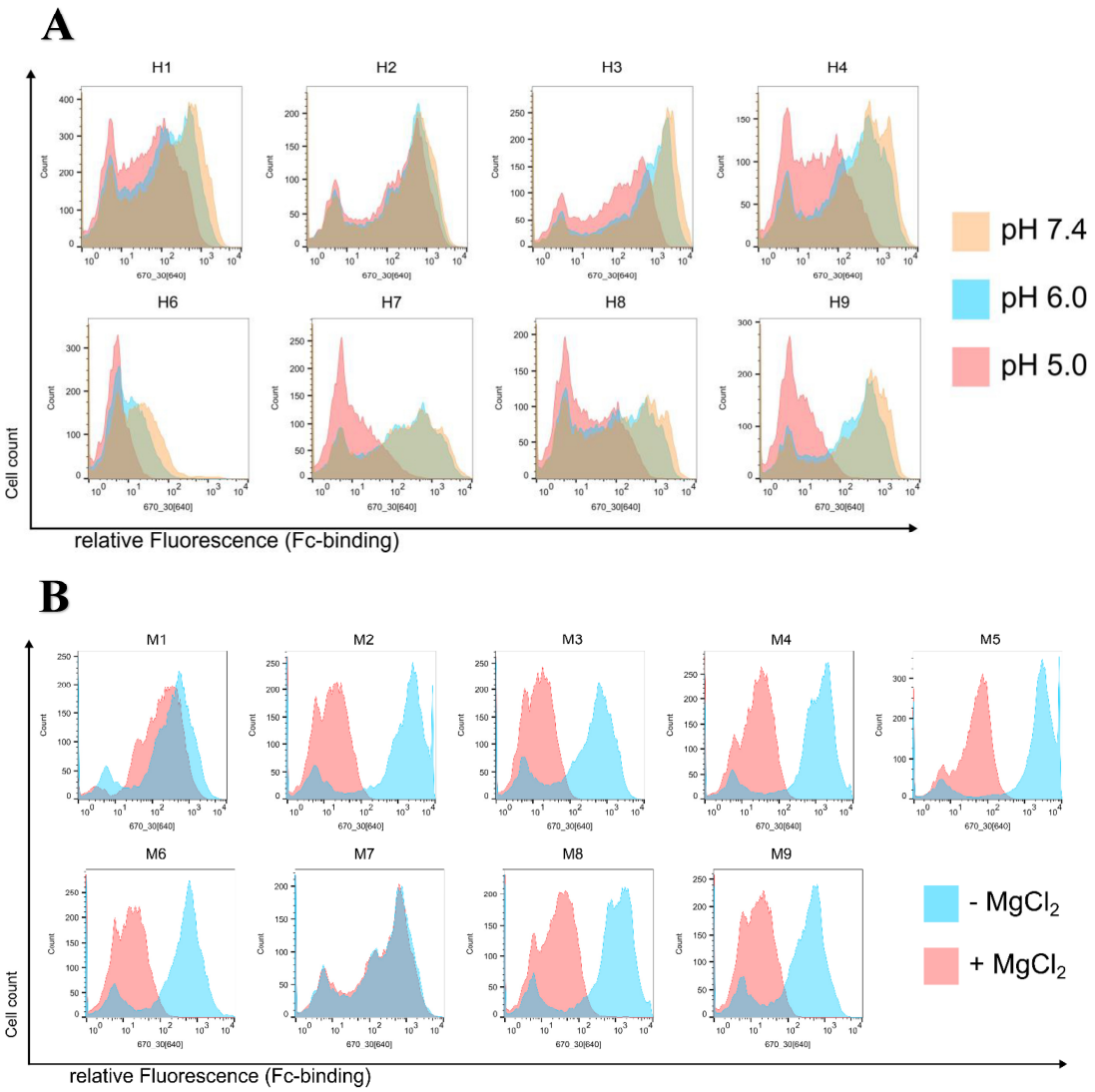


**Figure S4.** Summary of the single clone analysis by FACS. Each histogram contains 50,000 events with Fc-binding plotted on the x-axis and cell count on the y-axis. Detailed staining strategy is summarized in Table S1, the staining procedure in Table S2. **(A)** Analysis of isolated putative pH-responsive single clones. The washing step after target protein incubation was performed at pH 7.4 (orange), pH 6.0 (blue) or pH 5.0 (red), respectively. **(B)** Analysis of isolated putative magnesium-responsive single clones. The washing step was either performed with non-$MgCl_2$-containing Tris buffer (blue) or with Tris buffer containing 2 M $MgCl_2$ (red).

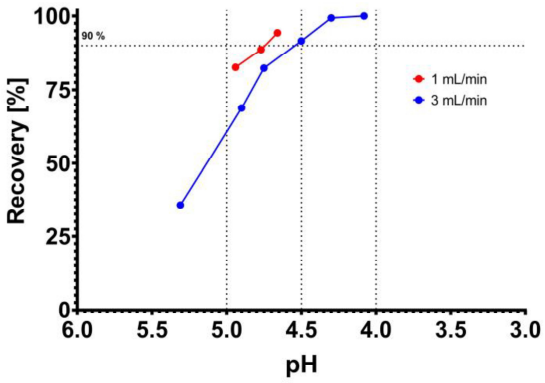


**Figure S5.** Recovery for H9 at different flow rates. The recovery is depicted on the y-axis, the pH value on the x-axis. Each dot represents a single measurement. Red data points indicate a utilized flow rate of 1 mL/min while blue data points depict a flow rate of 3 mL/min. Vertical dashed lines indicate pH 4.0, pH 4.5 and pH 5.0, respectively, horizontal dashed lines indicate 90% recovery.

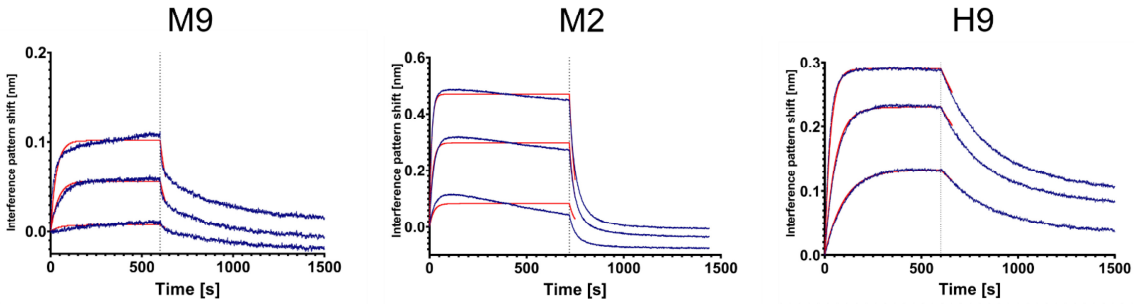


**Figure S6.** Binding kinetics of M9, M2 and H9 as determined via BLI on an Octet® RED96 system with the ForteBio data analysis software 9.0. Daratumumab was immobilized on FAB2G sensor tips and scFvs were subsequently associated at varying concentrations (M2: 720 s, M9/H9: 600 s). Dissociation was measured in PBS buffer at pH 7.4 for 600 s.

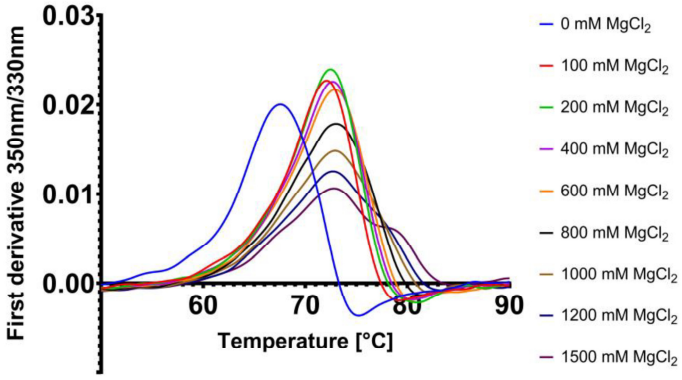


**Figure S7.** $T_M$ measurements of scFv M9 via Nano DSF at different $MgCl_2$ concentrations. Measurements were performed in singlets with a temperature gradient of 2°C/min.

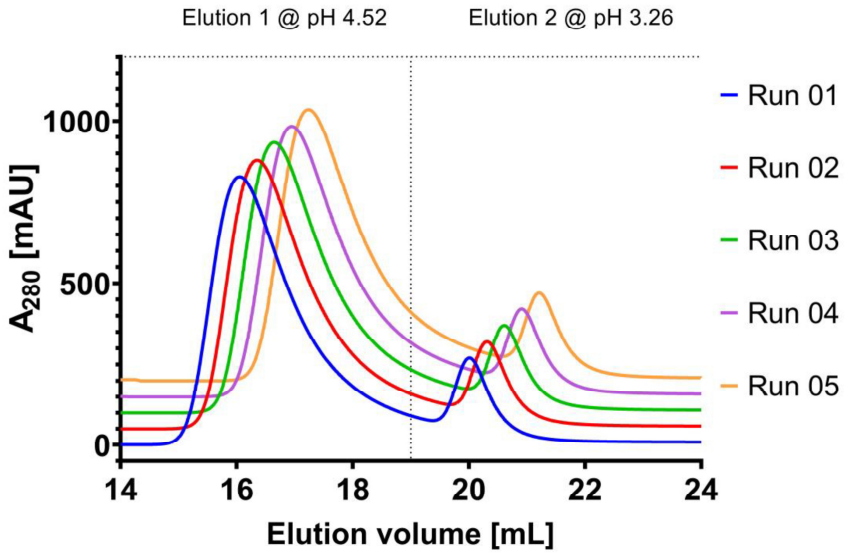


**Figure S8.** Repetition experiments for pH-responsive scFv H7. Five chromatography runs were performed with identical conditions. For this chromatogram, the elution from 14-24 mL elution volume are depicted. Elution step 1 is performed at pH 4.52, the second elution step at pH 3.26 Each run is indicated by a unique color, indicated on the right. Individual runs are nudged by 50 mAU and 0.3 mL.

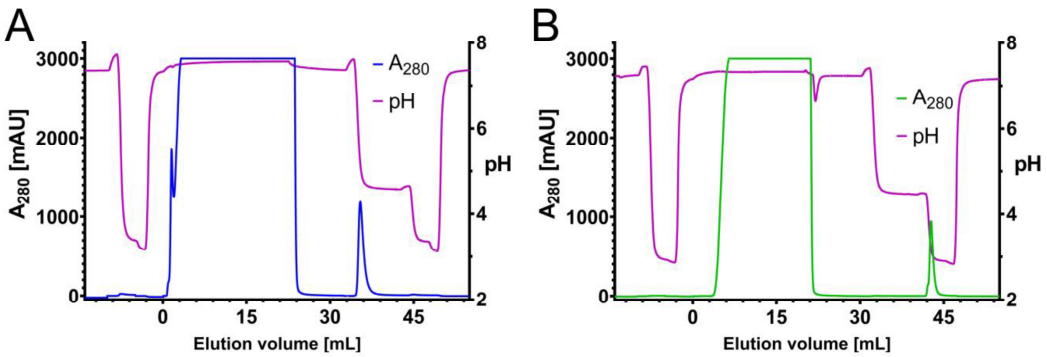


**Figure S9.** Trastuzumab purification from trastuzumab producing Expi293F cell culture supernatant. (A) Chromatogram of the purification of trastuzumab from 15 mL Expi293 supernatant. Absorbance at 280 nm is depicted on the left y-axis (blue), pH is shown on the right y-axis (violet). The elution volume is depicted on the x-axis. Elution was performed in two steps with pH 4.6 and pH 3.0, repectively. (B) Chromatogram of the purification of trastuzumab from 15 mL Expi293 supernatant with a Protein A HP column manufactured by GE Healthcare. Absorbance at 280 nm is depicted on the left y-axis (green), pH is shown on the right y-axis (violet). The elution volume is depicted on the x-axis. Elution was performed in two steps with pH 4.6 and pH 3.0, repectively.

9

# 5 Danksagung

In der folgenden Sektion möchte ich mich bei folgenden Personen bedanken:

Einen herzlichen Dank möchte ich an **Prof Dr. Harald Kolmar** richten. Insbesondere die kritische Diskussion von Daten halfen bei Beurteilung und Verfeinern von Experimenten ohne die die vorliegende Arbeit sicher nicht entstanden wäre. Auch Danke für das entgegengebrachte Vertrauen beim Organisieren der jährlichen Arbeitskreiskonferenz im Kleinwalsertal ohne die ich meine Skibegeisterung vermutlich nie entdeckt hätte ;-).

**Prof. Dr. Siegfried Neumann** danke ich für die Begutachtung meiner Arbeit und Übernahme des Koreferats.

**Prof. Dr. Beatrix Süß** und **PD Dr. Tobias Meckel** danke ich für ihre Arbeit als Fachprüferin und Fachprüfer meiner Arbeit.

**Prof. Dr. Stefan Hüttenhain** danke ich für motivierende Gespräche und entspannte Kaffeerunden während meines Bachelorstudiums, ohne die sich meine akademische Laufbahn vermutlich anders entwickelt hätte. **Dr. Andreas Krämer** gilt auch man Dank und seine sehr angenehme Betreuung meiner Bachelorarbeit.

Mein Dank gilt auch dem **MerckLab@TU Darmstadt** und all seiner Mitglieder. Allen voran **Dr. Gerhard Schwall** möchte ich für das Organisieren von internen Projekten, aber auch externen Kollaborationsprojekten danken. Hervorhebend danken möchte ich auch **Dr. Tina Bock** und **Dr. Dieter Spiehl** für das gemeinsame Bearbeiten von Projekten.

**Dr. Julius Grzeschik** für viele gemeinsame Stunden und Überstunden bei Getränken, fachliche Unterstützung sowie kulturgeschichtlicher Bildung hinsichtlich Skisport und mittelalterlicher Drachenkönige. Ich hoffe, dass auch Du irgendwann deine Handynummer auswendig kannst :3

**Dr. Stefan Zielonka** für Motivation, Ideen und Diskussion rund um fachspezifische und auch fachunspezifische Themen.

**Dr. Doreen Könning** für ihre Unterstützung/Ausbildung während meiner Masterarbeit und diversen Schwachsinn. **Adrian Elter** gilt mein Dank für die Assistenz bei Remoteeinreichung der Arbeit aus dem Ausland, romantische Stunden am See und der Zeit bei dem ein oder anderen Biergetränk. Solltest du Interesse haben neben System of a Down, Rammstein, Soundgarden, Linkin Park und Michael Jackson eine weitere Band kennenzulernen, kannst Du mich gerne fragen. **Jan Bogen** danke ich für die sehr gute gemeinsame Arbeit, die in

einer mehrfach ausgezeichneten Masterarbeit für ihn endete und das zu Recht! Bei **Dr. Simon Krah** bedanke ich mich für fachliche Beratung und Diskussion diverser Projekte, wie beispielsweise die Anschaffung einer neuen Brille. Auch die Erinnerung an gemeinsame Besuche von Fußballspielen möchte ich nicht missen :3.

Grüße gehen auch an „das andere Lager“, die Chemiker: **Dr. Hendrik Schneider** und **Simon Englert** danke ich für die fast perfekt dargestellte Bilderbuchehe. Hendrik für die gemeinsame Vorliebe für manche Vogelart (es gibt noch mehr als Adler btw.), das bisschen notwendige Chaos und meine Ausbildung als Pizzateigmasseur. Auch beobachte ich deine kontinuierliche Steigerung deines Biologenwissens wohlwollend. Simon danke ich für sehr viel hinz-ugewonnenes nutzloses Wissen und unzählbare spontane Themenwechsel in Diskussionen.

**Dr. Desislava Yanakieva** Нека бъдем честни, никой освен вас не може да прочете това. Благодаря ви за доброто и забавно сътрудничество. **Dr. Lukas Deweid** für seine meisterlich ausgearbeitete Geheimtaktik, die unserer Seleção den Chem Cup Sieg ermöglichte. Ein Sieg nicht für dich, nicht für mich, sondern für unsere gesamte Generation.

**Arturo Macarrón Palacios**, **Ataurehman Ali** aka. Ali Ata, **Dominik Happel** und **Bastian Becker** für gemeinsame Urlaubs- und Fahrraderlebnisse. Besonderen Dank möchte ich an Bastian für das geduldige Beantworten meiner technischen Fahrradfragen richten.

**Bei Dr. David Fiebig, Dr. Benjamin Mattes** und **Stefania Carrara** bedanke ich mich für eine wundervolle PEGS in Lissabon. Es war intensiv und bildend.

**Dr. Andreas Christmann,** danke das man bei Problemen deinen Rat einholen kann und manchmal sogar sinnvolle Antworten bekommt. :P

**Dr. Olga Avrutina, Dr. Anja Hofmann, Jan Habermann, Sebastian Bitsch, Valentina Hilberg, Sebastian Jäger, Aileen Ebenig, Lukas Pekar, Michael Ulitzka** und **etwaige Vergessene** danke ich für eine angenehme Arbeitsatmosphäre und die unbewusste Bereitstellung von Puffern und Material a Wochenenden.

Dank geht auch an: **Eva Baum.** Vielen Dank für deine große Hilfe in den Expressionstudien und für die unzähligen Arbeitsstunden, die du in deine Bachelorarbeit/Praktikum/Forschungsprojekt/HiWi,…etc. :P gesteckt hast.

**Ein großes Dankeschön geht auch Dr. Stephan Dickgießer** stellvertretend für die ganze „Dieter“-Gruppe. Die große Liebe, die uns alle eint.

Bei **Barbara Diestelmann** und **Dana Schmidt** möchte ich für die administrative Hilfe für Labor- und nicht-Laborpapierkram danken. Das erleichtert das Arbeiten enorm.

Bedanken möchte ich mich auch bei meiner Familie für den nötigen Rückhalt nicht nur während meiner Doktorarbeit, sondern auch während meines gesamten Studiums.

# 6 Affirmations

## Erklärung gemäß §8(1) Promotionsordnung

Hiermit erkläre ich, dass ich die vorgelegte Dissertation selbstständig und nur mit den mir zulässigen Hilfsmitteln angefertigt habe. Die Dissertation wurde in der vorgelegten oder einer ähnlichen Fassung zu keinem früheren Zeitpunkt an einer in- oder ausländischen Hochschule eingereicht. Die schriftliche Version stimmt zudem mit der elektronischen Version überein. Die identische elektronische Version für die Durchführung des Promotionsverfahrens liegt vor.
Außerdem erkläre ich, noch keinen Promotionsversuch unternommen zu haben.

Sion, 18.11.20
Ort, Datum

S. Hüng
Unterschrift

## Erklärung gemäß §9 Promotionsordnung

Hiermit versichere ich, dass ich die vorliegende Dissertation selbstständig angefertigt und keine anderen als die angegebenen Quellen und Hilfsmittel verwendet habe. Alle wörtlichen und paraphrasierten Zitate wurden angemessen kenntlich gemacht. Die Dissertation wurde in der vorgelegten oder einer ähnlichen Fassung zu keinem früheren Zeitpunkt an einer in- oder ausländischen Hochschule eingereicht.

Sion, 18.11.20
Ort, Datum

S. Hüng
Unterschrift

**ERKLÄRUNG ZUR BEGUTACHTUNG DER VERÖFFENTLICHUNGEN**

Kolmar
Referent

Neumann 02.11.2020
Koreferent Datum

Weder Referent (Prof. Dr. Harald Kolmar) noch Koreferent (Prof. Dr. Siegfried Neumann) der vorliegenden kumulativen Doktorarbeit waren an der Begutachtung nachstehender Veröffentlichungen beteiligt:

1. Dual function pH-responsive bispecific antibodies for tumor targeting and antigen depletion in plasma. *Frontiers in Immunology*
2. Simplifying the Detection of Surface Presentation Levels in Yeast Surface Display by Intracellular tGFP Expression. *Methods in Molecular Biology*
3. A generic procedure for the isolation of pH- and magnesium-responsive chicken scFvs for downstream purification of human antibodies. *Frontiers in Bioengineering and Biotechnology*
4. A simplified procedure for antibody engineering by yeast surface display: Coupling display levels and target binding by ribosomal skipping. *Biotechnology Journal*
5. Generation of Semi-Synthetic Shark IgNAR Single-Domain Antibody Libraries. *Methods in Molecular Biology*
6. Construction of Histidine-Enriched Shark IgNAR Variable Domain Antibody Libraries for the Isolation of pH-Sensitive vNAR Fragments. *Methods in Molecular Biology*
7. Yeast surface display in combination with fluorescence-activated cell sorting enables the rapid isolation of antibody fragments derived from immunized chickens. *Biotechnology Journal*
8. Facile generation of antibody heavy and light chain diversities for yeast surface display by Golden Gate Cloning. *Biological Chemistry*
9. Biophysical and biochemical characterization of a VHH-based IgG-like bi- and trispecific antibody platform. *mAbs*
10. Humanization of Chicken-derived scFv Using Yeast Surface Display and NGS Data Mining, *Biotechnology Journal*

Datum 2.11.2020

Referent
(Prof. Dr. Harald Kolmar)

Koreferent
(Prof. Dr. Siegfried Neumann)